UNIVERSITÀ DEGLI STUDI DI MILANO

SCUOLA DI DOTTORATO TERRA, AMBIENTE E BIODIVERSITÀ
Dipartimento di Bioscienze
Dottorato di Ricerca in Biologia Animale
Ciclo XXV

Biology of the dynamic connective tissues (MCTs) in invertebrate marine models: an integrated approach

Serena Tricarico

Tutors: Dr. Francesco Bonasoro e Prof.ssa M. Daniela Candia Carnevali
Coordinatore: Prof. Marco Ferraguti

Anno Accademico
2011/2012

This thesis was supervised by:

- Dr. Francesco Bonasoro
  Department of Biosciences, Università degli Studi di Milano, Milan, Italy

- Prof.ssa M. Daniela Candia Carnevali
  Department of Biosciences, Università degli Studi di Milano, Milan, Italy

The work described in this thesis was performed in:

- UNIMI - Università degli Studi di Milano, Milan, Italy

- INEB - Instituto de Engenharia Biomédica, Universidade do Porto, Portugal

The research described in this thesis was financed by:

Cariplo Foundation (Cassa di Risparmio delle Provincie Lombarde): Project MIMESIS 2009 (Marine Invertebrates Models & Engineered Substrates for Innovative bio-Scaffolds)

Table of contents

Abstract

Animal tissues are an immense source of inspiration for humans which actually mimic (biomimetic approach) and use them for novel material design and production. Connective tissue is the most important animal structural material and it (or its components) is often used as source of inspiration/model for different applications. Its main extracellular matrix (ECM) component is collagen. Currently, industrially available collagen is mainly of bovine origin that, however, carries a risk of transmission of serious diseases (bovine spongiform encephalopathy, BSE, and transmissible spongiform encephalopathy, TSE). Therefore, alternative and safer sources of collagen are required for regenerative medicine and one of the safer and recently exploited source are aquatic organisms.

The marine invertebrates that I used in this project (echinoderms, in particular sea urchins) possess peculiar and unique connective tissues, called Mutable Collagenous Tissues (MCTs), which could actually represent an alternative source of collagen. Moreover, MCTs undergo extremely rapid, drastic and reversible changes (completely independent from any muscular contribution) in their passive mechanical properties such as stiffness, tensile strength and viscosity under nervous control. Several evidences suggest that MCTs are probably one of the key elements of the striking regenerative capacities found in echinoderms, since they directly help the regenerative process, ex-ante creating the conditions and ex-post providing optimal growth-promoting environment and "dynamic" structures for tissue healing and regeneration. MCTs could therefore represent a valuable source of inspiration for biomaterial design addressed to biomedical applications.

The main general aim of this work was to acquire the appropriate knowledge of the model we want to get inspiration from (MCTs) and to understand how natural MCTs actually work. In particular, the specific objective was to define the basic biology of natural MCTs, particularly the key-components and their fundamental interactions; this will be achieved through morphological, biochemical, biomolecular and biomechanical characterizations.

This thesis is part of the MIMESIS Project financed by CARIPLO Foundation (2009). The very ultimate challenge of the project is to explore the possible development of a new class of biomimetic materials inspired to echinoderm MCT to be used for scaffolds for tissue regeneration and cell colture studies.

The first approach consisted in the investigation of the MCT structural key-components, including fibrillar proteins, proteoglycans (PGs) and glycosaminoglycans (GAGs) in order to deeply investigate how the natural tissue works. The transmission electron microscopy technique was used

to obtain micro-scale view to understand the micro-organization of the ECM components. With this detailed investigation the current knowledge of the structural organization of MCT ECM was expanded.

The biochemical analysis with SDS-PAGE and Western blot analysis on collagen and PGs/GAGs showed how complex MCTs are. We found that the fibrillar collagen has strong similarities with collagen type I and that all the PGs/GAGs families are represented in MCTs but with differences in quality and quantity according to the tissues analysed or to the related mechanical state.

Another major focus of this work was the biomolecular approach related to a presumptive key effector protein, tensilin. This factor, previously found and characterised in other echinoderms (holothurians), is considered as responsible for mutability phenomena. In our study, attention was addressed to “tensilin” possible presence and function in two common sea urchin species, *Strongylocentrotus purpuratus* and *Paracentrotus lividus.* We have successfully found and produced tensilin in *S. purpuratus* and performed fibril aggregation assays. On the basis of our results we can conclude that the *S. purpuratus* tensilin does not react with collagen like that isolated from holothurians and that the specific MCT environment is fundamental for its activity.

The last approach was addressed to extract effector molecules directly from fresh MCT tissues with chromatography and to characterize them with rheology tests. Very important data were collected: 1) the rheological characterization of insoluble and soluble echinoderm collagens in comparison with the ultrapure bovine sample showed that echinoderm collagen possesses peculiar mechanical properties that must be taken in account in view to build and produce an MCT inspired biomaterial; 2) moreover, some chromatographic fractions showed the capability to modify the standard collagen properties.

List of abbreviations

AA	Amino acid
AChSW	Acetylcholine in seawater
ASW	Artificial sea water
ATR-FTIR	Attenuated Total Reflectance - Fourier transform infrared
BLASTn	Basic Local Alignment Search Tool for nucleotide
BLASTp	Basic Local Alignment Search Tool for protein
BSE	Bovine spongiform encephalopathy
C1qBP	Complement component 1, q subcomponent binding protein
CDL	Compass depressor ligament
cDNA	Complementary deoxyribonucleic acid
C_f	Final concentration
CSC	Chondroitin-6-sulfate
DMA	Dynamic mechanical analyser
ECL	Enhanced chemiluminescence
ECM	Extracellular matrix
EDTA	Ethylenediamine tetraacetic acid
EGTA	Ethylene glycol tetraacetic acid
EST	Expressed Sequence Tags
FT-IR	Fourier transform infrared
G' (G prime)	Shear modulus elastic component
G" (G double prime)	Shear modulus viscous component
G* (G star)	Shear modulus complex component
GAG	Glycosaminoglycan
HRP	Horseradish peroxidase
JLC	Juxtaligamental cell
LM	Light microscope
LVER	Linear viscoelastic region
MCT	Mutable collagenous tissue
MMP	Metalloproteinase
mRNA	Messenger Ribonucleic acid

NCBI	National Center for Biotechnology Information
NEM	N-ethylmaleimide
NSF	Novel stiffening factor
OHPr	Hydroxyproline
ORF	Open reading frame
PBS	Phosphate buffered saline
PG	Proteoglycan
PM	Peristomial membrane
PMSF	Phenylmethanesulfonylfluoride
PPSW	Propylene phenoxetol in seawater
PTA	Phosphotungstic acid
PVDF	Polyvinylidine Fluoride membrane
RACE	Rapid amplification of cDNA ends
RNA	Ribonucleic acid
RT	Room temperature
RT-PCR	Reverse transcriptase-polymerase chain reaction
SDS-PAGE	Sodium dodecyl sulfate polyacrylamide gel electrophoresis
SURF	Sea urchin fibrillar module
TBST	Tris-Buffered Saline and Tween 20
TEM	Transmission electron microscope
TIMP	Tissue inhibitor metalloproteinase
Tris	Tris[hydroxymethyl]aminomethane
TSE	Transmissible spongiform encephalopathy
V_f	Final volume
γ (gamma)	Shear rate
η (eta)	Shear viscosity
σ (sigma)	Shear stress

Introduction

ECHINOIDS

Sea urchins are small, spiny, globular animals which constitute the class Echinoidea of the Echinodermata phylum. There are about 950 species of echinoids inhabiting all oceans from the intertidal to 5000 meters deep.

Regular echinoids are characterized by a roundish or globular test of solid plates; tube feet, which emerge through specific holes in the plates, form five conspicuous bands, running from the aboral to oral pole, called ambulacra. The areas interposed between these bands of tube feet are called interambulacra. Regular echinoids are roughly spherical, with a centrally located mouth at the intersection point of the five ambulacra; the anus is located on the opposite side in aboral position. Irregular sea urchins are elongated or flattened in shape, with the anus placed on the oral, lateral or aboral side of the body. In regular, and often, in irregular echinoids, the mouth is equipped with five jaws operating in a complex dental apparatus called Aristotle's lantern (Ruppert et al., 2007).

PARACENTROTUS LIVIDUS

Paracentrotus lividus is a species of sea urchin in the family Parechinidae commonly known as the purple sea urchin (see Fig. 1). It is the prototype species of the genus and occurs in the Mediterranean Sea and eastern Atlantic Ocean.

P. lividus has a circular, flattened greenish test with a diameter of up to seven centimetres in the adult. The test is densely covered by long and sharply pointed spines, usually purple but occasionally showing other colours including dark brown, light brown and olive green. There are five or six pairs of pores on each ambulacral plate (see Fig. 1; Ruppert et al., 2007).

P. lividus is a gonochoric species although hermaphroditism has been observed. Males and females aggregate for spawning and release gametes into the water column. The larvae form part of the zooplankton for about 28 days before settling and undergoing metamorphosis (Shpigel et al., 2004).

COMPASS DEPRESSOR LIGAMENT

The compass system consists of: (1) five compass ossicles which are located on the aboral (upper) surface of the lantern, (2) five compass elevator muscles which interconnect transversely the compasses, (3) ten compass rotular ligaments linking the compasses to the underlying rotular ossicles, and (4) ten compass depressors ligaments (CDL) of connective tissue which extend from the distal lobes of the compasses to the interambulacral processes of the perignathic girdle (inner edge of the test) at its junction with the flexible peristomial membrane (see Fig. 2; Wilkie et al., 1992).

The CDL of the sea urchin *P. lividus* is a very good experimental model, due to 1) their easy extraction, 2) their simple and typical mutable collagenous tissue (MCT) structure in comparison to others MCTs (see Fig. 3), 3) the advantageous absence of calcite ossicles inside the tissue.

PERISTOMIAL MEMBRANE

The peristomial membrane (PM) is an important component of the buccal apparatus in regular echinoids. It consists of a wide area of flexible body wall which surrounds the mouth and connects the lantern to the test (see Fig. 4). This membrane is a diaphragm-like viscoelastic ligament which has an important articular function and which is involved actively or passively in all the activities of the lantern. It has emerged from morphological, physiological and biomechanical studies (Lanzavecchia et al., 1988; Andrietti et al., 1990; Candia Carnevali et al., 1990; Wilkie et al., 1993, 1994) that the PM plays a key-role in the overall mobility of the lantern. It supports the lantern and can act antagonistically or synergistically with the muscles which control the movement and the position of the lantern. This functional eclecticity can be related closely to both the structural features and the mechanical properties of the membrane (Bonasoro et al., 1995).

The PM has a rather simple anatomical structure. In *P. lividus* the PM consists fundamentally of a collagenous dermis reinforced by scattered calcite ossicles, which is covered on its outer side by epidermis and on its inner side by a coelomic epithelium (Candia Carnevali et al., 1990). The thick dermal layer is the most significant component in terms of both structure and mechanical properties. Some investigations (Wilkie et al., 1993) provided evidence that the thick dermal layer consists of MCT, i.e., that it can both behave like a typical non-linear viscoelastic biomaterial and undergo reversible changes of tensility (stiffening or softening) under nervous control.

In further studies (Wilkie et al., 1994) the microarchitecture of the fibrous dermis and its functional differentiation were analysed in detail and correlated with the complex mechanical behaviour of the PM.

MCTs

One of the key factors responsible for the ecological success of echinoderms is the ubiquitous presence of mutable collagenous tissues (MCTs). These tissues, although composed of the usual collagenous tissue elements (collagen fibrils, microfibrils, amorphous matrix and cells), are able to change reversibly their viscoelastic properties under nervous control in an extremely short time-span (Motokawa and Tsuchi, 2003). This potential is in part due to the active involvement of partially characterized glycoproteins that transiently cross-link collagen fibrils.

Mutability is an extreme and rapid phenomenon (occurring in <1 s in some cases) involving nervously mediated changes in connective tissue mechanical properties (Wilkie et al., 1993). These changes are accompanied by a rearrangement of the extracellular matrix (ECM) that nevertheless maintains its intrinsic features in terms of structural components. Dynamic phenomena comparable to these changes occur also in other animal models: for instance, the normally stiff uterine cervix of mammals becomes compliant to allow the passage of the foetus (Timmons et al., 2010). The time scale of such phenomena varies a lot: from under 1 s in echinoderms to hours or days in mammals.

In terms of tensile properties, MCT can strengthen and stiffen significantly or, in contrast, completely lose resistance to tensile force (Wilkie, 2005). In the few cases where muscle cells are present, the high tensile strength and stiffness that can be generated and the high ECM-muscle ratio indicate that mutability does not depend on active contractile mechanisms (Takemae and Motokawa, 2005; Wilkie, 2002).

Mutable collagenous structures exhibit both functional and structural, including ultrastructural, diversity (Wilkie, 2005). Three main patterns of tensile changes can be expressed by a mutable tissue: (1) only reversible stiffening and destiffening (e.g. sea urchin PM and CDLs; Wilkie et al., 1992, 1993); (2) only irreversible destiffening (always associated with autotomy; e.g. crinoid syzygial ligament; Wilkie et al., 1999; ophiuroid tendons; Wilkie and Emson, 1987); (3) irreversible destiffening as well as reversible stiffening and destiffening (e.g. ophiuroid intervertebral ligament; Wilkie, 1988). These significantly different behaviours make very complicate to interpret the phenomenon in its basic mechanisms.

MCTs can be considered as composite materials in which collagen fibrils act as tensile elements, while the interfibrillar matrix (partly composed of glycosaminoglycans - GAGs)

represents the compression-resistant element (Ottani et al., 2001). Although MCTs share these structural and functional principles with vertebrate connective tissues, they fulfil additional functions. They are involved in echinoderm locomotion (Santos et al., 2005), low-energy maintenance of posture (Emson, 1984; Takemae et al., 2009) and defensive self-detachment of body components (autotomy), followed by regeneration (Candia Carnevali and Bonasoro, 2001a, b; Wilkie, 2001). The regeneration process itself may be facilitated by the presence of MCTs; e.g. when structural loss occurs at the level of mutable collagenous structures, regeneration is usually quicker and the development of anomalies is greatly reduced in comparison with regeneration following traumatic amputation performed at another level (Candia Carnevali and Bonasoro, 2001a, b). Furthermore, MCT may be involved in the "fission" processes associated with asexual reproduction in echinoderms (Sterling and Shuster, 2011; Wilkie et al., 1984). From all these points of view, MCT has clearly contributed to the ecological success of echinoderms (Motokawa and Tsuchi, 2003).

Recent and important information comes from the analysis of the water content of MCTs in different mechanical states. Both Tamori et al. (2010) and Ribeiro et al. (2012) confirmed that compliant samples have a higher content of water respect to stiffened samples. Interestingly, in sea urchin CDL ligaments (Ribeiro et al., 2012), this difference resulted to be due to a translocation of water from the interior to the surface of compass depressor ligaments during the stiffening process. As suggested by the authors, the water molecules, hydrating the standard or compliant samples and interacting with extracellular matrix components, could be replaced by putative stiffening effectors, resulting in water displacement.

Typical variable tensility phenomena have been demonstrated in many echinoderm collagenous structures including sea urchin spine ligaments (Hidaka and Takahashi, 1983; Morales et al., 1989) and PM (Candia Carnevali et al., 1990) and CDLs (Wilkie et al., 1992).

MCTs: general architecture

The mutable collagenous tissues can be considered as typical composite materials, constituted by a dense ECM of collagen fibrils, fibrillin microfibrils, proteoglycans (PGs, insoluble and soluble), water and a number of specific constitutive and regulative proteins (effector proteins) identified so far and characterized only in holothurian dermis (see Figs. 5, 6; Wilkie, 2005; Barbaglio et al., 2012). As MCTs are present in several anatomical locations, they perform the same mechanical functions as the collagenous connective tissue at analogous locations in the bodies of vertebrates: these functions can be generally related to resisting, transmitting and dissipating

energy, as far as the fibrous components is concerned, whereas the interfibrillar matrix gives resistance to compression maintaining the tissue hydrated (Silver and Landis, 2008).

Besides collagen, other supramolecular assemblies are present in all studied MCTs. This is the case of the loose networks of microfibrils endowing tissues with elasticity (Wilkie, 2005; Barbaglio et al., 2012). An extensive morphological, biochemical and immunological characterization of these structures from *Cucumaria frondosa* revealed that they resemble fibrillin-containing microfibrils of mammalian connective tissues (Thurmond and Trotter, 1996; Thurmond et al., 1997). The microfibrils network extracted from holothurian dermis and tested by tensile testing showed to be extensible/reversible up to 300% of their initial length. It seems that this protein can help MCT in a compliant state to return its initial length after it has undergone a relevant deformation (Thurmond and Trotter, 1996; Thurmond et al., 1997).

Although other cell types are present (e.g. fibroblast-like, phagocytes and myocytes), all confirmed MCTs are permeated by or in contact with very peculiar cell types, the juxtaligamental cells (JLCs; Wilkie, 1979; Wilkie et al., 1992; Wilkie, 2005). JLCs have been suggested to be part of the nervous system due to their close association with neuronal processes (functional contact with axons sometimes at chemical synapse-like junctions) providing MCT direct innervation. Neural inputs to MCTs seem to include both cholinergic and aminergic components. The activities of these cells are controlled at least partly by cholinergic pathway, although there is also evidence of the presence of aminergic innervation (see Fig. 6; Wilkie, 1979; Wilkie et al., 1992; Wilkie, 2005).

In most MCTs structures it is possible to identify cells characterised by more than one population of granules, which can be distinguished by shape (circular or oval profiles), size and variable electron density (see Fig. 7; Koob et al., 1999). These cellular elements are considered as the effector cells responsible for MCT tensility, since they are developed only within MCT, they are in close contact with the nervous system and, their granules contain molecules (identified only in the dermis of the holothurian *C. frondosa*) that influence the interfibrillar cohesion (Trotter et al., 1996; Tipper et al., 2002). Also in the sea cucumber model, more than one population of JLCs could be distinguished morphologically (JLC1 and JLC2), suggesting that one cell type could be responsible for the release of the stiffening protein and the other for release of the de-stiffening protein, resulting in the stiff and compliant mechanical state respectively (Koob et al., 1999).

MCTs: collagen and fibrillin

Based on current evidence, it appears that most MCTs consist of parallel aggregates of discontinuous, spindle-shaped collagen fibrils with paraboloidal tips to which PGs are covalently or

non-covalently attached (Matsumura, 1974; Trotter et al., 1995). This seems to be the perfect arrangement for fibrils that strengthen a discontinuous fibre composite in order to avoid shear-stress concentration near the ends (Trotter and Koob, 1989; Trotter et al., 2000).

Although the main fibrillar extracellular components are common in the matrix of all MCT structures, their organization and spatial arrangement can vary a lot. In sea urchins, for example, the CDL as well as the spine ligament present a structure with predominantly parallel fibre array. However, the PM shows distinct layers with orthogonal fibre arrays. This structural diversity of MCTs is rather comparable to that of mammalian connective tissues (Wilkie et al., 1992, 1994; Wilkie, 2005; Shoulder and Raines, 2009).

Similarities were also found between vertebrate collagen type I fibrils and sea urchin collagen fibrils regarding D-banding pattern, amino-acids composition, crosslink chemistry and gene organization (Trotter et al., 1994; Wilkie, 2005; Szulgit, 2007). Although the work performed by Trotter et al. (1994) suggested some close resemblance between the D-banding pattern of collagen from sea urchin spine ligament, holothurian body wall and mammalian type I fibrils have some differences in the staining intensity, suggesting that dissimilarities might occur at the amino acid sequences (Trotter and Koob, 1989, 1994). Also some differences were found regarding the chain composition of echinoid and holothurian collagen molecules, their solubility and amino acid composition (Trotter and Koob, 1994; Trotter et al., 1995).

Interestingly Exposito et al. (2002, 2010) have demonstrated the presence of heterotypic fibrils with collagen molecules that undergo distinct maturation in their N-propetide domain. This domain seems to be specific of echinoderm phylum and consist of a 140 amino acid long motif (sea urchin fibrillar module - SURF). Although they seem to be exclusive of echinoderms and are present in MCTs structures, their contribution to the variable tensility is still speculative since SURF molecules also appear in several tissues that are not mutable (Cluzel et al., 2000, 2003; Exposito et al., 2002, 2010).

During the last decade numerous investigations have characterized the fibrillar collagen chains in *Hydra*, nematodes, rat, bovine and sea urchin. These data support the concept that in both invertebrates and vertebrates the triple helix is conserved, despite the presence of some imperfections and sometimes low levels of sequence identity (Exposito et al., 2002).

Sea urchin collagen literature identifies the presence of two fibrillar α chains (1 α and 2 α) involved in the formation of heterotrimeric molecules [$(\alpha_1)_2$ α_2] that are characteristic of mammalian type I collagen (Robinson, 1997; Cluzel et al., 2000, 2003; Exposito et al., 2002, 2010). Phylogenetically, echinoderm striated collagen fibrils are also close to mammalian type I fibrils.

The phylogenetic tree of the collagen genes recently presented by Wada et al. (2006) demonstrated the proximity of sea urchin collagen genes to those coding collagens of mammalian type I fibrils.

The variable tensility of MCT does not involve any changes in both the mechanical properties and the morphology of the collagenous fibrils themselves. All the ultrastructural studies performed were unsuccessful to demonstrate that MCT tensility is accompanied by modifications in fibrils diameter or even by changes in D-banding pattern. Furthermore, the fusiform shape of the fibrils is not related with MCT variable tensility (Wilkie, 2005; Barbaglio et al. 2012).

Fibrillin microfibrils were already biochemically and ultrastructurally characterized by Thurmond and Trotter (1996). However, their involvement in the mutability phenomenon is inconclusive since they are present also in connective tissues that are not mutable (Thurmond et al., 1997).

MCTs: molecular interactions involved in the interfibrillar cohesion

MCTs can be maintained stiff or compliant due to the ground substance molecules that interconnect fibrils, this process being strongly influenced by the extracellular ionic composition and concentration, suggesting that the capacity of the fibrils for reciprocal sliding can be controlled through alterable interaction of specific charges that constitute the extracellular matrix (Motokawa, 1984; Hayashi and Motokawa, 1986). They are extremely sensitive to the ionic surrounding medium; their tensile strength is pH dependent and the stiffness decrease with monovalent cation concentration (e.g. K^+). It is possible that monovalent cations mask GAG anionic sites reducing collagen-GAG and GAG-GAG interactions. Divalent cations (Ca^{2+} and Mg^{2+}), have an opposite influence on MCT stiffness regarding the monovalent cations; it is possible that they can act as divalent cross-linkers. However, the current hypothesis suggests that their role on the variable tensility is more related with their action on the cellular components (JLCs) rather than the ECM itself (Motokawa, 1984; Hayashi and Motokawa, 1986; Hill, 2001; Wilkie, 2005).

As in mammalian connective tissues, PGs are one of the main molecular components involved in interfibrillar cohesion: PGs are covalently or non-covalently attached to collagen fibrils, serving as binding sites for the effector molecules responsible for interfibrillar cohesion (Erlinger et al. 1993; Raspanti et al., 2008). PGs with their typical glycosaminoglycans (GAGs) side chains were already characterized in the echinoid spine ligament, where GAGs mainly belong to the chondroitin-dermatan sulfate family (Trotter and Koob, 1989; Trotter et al., 1995). In holothurian dermis, highly sulfated fucose GAGs were also observed and associated with collagen fibrils (Trotter and Koob, 1989; Szulgit, 2007).

It seems that the integrity of the ECM of MCT in contact with the ionic composition of sea-water depends on the electrostatics interactions that are very important to maintain the interfibrillar cohesion (Motokawa, 1984; Hayashi and Motokawa, 1986).

MCT tensility seems to be adjusted through changes in the type or even density of interactions between adjacent PGs molecules or between PGs and collagen fibrils. While PGs-PGs interactions are poorly characterized, it is agreed that collagen-PGs interaction are mainly electrostatic and the softening of MCT may result from the weakening or even suppression of PG-collagen interaction, which allows the interfibrillar slippage to occur (Motokawa, 1984; Wilkie, 2005; Barbaglio et al., 2012).

MCTs: effector molecules

In terms of molecules responsible for interfibrillar cohesion, clear interfibrillar bridges were already visualized (with electron microscopy techniques), and some of the proteins involved were already identified in the sea cucumber model (see Fig. 6; Trotter et al., 1996; Koob et al., 1999; Yamada et al., 2010; Barbaglio et al., 2012).

The molecule that is more likely to have a role in the standard tensile state is stiparin, the most abundant glycoprotein that interacts with collagen fibrils via surface-bound PGs (Trotter et al., 1996). MCT re-stiffening from the ‘compliant’ state has been attributed to tensilin, a glycoprotein that binds to collagen fibrils via surface GAGs forming interfibrillar bridges between collagen fibrils, preventing interfibrillar slippage (Trotter et al., 1998; Tipper et al., 2002).

Tensilin was isolated from *C. frondosa* with agents causing cell lysis, indicating that it is secreted from cells: however tensilin was also localized extracellularly and this depends on the mechanical state of the tissue (Trotter et al., 1998; Tipper et al., 2002). The hypothesis at the moment is that collagen fibrils are held together by stiparin through weak bonds (since stiparin is easily extracted with seawater) that can facilitate the action of effector molecules such as tensilin (see Fig. 6).

Another stiffening agent has been recently identified. The MCT stiffening from the standard to the maximally stiffened state was recently attributed to a novel stiffening factor (NSF). However it essential to elucidate if the stiffening activity of NSF is due to its direct action on extracellular components or to indirect effects on cells (Yamada et al., 2010).

The potential destiffening agent has not yet been identified. It has been suggested that specific enzymes might have such role. The hypothesis of tensilin-tensilin protease proposed by Wilkie et al. (2005) appears plausible, since the C-terminus of tensilin (that contains a collagen-binding domain) undergoes proteolysis *in vitro*. It has been suggested that tensilin-induced

stiffening is reversed *in vivo* by a specific protease. Also, as the amino acid sequence of tensilin has 21-36% homology with a tissue inhibitor metalloproteinase (TIMP), this raises the possibility that the mutability mechanism may have evolved from a MMP (metalloproteinases) -TIMP system (Wilkie, 2005). It seems that, once released in the extracellular matrix, this protease will cleave tensilin near the GAG binding site, allowing fibrils to slide past each other and resulting in a compliant condition. Reversibility is obtained by the release of "fresh" tensilin to the ECM that will form and reform new bonds restoring the tissue in its initial mechanical properties (Wilkie, 2005).

A "stiparin inhibitor" and a "plasticiser factor" were also identified as responsible for the transition from the standard to the compliant state (Koob et al., 1999; Trotter et al., 1999; Wilkie, 2005). Till now, the factor(s) that return MCT from the maximally stiffened state to the standard state were not identified. It can be hypothesized that different mechanisms and proteins effectors can be involved in the different transitions (see Fig.6).

MMPS AND TIMPS

The fact that the amino acid sequence of tensilin indicates 21-36% homology with mammalian TIMPs raises the intriguing possibility that MMPs may be directly involved in the mutability phenomenon or that the regulatory mechanism has evolved from a MMP-TIMP system (Wilkie, 2005).

MMPs are a family of enzymes that can degrade all ECM components and are extensively involved in the ECM remodeling that accompanies morphogenesis and wound healing in mammals (Wilkie and Emson, 1987), and development and regeneration in echinoderms (Hidaka and Takahashi, 1983).

Furthermore, MMPs contribute to the destiffening of the mammalian uterine cervix, which precedes and facilitates the dilatation of the cervix during foetal delivery (Barbaglio et al., 2012). Whilst the uterine cervix can also be regarded as a mutable collagenous structure, its changes in mechanical properties differ from those of echinoderm MCTs in having a much longer time course (hours to weeks) and in being under primarily endocrine rather than neural control (Brockes and Kumar, 2008). Another important difference is that cervical destiffening is achieved partly through the degradation of collagen fibrils (Brockes and Kumar, 2008; Wilkie et al., 2010), whereas there is no evidence that this accompanies the destiffening of echinoderm MCTs and indeed the capacity of most of these tissues to rapidly re-stiffen makes this highly unlikely a priori (Santos et al., 2005).

MMPs could, however, destabilize echinoderm MCTs by hydrolysing non-collagenous components that contribute to interfibrillar cohesion. Such a mechanism may be responsible for the

dermal “liquefaction” shown by some holothurians, which appears to result from the digestion of interfibrillar molecules (possibly PGs) by a gelatinolytic enzyme that has no discernible effect on the collagen fibrils themselves (Castillo et al., 1995).

New interesting data came from the analysis of MMPs activity (Ribeiro et al., 2012a). Galardin, an inhibitor of MMPs (MMPs 1, 2, 3, 8, 9), reversibly increased the stiffness and storage modulus of CDLs. Furthermore, a progressive increase in total gelatinolytic activity from the compliant to the stiff state was registered (Ribeiro et al., 2012a). Gelatin-zymography detects the presence of activated MMPs, inactive pro-MMPs and some MMPs previously bound to TIMPs. The positive correlation between degree of stiffness and increasing levels of higher molecular weight complexes (probably resulting from increasing inhibition of activated MMPs) is in accord with the hypothesis of an involvement of MMPs in the mutability mechanism.

PGS AND GAGS

Proteoglycans (PGs) are proteins that are heavily glycosylated. The basic PG unit consists of a “core protein” with one or more covalently attached glycosaminoglycan (GAG) chain(s) (see Fig. 8; Meisenberg and Simmons, 2006).

GAGs or mucopolysaccharides are long unbranched polysaccharides consisting of a repeating disaccharide unit. The repeating unit consists of a hexose (six-carbon sugar) or a hexuronic acid, linked to a hexosamine (six-carbon sugar containing nitrogen). In the PGs the point of attachment is a Ser residue to which the GAGs are joined through a tetrasaccharide bridge (For example: chondroitin sulfate-GlcA-Gal-Gal-Xyl-PROTEIN). The chains are long, linear carbohydrate polymers that are negatively charged under physiological conditions, due to the occurrence of sulfate and uronic acid groups (see Fig. 8).

PGs are a major component of the animal ECM, the “filler” substance existing between cells in an organism. Here they form large complexes, both to other PGs, to hyaluronan and to fibrous matrix proteins (such as collagen). They are also involved in binding cations (such as sodium, potassium and calcium) and water, and also regulating the movement of molecules through the matrix. Evidence also shows they can affect the activity and stability of proteins and signalling molecules within the matrix. Individual functions of PGs can be attributed to either the protein core or the attached GAG chain and serve as lubricants (Meisenberg and Simmons, 2006).

PGs can be categorised (see Table 1) depending upon the nature of their GAG chains or by size (kDa):

Glycosaminoglycans	Small proteoglycans	Large proteoglycans
chondroitin sulfate/dermatan sulfate	decorin, 36 kDa biglycan, 38 kDa	versican, 260-370 kDa, present in many adult tissues including blood vessels and skin
heparan sulfate/chondroitin sulfate	testican, 44 kDa	perlecan, 400-470 kDa
chondroitin sulfate		neurocan, 136 kDa aggrecan, 220 kDa, the major proteoglycan in cartilage
keratan sulfate	fibromodulin, 42 kDa lumican, 38 kDa	

Table 1. Classification of GAGs and PGs. According to the specific GAG considered, it can be assembles in small or large PGs. Jeffrey and Watt, 2003.

COLLAGEN FIBRILS AGGREGATION ASSAY

The first aggregation assays were described by Trotter et al. (1996, 1999; see Fig. 9). Collagen fibrils extracted from the dermis of the holothuroid *C. frondosa* were mixed with stiparin protein, purified directly from dermis with different anion-exchange column. In particular, they mixed 1 ml volume containing 60 µg (collagen) fibrils, 0.3 M NaCl, 20 mM Tris-HCl, pH 7.8, and aggregating protein quantities between 0.1 and 2 µg. Collagen fibrils were aggregated was observed by eye.

The last assay was described by Tamori et al. (2006; see Fig. 10) in which collagen fibrils extracted from the dermis of the holothuroid *Holothuria leucospilota* were mixed with the tensilin protein, purified directly from dermis with different anion-exchange column. In particular, they mixed a suspension (20 µl) that contained collagen fibrils with the same volume of test solution either in the presence of calcium or in its absence. A clot of fibrils was formed in the collagen-suspension solution when it was mixed with an equal amount of buffer solution containing *H-tensilin*. The fibril formation was observed both in media with Ca^{2+} and without Ca^{2+}.

RHEOLOGY

Rheology is the study of the flow of matter, primarily in the liquid state, but also as ‘soft solids’ or solids under conditions in which they respond with plastic flow rather than deforming elastically in response to an applied force. It applies to substances which have a complex molecular structure, such as muds, sludges, suspensions, polymers and other biological materials (Schowalter, 1978).

Newtonian fluids can be characterized by a single coefficient of viscosity for a specific temperature. Although this viscosity will change with temperature, it does not change with the flow rate or strain rate. Only a small group of fluids exhibit such constant viscosity, and they are known as Newtonian fluids. But for a large class of fluids, the viscosity change with the strain rate (or relative velocity of flow) and are called non-Newtonian fluids. Rheology generally accounts for the behaviour of non-Newtonian fluids, by characterizing the minimum number of functions that are needed to relate stresses with rate of change of strains or strain rates (Schowalter, 1978).

Viscoelasticity is the property of materials that exhibit both viscous and elastic characteristics when undergoing deformation. Viscous materials, like honey, resist shear flow and strain linearly with time when a stress is applied. Elastic materials strain instantaneously when stretched and just as quickly return to their original state once the stress is removed. Viscoelastic materials have elements of both of these properties and, as such, exhibit time dependent strain. Whereas elasticity is usually the result of bond stretching along crystallographic planes in an ordered solid, viscosity is the result of the diffusion of atoms or molecules inside an amorphous material (Meyers and Chawla, 1999).

In rheology viscometry tests are carried out to determine the viscosity, as a function of the applied shear stress or shear strain changing the frequency, temperature or time and oscillation tests are used to determine the strength and stability of a material. This last gives a clear indication of the behaviour of the sample, whether viscous or elastically dominated, over a given frequency range.

The fundamental viscometry and oscillation parameters are summarized below:

- Shear strain: the total angular displacement since the start of the action. It is the angular displacement multiplied by the shear strain constant of the geometry;
- Shear rate γ (gamma) (s^{-1}): Shear strain / time. A measurement of how fast the sample is flowing. Also known as shear strain rate. This is the shear rate experienced by the sample. The rate of change of shear strain with respect to time. It is calculated as the angular velocity multiplied by the shear strain constant of the geometry;
- Shear stress σ (sigma)(Pa): Force / surface area. This is the stress experienced by the sample. The shear stress applied to the sample. It is calculated from the applied torque and the shear stress constant of the geometry. The value is the average taken over the integration period;
- Shear viscosity η (eta)(Pa*s): Viscosity (shear stress / shear rate). Shear viscosity can be steady state or instantaneous. The steady state variable will always be available even in ramp modes. System sequences will have their graphs labelled to indicate whether the test was a steady state test or a ramp test;

- Shear modulus complex component G*(Pa): Oscillatory stress / oscillatory strain. This shows the measured sample's stiffness. The units are Pascal. Sometimes called G star;
- Shear modulus elastic component G'(Pa): G*cos phase angle. Also called the storage modulus, this shows the magnitude of the elastic component in the sample at the measured frequency. Called G prime;
- Shear modulus viscous component G"(Pa): G*sin phase angle. Also called the loss modulus, this shows the magnitude of the viscous component in the sample at the measured frequency. Called G double prime;
- Shear viscosity (complex component) η*(Pa*s): Complex modulus / frequency (rad/s). The complex viscosity can be related to the shear viscosity using the Cox-Mertz rule, where complex viscosity is analogous to shear viscosity, and angular frequency is related to shear rate. Works best for unfilled, linear polymers.

Collagen rheology

Collagen suspensions can be considered as a viscoelastic fluid (Wilkie, 2005) and so can be studied by rheology methods.

The increasing variety and availability of purified extra- and intracellular matrix proteins provides an unprecedented opportunity to quantify the mechanical properties of the cellular environment. Reconstituted biopolymer fibre networks can exhibit nonlinear rheology that is dramatically different than synthetic polymer gels (Djabourov et al., 1993).

Fibrin gel and articular cartilage, both of which have entangled fibrillar networks similar to collagen gel, have been studied in some detail (Allen et al., 1984; Barocas et al., 1995) and provide a valuable basis for our study.

Collagen gel behaviour results from the intrinsic properties of and interaction between two component phases: a network of collagen fibrils and interstitial solution, typically, tissue culture medium. The fibrils form a sparse (<1% volume) but highly entangled network (Allen et al., 1984) that effectively resists shear and extension but has little compressive strength. Resistance to the interstitial flow of the solution through the network, however, can lead to high solution pressures, which allow the gel to withstand compressive loads. Thus, when the gel is subjected to shear or tension, the physically crosslinked network supports virtually the entire load; under compression, however, the network transfers much of the load to the interstitial solution, the incompressibility of which prevents network collapse (Allen et al., 1984).

Aims

The main general aim of this project was to acquire the appropriate information on the model we want to get inspiration from, MCTs, and to understand how it natural actually works. The research work was developed according to the specific objectives to define the basic biology of natural MCTs, particularly the key-components and their fundamental interactions; this was achieved through morphological, biochemical, biomolecular and biomechanical characterizations of two established MCT models, peristomial membranes and compass depressor ligaments, and of two representative sea urchin species *P. lividus* and *S. purpuratus*.

The objectives of my PhD thesis were:

1) extraction and characterization of collagen;
2) histological and biochemical analysis of proteoglycans and glycosaminoglycans associated to collagen fibrils both in the intact tissues and in the extracted collagen;
3) biomolecular analysis of the glycoprotein tensilin, one of the principal molecule responsible for MCT properties;
4) test of the modulation properties of tensilin on the aggregation state of extracted collagen fibrils;
5) extraction with ion-exchange chromatography of all the possible active fractions and their characterization with rheological tests in order to recognize in some of them any mechanical activity.

This PhD thesis work is part of the extensive MIMESIS Project which is addressed to the innovative perspective of developing a new biomaterial, designed at the nanoscale, simulating some MCT analogous properties.

Since reproducing the complex natural structure of MCT is virtually impossible, a starting point can be manipulating simpler components in order to produce a composite with tuneable mechanical properties and whose biocompatibility was tested in cell colture studies.

This project has a wide potential impact and scientific/technical benefits in different scientific fields, including animal biology, engineering and biomedicine. The idea of a dynamic scaffold capable of adapting its stiffness/structural integrity according to the needs of a growing tissue is a radical concept which may chance the scenario of intelligent materials for Tissue Engineering.

Materials and methods

EXPERIMENTAL MODELS

Specimens of *P. lividus* were collected in the Ligurian Sea (Italy) at depth of 3-5 meters, thanks to the permission of the Marine Protected Areas of Portofino and Bergeggi. The animals were transported to Milano and maintained at 16°C in aerated 50 L aquaria with artificial sea water (Instant Ocean®, Aquarium System) and feed with "Invert Meal" at approximately weekly intervals. Periodically we collected 30-50 sea urchins in the Ligurian Sea and placed 8-10 animals in each aquarium. Water parameters such as temperature, density, pH, salt, ion and anion concentrations were constantly checked in order to guarantee optimal conditions throughout the experiments. Animals were exposed to 8 hours/day of light in order to reproduce as much possible natural conditions.

Specimens of *S. purpuratus* were collected along the Connecticut coast (USA) and then the dissected PM delivered to Milan in RNAlater solution.

ISOLATION OF CDL AND PM

CDLs were dissected from the sea urchin Aristotle's lantern as follow: the whole test is cut in two halves with scissors separating the oral part and the aboral one; working on the oral part the test CDLs are dissected from the compass and the perignathic girdle using micro-scissors and tweezers.

PMs were dissected from the oral half of the sea urchin: the test is reduced to produce an approximately round piece of test surrounding the perignathic girdle with the membrane inside, the PM is isolated by the perignathic girdle using micro-scissors; then, the external epidermis is carefully removed with a razor blade.

Throughout all of these operations the specimen was kept moist or was submerged in ASW at RT.

In order to compare CDL and PM characteristics in different functional states, animals were subjected to three different treatments. To obtain the 'compliant' condition, the lower half of an animal, which includes the lantern, PM and CDLs, was immersed in an anaesthetic solution of 0.1% propylene phenoxetol in seawater (PPSW) for 45 minutes; this treatment results in the protraction (lowering) of the lantern and slackening of the CDLs. To obtain the 'stiff' condition, half animals

were immersed in 1mM acetylcholine chloride in seawater (AChSW) for 15 minutes, which causes retraction (raising) of the lantern and stretching of the CDLs. Controls, which were in the 'standard' condition, were kept in ASW for 45 minutes (PPSW control) and 15 minutes (AChSW control).

COLLAGEN EXTRACTION

Insoluble collagen extraction was performed according to the protocol of Matsumura (1974) on CDLs and PM of *P. lividus* and on the PM of *S. purpuratus*. The disaggregation was carried at 4°C. The tissue was suspended in a solid/solvent 1:20 (w/v) 0.5 M NaCl, 0.05 M EDTA-Na, 0.1 M Tris-HCl buffer (pH 8.0) and 0.2 M β-mercaptoethanol solution. The suspension was stirred for 2 days at 4°C and then filtered through Nylon gauze. The filtered material containing fibrous components was centrifuged two times at 10000g 1h and the supernatant was discarded. The pellet was dialysed against 0.5 M EDTA-Na solution (pH 8.0) and successively against distilled water. The collagen solution was stored at -20°C and then used for the preparation of collagen biofilm.

Soluble collagen extraction was performed according to the protocol of Burke et al. (1989). The initial samples were both insoluble collagen and fresh tissue. The sample is washed with 0.5 M acetic acid solution and then stirred in a solid/solvent 1:20 (w/v) 0.5 M acetic acid + 1mg/ml pepsin solution for 48h at 4°C. After a centrifuge 17000g 1h 4°C the supernatant is saved. The precipitation of soluble collagen is obtained mixing the supernatant with NaCl to reach a final concentration of 4 M NaCl. The sample is stirred for 24h at 4°C and centrifuged 17000g 1h 4°C. The transparent gel obtained is saved. It was use immediately or stored at 4°C with 0.5 M acetic acid for maximum 1 week.

COLLAGEN QUANTIFICATION

Insoluble collagen quantification was performed on the insoluble collagen dialysed against distilled water weighting the pellet after a centrifuge 10000g 1h.

Soluble collagen quantification was performed according to the protocol of Taşkiran et al. (1999). Sirius red F3BA, a strong anionic dye, stains collagen by reacting, via its sulphonic acid groups, with basic groups present in the collagen molecule. The samples were both insoluble collagen and fresh tissue. The sample was lyophilized and added to a solution of 1mg/ml pepsin in 0.5 M acetic acid for 48h at 4°C. Undigested material was removed by centrifugation at 17000g 1h 4°C. The supernatant was diluted with 1.8 ml of 0.5 mM Sirius red in 0.5 M acetic acid and incubated at room temperature for 20 minutes. The samples were centrifuged at 2500g for 10

minutes and supernatant absorbance was read at 528 nm against 0.5 M acetic acid as blank. The assay was calibrated using type I collagen purified from rat tail (Sigma). The method sensitivity was found to be in the range of 5 to 40 mg/ml of collagen.

COLLAGEN NEGATIVE STAIN

The intact PMs and CDLs were fixed overnight at RT in 2% glutaraldehyde in 0,1M cacodylate buffer over night at 4°C. Samples were treated with 1% osmic acid in 0.1% cacodylate buffer for 2h and then washed twice in distilled water. After fixation, samples were treated with uranyl acetate solution in 25% ethanol for 2h, dehydrated in a graded ethanol series and embedded in an Epon-Araldite resin. Sections (70-100 nm) were cut with an LKB Ultrotome V using a diamond knife, stained with aqueous 2% uranyl acetate in distilled water.

For negative staining of the extracted fibrils, a 5 µl drop of insoluble or soluble isolated collagen was applied to a 200 mesh Formvar-coated grid and allowed to remain for 1 minutes, after which it was removed of the grid with a piece of filter paper and replaced with a 10 µl drop of 0.5% potassium phosphotungstate (PTA) at pH 7.3. After 1 minutes the bulk of the stain was removed and the grid was allowed to dry in air before inserting it into the microscope column.

Samples were observed in a JEOL 100SX TEM. Measurements of the lengths of negatively stained fibrils were made directly from electron micrographs**.**

COLLAGEN BIOINFORMATIC ANALYSIS

P. lividus collagen gene was analysed in GenBank database on www.ncbi.nlm.nih.gov internet website. BLASTn and BLASTp (Basic Local Alignment Search Tool for nucleotide and protein) algorithms were used to make comparisons.

COLLAGEN CHARACTERIZATION: SDS-PAGE AND WESTERN BLOT ANALYSIS

Intact PMs and CDLs were treated with PPSW, AChSW, ASW 15 minutes and ASW 45 minutes to produce samples in different mechanical states and in particular respectively in compliant, stiffen, control stiffen and control compliant states. The insoluble collagen was isolated according to the protocol of Matsumura (1974) and then solubilized according to Burke et al. (1989). The transparent gel obtained was assessed by SDS-PAGE by the Laemmli (1970) system with a 10% precast gel (Bio-Rad). Samples were diluted prior to electrophoresis using sample

buffer and then were boiled at 100°C for 5 minutes. Gels were run at 150V 1h at RT (Fisher et al., 1983). On completion of electrophoresis, gels were fixed and stained with Coomassie Blue R-250. The gel was then transferred to destaining solution and subsequently photographed.

After the SDS-PAGE the proteins were transferred to a PVDF membrane previously washed with water and transfer buffer. The blotted PVDF membrane was blocked in freshly prepared 5% non-fat dry milk at RT 1h with constant agitation. The PVDF was incubated with 1:125 dilution of Monoclonal Anti-Collagen Type I antibody produced in mouse (Sigma C 2456) or Monoclonal Anti-Collagen Type III antibody produced in mouse (Sigma C 7805), diluted in freshly prepared 5% non-fat dry milk overnight with agitation at 4°C. After 3 washes in TBST, the PVDF was incubated in the secondary antibody anti-Mouse IgG HRP produced in rabbit (Sigma A 9044; 1:10000 dilution) in 5% non-fat dry at RT 1h with constant agitation. Type I collagen purified from rat tail tendon (Sigma C 3867) and collagen III protein (abcam ab 7535) were used as standards. For the protein detection in Western blot was used the ECL™ Western Blotting Detection Kit (GE Healthcare) and to visualize labeled protein were used Autoradiography (X-ray) films (Ultracruz sc-201696).

COLLAGEN FT-IR ANALYSIS

Insoluble and soluble collagen isolated from the *P. lividus* PM and bovine ultrapure collagen (Sigma C 4243) were analysed by FT-IR using a Perkin Elmer 2000 spectrometer. The specimens were analysed with attenuated total reflectance (ATR-FTIR) using the SplitPea™ accessory (Harrick Scientific), provided with a silicon internal reflection element and configured for external reflectance mode, where the spectra were acquired from a 200 μm diameter sampling area. At least five different areas from each sample were analysed. All samples were run at a spectral resolution of $4cm^{-1}$ and two hundred scans were accumulated in order to obtain a high signal-to-noise level. A nitrogen purge of the sample compartment was performed to minimize artefacts that could arise from residual air bands (CO_2 and H_2O vapours). All spectra were automatically smoothed, and normalized using Spectrum software, version 5.3.

CELLS AND PGS/GAGS HISTOLOGY

Intact PMs and CDLs were treated with 4 M Guanidine chloride in 0.05 M sodium acetate (pH 5.8) or 0.1 M NaOH to remove PGs. Samples were continuously stirred in one of these two solutions at 4°C for 24 h. After a centrifuge at 17000g for 1h at 4°C the tissue was recollected.

Other intact PMs and CDLs were treated with PPSW, AChSW, ASW 15 minutes and ASW 45 minutes to produce samples in different mechanical states and in particular respectively in compliant, stiffen, control stiffen and control compliant states.

Moreover, insoluble collagen isolated from the PM was treated with 4 M Guanidine chloride in 0.05 M sodium acetate (pH 5.8) or 0.1 M NaOH to remove PGs. Samples were continuously stirred in one of these two solutions at 4°C for 24 h. After a centrifuge at 17000g for 1h at 4°C the pellet was collected.

Milligan's Trichrome and Alcian blue

Intact PMs and CDLs treated with purifying solutions or with solutions to induce the different mechanical states were then fixed with 4% paraformaldehyde in PBS, dehydrated in an ethanol series, cleared in xylene and embedded in paraffin wax. Sections 10 µm thick were cut in Reichert Jung microtome, deparaffinized with xylene and hydrated to distilled water.

Cells were identified by their location in sectioned tissues by their staining characteristics in Milligan's Trichrome-stained sections. Milligan's Trichrome staining (Milligan, 1946) was conducted as follows. After treatment with 100% xylene to remove the paraffin, sections stained light pink or were rinsed successively in 100 % and 95 % ethanol, allowed to mordant in potassium dichromate-HCl for 2 minutes, and stained with acid fuchsin for l minute. The stain was fixed in phosphomolybdic acid for 3 minutes. Subsequently, acid fuchsin-stained slides were counterstained with orange G for 5 minutes, with fast green for 10-15 minutes and washed with 1 % acetic acid for 3 minutes. Finally, the stained sections were dehydrated in 95 % and 100 % ethanol. Milligan's Trichrome stains cells in dark red and collagen in green.

PGs were identified by Alcian blue 8GX-stained sections (Sigma-Aldrich 05500). The sectioned PMs treated with purifying solutions or with solutions to induce the different mechanical states were stained with Alcian blue staining solutions prepared at 3 different pH 0.2, 3.1 and 5.6 (Sheehan and Hrapchak, 1980) to characterize PGs presence/removal using different purifying solutions or in the different mechanical states. The Alcian blue staining protocol is similar to the Milligan's Trichrome one replacing all the staining steps with the single step Alcian blue staining solution.

Samples were mounted in Eukitt®. Stained sections were observed under the Jenaval light microscope.

Cuprolinic blue

The intact PMs and CDLs were fixed overnight at RT in 0.1% Cuprolinic blue solution containing 2.5% glutaraldehyde in 0.025 M sodium acetate and 0.3M $MgCl_2$ (pH 5.6). Samples were washed twice in 0.025 M sodium acetate and 0.3M $MgCl_2$ (pH 5.6) followed by a wash in distilled water. After fixation, samples were washed in ethanol 25%, and in 0.5% sodium tungstate in ethanol 50%, dehydrated in a graded ethanol series and embedded in an Epon-Araldite resin. Sections (70-100 nm) were cut with an LKB Ultrotome V using a diamond knife, stained with aqueous 2% uranyl acetate in distilled water, and observed in a JEOL 100SX TEM. Tissues in ASW were used as a control.

The isolated and treated collagen samples were applied to 200 mesh Formvar-coated grid. The fibrils were stained with Cuprolinic blue by exposing them sequentially to the following solutions for the indicated times and number of changes (Trotter and Koob, 1989): 500 mM NaC1 (60 s x 1), fixative (60 s x 1), Cuprolinic blue (60 s x 1), fixative (30 s x 2), tungstate (60 s x 1), water (30 s x 2), 1% uranyl acetate (60 s x 1), and water (30 s x 2). The isolated and untreated fibrils were used as a control. The grids were then observed in a JEOL 100SX TEM.

TEM micrographs were acquired and measurements of the collagen D-periods were obtained in each micrograph, using the program ImageJ 1.41o.

PGs/GAGs QUANTIFICATION: ALCIAN BLUE STAIN

The isolation and quantification of PGs/GAGs was performed according to the protocol of Vogel and Peters (2001). Intact PMs and CDLs were isolated from the animals, treated with PPSW for 45 minutes, AChSW for 15 minutes and ASW for 45 and 15 minutes, and immediately frozen with liquid nitrogen. Moreover, previously isolated insoluble collagen and treated insoluble collagen with 4 M Guanidine chloride in 0.05 M sodium acetate (pH 5.8) or 0.1 M NaOH were analysed. PGs/GAGs were extracted using 4 M Guanidine chloride in 0.05 M sodium acetate (pH 5.8) solution for 15 minutes from intact tissues and isolated collagen samples. The supernatants were mixed with Alcian blue solutions prepared at three different pH 0.2, 1.4 and 5.6. PGs/GAGs were collected by centrifugation at 4°C 17000g 15 minutes. Excess stain in the pellet is removed by washing in DMSO solution. The PGs/GAGs-Alcian blue complexes are dissolved and dissociated in a 4 M Guanidine chloride/propanol mixture and are then recovered by centrifugation. The amount of PGs/GAGs is directly proportional to the Alcian blue concentration measured as absorbance at 605 nm.

The tube/absorbance assay has a measuring range of 1-20 μg of GAG (Vogel and Peters, 2001). The calibration curve was prepared with chondroitin-6-sulfate (CSC) from 0.0125 to 0.4 mg/ml.

Statistical analysis

Since the data were not normally distributed (D'Agostino and Pearson test), the Mann–Whitney U test was used to compare the amount of PGs/GAGs of PM and CDL in the three different mechanical states at the same pH of the Alcian blue solution and in the three different pH of the Alcian blue solution at the same mechanical state. Results were considered statistically significant when $p<0.05$. Means are given ± standard deviation. Statistical differences among the treatments were determined using Kruskal-Wallis one-way analysis of variance (ANOVA) with Dunn's post-hoc test (Zani, 1994). All statistics were performed using GraphPad Prism 4 software.

PGs/GAGs CHARACTERIZATION: SDS-PAGE AND WESTERN BLOT ANALYSIS

PMs and CDLs were isolated from the animals, treated with ASW for 45 and 15 minutes, PPSW for 45 minutes and AChSW for 15 minutes. The tissues were immediately frozen with liquid nitrogen and the PGs/GAGs were then extracted in 4 M Guanidine chloride in 0.05 M sodium acetate (pH 5.8) for 15 minutes. Following centrifugation at 3440g 10 minutes, the supernatant was exchanged by dialysis into 7 M urea and 0.1 M NaCl. The dialysed extract was lyophilized, precipitated in ethanol (solid/solvent 1:8) to prepare samples for gel electrophoresis. After a centrifugation 1000g 10 minutes the pellet was solubilized in 25 μl of gel sample buffer and heat to 100°C for 5 minutes in a heat bath. The samples were analysed by SDS-PAGE using gels containing a linear gradient of 4-20% acrylamide run at 150V for approximately 1h at RT (Fisher et al., 1983). Gels were stained with Coomassie Blue R-250 to visualize protein bands and with Alcian blue to visualize sulfated GAGs and PGs (Trotter and Koob 1989). The gel was then transferred to destaining solution and subsequently photographed.

After the SDS-PAGE the proteins were transferred to a PVDF membrane previously washed with water and transfer buffer. The blotted PVDF membrane was blocked in freshly prepared 5% non-fat dry milk for at RT 1h with constant agitation. The PVDF was incubated with 1:250/500 dilution of Versican (H-56) rabbit polyclonal antibody (Santacruz sc-25831) or Heparan sulfate proteoglycan rat monoclonal antibody (abcam A 7L6), diluted in freshly prepared 5% non-fat dry milk overnight with agitation at 4°C. After 3 washes in TBST, the PVDF was incubated in the secondary antibody anti-rabbit and anti-rat IgG HRP (1:10000 dilution) in 5% non-fat dry milk for

at RT 1h with agitation. Type I collagen purified from rat tail tendon (Sigma C 3867) and CSC (Sigma) were used as a standard. For the protein detection in Western blot was used the ECL™ Western Blotting Detection Kit (GE Healthcare) and to visualize labelled protein were used Autoradiography (X-ray) films (Ultracruz sc-201696).

FIBRILLIN BIOINFORMATIC ANALYSIS

Fibrillin gene was analysed in GenBank database on www.ncbi.nlm.nih.gov internet website. BLASTn and BLASTp (Basic Local Alignment Search Tool for nucleotide and protein) algorithms were used to make comparisons.

FIBRILLIN EXTRACTION

The extraction of fibrillin was performed modifying the protocol by Thurmond et al. (1997). Dissected CDLs and PMs were suspended and gently agitated at 4°C for 24 h in a solid/solvent 1:10 (w/v) 6 M Guanidine chloride in 0.05 M sodium acetate (pH 5.8) and 10 mM NEM. After a centrifugation 16000g 30 minutes 4°C the supernatant 1 was decanted at 4°C whereas the pellet 1 was extracted for another 24 h in fresh extracting solution under the same conditions. After a centrifugation 16000g 30 minutes 4°C the supernatant 2 was decanted at 4°C whereas the pellet 2 was resuspended in the same volume of collagenase buffer: 200 mM NaCl, 50 mM Tris-HCl, 10 mM $CaCl_2$, 3.1 mM NaN_3, pH 7.4, six changes of collagenase buffer were used. Protease inhibitors were added to the last change of collagenase buffer to give 1 mM PMSF and 1 mM NEM. Collagenase Type I (GIBCO™) was added to the solution at a concentration of 150 units of collagenase activity per gram of starting material. The tissue was exposed to collagenase for 24 h at 37°C. After a centrifugation 16000g 30 minutes 4°C the supernatant 3 was decanted at 4°C whereas the pellet 3 was again digested with collagenase for 24 h at 37°C. After a centrifugation 16000g 30 minutes 4°C the supernatant 4 was decanted at 4°C whereas the pellet 4 was extracted for 24 h at 4°C in four changes of 6 M Guanidine chloride extraction buffer (described above) containing 1 mM NEM. All the supernatants were dialysed against MilliQ water.

FIBRILLIN CHARACTERIZATION: SDS-PAGE

The lyophilized fibrillin was assessed by SDS-PAGE by the Laemmli (1970) system with a 10% precast gel (Bio-Rad). Samples were diluted prior to electrophoresis using sample buffer and

then boiled at 100°C for 5 minutes. Gels were run at 150V 1h at RT (Fisher et al., 1983). On completion of electrophoresis, gels were fixed and stained with Coomassie Blue R-250 for 1 h. The gel was then transferred to destaining solution and subsequently photographed.

TENSILIN BIOINFORMATIC ANALYSIS AND BIOMOLECULAR CHARACTERIZATION

Tensilin was analysed in GenBank database on www.ncbi.nlm.nih.gov internet website. BLASTn and BLASTp (Basic Local Alignment Search Tool for nucleotide and protein) algorithms were used to make comparisons.

S. purpuratus tensilin cDNA were isolated from the PM by means of RT-PCR using gene-specific primers designed on the sequence (acc. number: XM775549.2) available in the GenBank database (Sp_F, Sp_R; see Table 2). *P. lividus* tensilin cDNA was amplified from the PM using primers (P liv ESON F1, P liv ESON F2, P liv ESON F3, P liv ESON R1, P liv ESON R2, P liv ESON R3; see Table 2) based on the EST clone available in the GenBank database (acc. number: AM565277.1). The RNA extraction step was performed with RNeasy Fibrous Tissue Mini Kit (Qiagen), the gel extraction step was performed with QIAquick Gel Extraction Kit (Qiagen), the reverse transcription step was performed with AMV Reverse Transcriptase (Promega), the cloning step was performed with TOPO TA Cloning® (Invitrogen) and the plasmid extraction was performed with QIAprep Spin Miniprep Kit (Qiagen). The PCR reagents were purchased from GeneSpin, DNA Oligos primers were purchased from Invitrogen and the sequencing step was assign to Primm srl Milano.

PRIMER	DIRECTION SEQUENCE
Sp_F	forward 5' - CACATC TACTCAGCACCATG
Sp_R	reverse 5' - CGTTGGTCGTGTGTGCTAAT
S purp 5'AP	forward 5' –ATATCTCGAGCGGCCGCTAGCTAATACGACTCACTATAGGGAGACC ACAACGGTTTCCCTCTAGAAATAATTTTG TTTAACTTTAAGAAGGAGAGCCACC
S purp 3'AP	reverse 5' – AAATATTCAATAACAAAAAAATGTATCTTTACATTTAGGTTTATTTAA ATACCCGCACCAATTAGTGGTGATGGTGATGATG
P liv ESON F1	forward 5' - CAGTTATGAAGGTGAAAATCAC
P liv ESON F2	forward 5' - GGACGCTGACAACGAGGCA
P liv ESON F3	forward 5' - GTCCATGCAAAAAGCAGTTTTG
P liv ESON R1	reverse 5' - TTACCTCCTATCACATAAGTATC
P liv ESON R2	reverse 5' - GGTGTAGGGATGGAGCAGG
P liv ESON R3	reverse 5' - CTAGGTGAGTAGAAGAAGATGT

Table 2. Primers used in amplification and sequencing of tensilin full-length from *S. purpuratus* and *P. lividus*. Sp_F and Sp_R, forward and reverse primers to amplify *S. purpuratus* full-length tensilin; S purp 5' AP and S purp 3' AP, forward and reverse adapter primers for the *in vitro* translation; P liv ESON F1 and P liv ESON R1, first set of forward and reverse primers to amplify *P. lividus* full-length tensilin; P liv ESON F2, P liv ESON F3,

P liv ESON R2 and P liv ESON R3, second set of forward and reverse primers to amplify *P. lividus* full-length tensilin.

PROTEIN PRODUCTION

A second round of amplification on *S. purpuratus* sample was performed using an aliquot of the first reaction with two adapter primers (S purp 5'AP, S purp 3'AP; see Table 2) in order to include in the amplicon the 5' and 3' sequences necessary for the following *in vitro* translation. The cDNA was gel-purified and *in vitro* translated using the EasyXpress Insect Kit II (Qiagen) for *in vitro* synthesis of proteins with post-translational modifications using insect-cell lysates, according to the manufacturer's specifications. The proteins were purified with Ni-NTA Magnetic Agarose Beads (Qiagen), for high-throughput, micro-scale purification of 6xHis-tagged protein.

Proteins were quantified with the colorimetric and spectrophotometric BCA Assay (Pierce) and then used for the fibril aggregation assay.

COLLAGEN FIBRILS AGGREGATION ASSAY

Aggregation assays were carried out as previously described by Trotter et al. (1996), Koob et al. (1999) and Tamori et al. (2006).

Pre-Aggregation Assays without protein were performed to test collagen self-aggregation with different collagen quantities, different medium solutions, different temperature degree, and different stirring speeds.

The final buffer solution chosen is EGTA-ASW (0.5 M NaCl, 0.05 M $MgCl_2$, 7.2 mM EGTA, 0.01 M KCl and 0.01 M Mops, pH 8.0). The elution buffer is the buffer inside which the protein is diluted in the final step of the production protocol (50 mM NaH_2PO_4, 300 mM NaCl, 250 mM imidazole, 0.05% Tween 20, pH 8.0). The elution buffer was analysed as sample to eliminate the possibility that this buffer can represent an artefact.

I decided to perform the fibril aggregation test both with *P. lividus* and *S. purpuratus* collagen using only *S. purpuratus* tensilin protein to verify the species-specificity of the protein itself. *P. lividus* and *S. purpuratus* collagen was extracted according to the protocol of Matsumura (1974).

The aggregation activity was monitored in the 1^{st}, 2^{nd} and 4^{th} tests with the stereomicroscope, whereas in the 3^{rd} test with the light microscope.

The experimental plan of the aggregation assays is summarized as follow:

- Test 1: - EGTA-ASW 910 µl + 90 µl *P. lividus* collagen; - EGTA-ASW 885 µl + 90 µl *P. lividus* collagen + 25 µl tensilin; - EGTA-ASW 910 µl + 90 µl *S. purpuratus* collagen; - EGTA-ASW 885 µl + 90 µl *S. purpuratus* collagen +25 µl tensilin; V_f = 1 mL, $C_{f\ collagen}$ = 0.09 mg/ml, stirring at 100 rpm 2 h RT;
- Test 2: - EGTA-ASW 410 µl + 90 µl *P. lividus* or *S. purpuratus* collagen; - EGTA-ASW 385 µl + 90 µl *P. lividus* or *S. purpuratus* collagen + 25 µl Elution buffer (dialysed); - EGTA-ASW 385 µl + 90 µl *P. lividus* or *S. purpuratus* collagen + 25 µl tensilin; V_f = 0.5 ml, $C_{f\ collagen}$ = 0.18 mg/ml, stirring at 100 rpm 2 h RT;
- Test 3: - EGTA-ASW 135 µl + 90 µl *P. lividus* or *S. purpuratus* collagen; - EGTA-ASW 135 µl + 90 µl *P. lividus* or *S. purpuratus* collagen + 25 µl Elution buffer (dialysed); - EGTA-ASW 135 µl + 90 µl *P. lividus* or *S. purpuratus* collagen + 25 µl tensilin; V_f = 250 µl, $C_{f\ collagen}$ = 0.36 mg/ml, no stirring, monitoring with TimeLapse 2h;
- Test 4: - 250 µl *S. purpuratus* collagen; - 250 µl *P. lividus* collagen; - 250 µl *S. purpuratus* collagen + 25 µl Elution buffer (dialysed); - 250 µl *P. lividus* collagen + 25 µl Elution buffer (dialysed); - 250 µl *S. purpuratus* collagen + 20 µl tensilin (3 productions concentrated in 20 µl); - 250 µl *P. lividus* collagen + 20 µl tensilin (3 productions concentrated in 20 µl); V_f = 275 µl, $C_{f\ collagen}$ = 0.36 mg/ml, stirring at 50 rpm 2 h RT.

FRACTIONS EXTRACTION AND CHARACTERIZATION: CHROMATOGRAPHY

The fraction extraction protocol was inspired to Tipper et al. (2003). Ten frozen *P. lividus* PMs (total weight about 0.5g) were minced into pieces (1 mm^3) and suspended in 1.67 ml of chilled 20 mM Tris-HCl, pH 7.8, 0.8 M NaCl, 5 mM benzamidine HCl, 10 mM NEM, 1 mM PMSF, 2 mM EDTA solution. The tissues suspended were frozen at -80°C and thawed at 15°C five times to effect complete cell lysis. The freeze/thaw suspension was adjusted to ten volumes/g tissue (wet wt., 5 ml) by the addition of the first chilled solution with enzyme inhibitors and stirred overnight at 4°C. The suspension was centrifuged at 20000*g* for 30 minutes at 4°C. The resulting supernatant was applied to a 1 ml HiTrapQ HP (GE Healthcare 17-1153-01) in a BioLogic DuoFlow System (Bio-Rad) and washed and eluted with 25 ml of 3.0 M NaCl in 20 mM Tris-HCl, pH 8.0. Both stiffening and plasticizing activities were found exclusively in the unbound fractions (Tipper et al., 2003). The unbound fraction was dialysed against an appropriate volume of 20 mM Tris-HCl, pH 7.8, at 4°C to adjust the final concentration of NaCl to 0.05 M. It was applied to a second HiTrapQ column equilibrated in 20 mM Tris-HCl, pH 7.8, 0.05 M NaCl. This column was eluted with a linear gradient of 0.05-1 M NaCl in 20 mM Tris-HCl, pH 7.8.

The quantification of each single fraction was performed with the DC Protein Assay (Bio-Rad) that is a colorimetric assay for protein concentration following detergent solubilisation.

SDS-PAGE with silver staining technique was performed because provides a very sensitive tool for protein visualization with a detection level down to the 0.3-10 ng level (Switzer at al., 1979; Rabilloud, 1999). The SDS-PAGE gel used were CriterionXT^{TM} Precast Gel 3-8% (Bio-Rad). After electrophoresis, the gel was placed into the fixing solution for 2h (50% ethanol or methanol, 12% acetic acid, 0.05% formalin). After washes with 20% ethanol the gel was incubated for 2 minutes with gentle rotation into the sensitizing solution (0.02% (w/v) sodium thiosulfate (Na_2S2O_3)). After washes the cold silver staining solution (0.2% (w/v) silver nitrate ($AgNO_3$), 0.076% formalin) was added and shaken for 20 minutes to allow the silver ions to bind to proteins. After washes the gel was shortly rinsed with the developing solution (6% (w/v) sodium carbonate (Na_2CO_3), 0.0004% (w/v) sodium thiosulfate ($Na_2S_2O_3$), 0.05% formalin) for 2 - 5 minutes. The reaction was stopped adding the terminating solution (12% acetic acid). The gel was then photographed.

FRACTIONS ANALYSIS: RHEOMETER TESTS

The Rheometer Kinexus Malvern (see Fig. 11) with geometry cone plate (CP 0.5/40 SR0432 SS) and solvent trap (55mm C0127 SS) was used to analyse the rheological properties of the insoluble and soluble collagen isolated from the *P. lividus* PM and bovine ultrapure collagen (Sigma C 4243) and samples made mixing all the collagens with all the chromatographic fractions. A mix of collagen and only protein buffer (from 0 M to 1 M NaCl 20 mM Tris-HCl, pH 7.8) was used as a control. All the tests were performed at 25°C and 37°C.

The following viscometry tests were performed: (1) Table of shear rates log (Start shear rate 0.1 s^{-1}, End shear rate 100 s^{-1}); (2) Shear rate ramp log isothermal (Start shear rate 0.1 s^{-1}, End shear rate 10 s^{-1}, Ramp time 2 minutes); (3) Shear stress ramp with yield stress analysis (Start shear stress 0.10 Pa, End shear stress 100.00 Pa, Ramp time 1 minute).

The following oscillation test was performed: Amplitude sweep stress controlled with LVER determination for low viscosity materials (Start shear stress 0.10 Pa, End shear stress 10.00 Pa, Frequency 1.00 Hz).

Results

COLLAGEN EXTRACTION

The extraction of the insoluble collagen from PM and CDLs of the sea urchin *P. lividus* and PM of *S. purpuratus* was performed according to the protocol of Matsumura (1974). Collagen fibrils were isolated from the tissues and examined in the transmission electron microscope after negative staining with PTA. TEM analysis of extracted collagen fibrils demonstrated the effectiveness of the collagen extraction protocol on the analysed mutable tissues of *P. lividus* and *S. purpuratus*. In Fig. 12 are represented isolated fibrils from *P. lividus* CDL, in Fig. 13 are represented isolated fibrils from *P. lividus* PM.

Effective isolation required the presence of all three active reagents in the disaggregating solution: NaC1, EDTA, and β-mercaptoethanol. Omission of any one made it impossible to isolate single intact fibrils. This observation is in agreement with previous studies on other echinoderms: Matsumura (1973, 1974) and coworkers (1973) first showed that whole collagen fibrils can be isolated from sea cucumber *Stichopus japonicus* and starfish *Asterias amurensis* by exposure of tissues to a disaggregating solution containing 0.5 M NaCl, 0.2 M β-mercaptoethanol, 0.05 M EDTA, 0.1 M Tris-HCl, pH 8.0. Matsumura's method was used subsequently to isolate fibrils from sea urchin *Eucidaris tribuloides* ligaments (Trotter and Koob, 1989). We tested two different disaggregating solutions, which included 0.1 M or 0.2 M β-mercaptoethanol. We found that, although tissues began to disaggregate in 0.1 M β-mercaptoethanol, much more collagen could be extracted in 0.2 M β-mercaptoethanol.

The extraction of the soluble collagen was also successfully performed from the PM and CDLs of the sea urchin *P. lividus* according to the protocol of Burke et al. (1989). Soluble collagen was isolated from the tissues and examined to TEM after negative staining with PTA. TEM analysis of extracted collagen demonstrated the effectiveness of the soluble collagen extraction protocol on the analysed mutable tissues of *P. lividus* (data not shown).

COLLAGEN QUANTIFICATION

The results here showed referred only to *P. lividus* PM because, even if TEM and SDS-PAGE analysis confirm the effectiveness of the extraction protocol form CDL, the weight

measurements and Sirius red quantification on CDL are not quantitative significant due to the little amount of starting material.

Considering that *P. lividus* PM is about 60 mg wet weight, the different components are represented as below: 50% water, 25% calcareous material, 10% insoluble collagen and 2% soluble one.

From our experiments and relative weight measurements, it results that the disaggregating solution can extract from one PM about 10-15 mg insoluble collagen.

Whereas for the soluble collagen quantification, we used the Sirius red assay that is a reliable, easy and inexpensive method requiring low cost reagents and equipment and might be used for quantification of the total collagen content in tissues as an alternative to other more expensive methods (e.g. hydroxyproline test: Bergman and Loxley, 1963). Sirius red F3BA, a strong anionic dye, stains collagen by reacting, via its sulphonic acid groups, with basic groups present in the collagen molecule. Acetic acid solution with pepsin can extract from one PM 0.2-1 mg soluble collagen, which is comparable with literature data concerning collagen quantification by different methods (e.g. hydroxyproline test: Bergman and Loxley, 1963).

COLLAGEN NEGATIVE STAIN

The thin sections of embedded *P. lividus* CDL and PM and isolated insoluble collagen fibrils from *P. lividus* CDL and PM were stained with PTA and then observed to TEM (see Figs. 12, 13, 14).

Measurements of the diameters of collagen fibrils in thin sections yielded the following results: for CDLs the diameter range was 20-150 nm (n = 250); for PM the diameter range was 30-380 nm (n = 250).

Measurements of the D-period of collagen fibrils in thin sections yielded the following results: for CDLs treated in ASW the D-period range was 58-63 (mean ± SD 60.76±2.22; n= 50); for intact PM treated in ASW the D-period range was 59-63 nm (mean ± SD 61.33±2.63; n = 30).

For isolated collagen from *P. lividus* PM the D-period range was found to be different from the previous information and it was 62-66 nm (mean ± SD 64.0±2.8; n = 52).

All these values are comparable to those found in the literature for echinoderms (Matsumura, 1973, 1974; Matsumura et al., 1973; Trotter and Koob, 1989).

COLLAGEN BIOINFORMATIC ANALYSIS

The comparison of nucleotide or protein sequences from the same or different organisms is a very powerful tool in molecular biology. By finding similarities between sequences, scientists can infer the function of newly sequenced genes, predict new members of gene families, and explore evolutionary relationships. For this reasons, I used the BLASTp and BLASTn tools on http://blast.ncbi.nlm.nih.gov/ website to analyse the known sequences of the *P. lividus* and *S. purpuratus* collagen proteins and nucleotides making comparisons with all the know sequences present in the databases. In particular, focusing the attention on the similarities with the human species it seems that the major homology is with the alpha 2 chain of the type I collagen (see Table 3).

Homo sapiens **collagen**	***Paracentrotus lividus*** **collagen**	***Strongylocentrotus purpuratus*** **collagen**
Type I alpha 2	Max score=345 Query coverage=100%	Max score=446 Query coverage=97%
Type XXIV alpha 1	Max score=303 Query coverage=99%	Max score=434 Query coverage=97%
Type V alpha 3	Max score=249 Query coverage=100%	Max score=366 Query coverage=97%
Type III alpha I	Max score=208 Query coverage=96%	Max score=235 Query coverage=97%
Type II alpha I	Max score=203 Query coverage=69%	Max score=226 Query coverage=59%

Table 3. Results of the BLASTp tool for the comparison of *P. lividus* and *S. purpuratus* collagen protein sequences with all the human proteins. Max score is a score that indicates how well the sequence matches; the query coverage tells how long piece of *P. lividus* and *S. purpuratus* sequences are covered by the human found.

COLLAGEN CHARACTERIZATION: SDS-PAGE AND WESTERN BLOT ANALYSIS

SDS-PAGE analysis of the *P. lividus* PM and CDL collagen is presented in see Fig. 15. Both samples are characterized by the presence of species of apparent molecular masses 140 and 116 kDa (lane 2, 3) while the rat tail tendon preparation contained the expected species at 126 and 123 kDa (lane 4). Both preparations were also characterized by the variable presence of additional species of 55 and 53 kDa. These latter species were found to be contaminants derived from the pepsin used in the purification protocol. Furthermore, bands at about 250 kDa are present and are related to the formation of collagen β sheets.

The relative staining intensities of the 116 and 140 kDa species were determined by eye but densitometric gel analyses in literature suggested that the 116 and 140 kDa species are present in a

2:1 molar ratio and organized in a $(116)_2$ $(140)_1$ configuration similar to the α_1 and α_2 chains of type I rat tail tendon collagen (Robinson, 1997).

SDS-PAGE analysis of the *P. lividus* PM and CDL collagen isolated from tissues previously treated to induce the different mechanical states is presented in see Fig. 16. All the samples are characterized by the presence of species of apparent molecular masses 140 and 116 kDa (lane 2, 3) independently from the mechanical state.

Western blot analysis of the *P. lividus* PM and CDL collagen is presented in Fig. 17. *P. lividus* PM and CDL collagens were blotted with Monoclonal Anti-Collagen Type I antibody or with Monoclonal Anti-Collagen Type III antibody, using Type I collagen purified from rat tail tendon and collagen III protein as standards. Blotting samples with Anti-Collagen Type I antibody results that both PM and CDL and rat tail collagens were recognised by the antibody. On the contrary, blotting samples with Anti-Collagen Type III antibody, it results that only the collagen III of control was recognised by the antibody. The Anti-Collagen Type III antibody did not recognise neither PM collagen nor the CDL one.

COLLAGEN FT-IR ANALYSIS

These results arise from the collaboration and technical support of our colleagues at INEB.

Insoluble and soluble *P. lividus* collagens isolated from the PM and bovine ultrapure collagen were analysed by FT-IR using a Perkin Elmer 2000 spectrometer (see Fig. 18) and the picks were measured using the software Spectrum version 5.3.

A comprehensive assignment of the major bands was derived from literature (Petibois et al., 2006). The main bands of collagens arose from the peptide bond vibrations: the heights of the peaks of amide I (1640 cm^{-1}, C=O stretch), amide II (1550cm^{-1}, C-N stretch and N-H in-plane bend) 1450 cm^{-1} (CH bending) and the one between 3100 cm^{-1}-3600 cm^{-1} (OH and NH) of CDLs and collagen spectra.

All the types of collagen exhibited absorptions at 1033, 1059, and 1083 cm^{-1}, which arise from the C–OH stretching vibrations of the carbohydrate moieties attached to the protein. Absorption features at 1451, 1399, 1339, 1282, 1236, and 1203 cm^{-1} are attributed to CH_2 and CH_3 wagging and deformation, and C–N stretching of collagen. Amides I and II absorptions were revealed at 1658 and 1555 cm^{-1} and the shoulder appearing at 1637 cm^{-1} could be attributed to the triple helix absorption of collagens. All the types of collagen exhibited very similar absorptions although one could notice that type I bovine ultrapure collagen presented higher intensities for the spectra.

FT-IR spectra of isolated collagen from PM exhibited bands assignable to collagen, since the striking resemblance between the spectra was immediately apparent. The characteristic absorbance bands of PM were amide I (1640 cm^{-1}), amide II (1550 cm^{-1}) and amide III (1239 cm^{-1}), arising from the peptide bonds vibrations of the main structural proteins, namely collagen.

CELLS AND PGS/GAGS HISTOLOGY

Milligan's Trichrome and Alcian blue

About cell removal characterization using different purifying solutions, it results that in PM treated with ASW and 4M Guanidine chloride solution could be identified cells in sections stained with Milligan's Trichrome but nor in 0.1 M NaOH solution treated samples. The results obtained by Milligan's Trichrome staining are shown in Fig. 19 and they suggest that cellular material appears to have been unaffected by 4M Guanidine chloride but was removed entirely by 0.1 M NaOH, using ASW sample as control.

Using Alcian blue dye, that binds by electrostatic forces the negatively charged acidic polysaccharides, is possible to discriminate the PGs/GAGs present in the sample in the different acid conditions: at pH more acid (0.2) only the PGs/GAGs with a strong sulfate group will be stained by Alcian blue; at pH less acid (5.6) all the PGs/GAGs with a sulfate group will be stained, giving us information of the total amount of the PGs/GAGs present (Hayat, 1993).

Using Alcian blue staining solutions on sectioned PMs treated with purifying solutions, results that, again, whilst 4M Guanidine chloride does not affect the intensity of staining of the collagen fibres, this is significantly reduced by 0.1 M NaOH. In PMs purified with 4M Guanidine chloride there is no decrease of PGs blue staining, whereas in the tissue treated with 0.1 M NaOH there is a strong decrease of PGs blue staining. This confirms that 0.1 M NaOH solution is the best to purify PM from PGs (see Fig. 20).

Furthermore, looking to the results obtained staining the PMs treated with the different purifying solutions with the Alcian blue solutions at different pH is evident that in the PM the strongly sulfated mucins are the dominant component, whereas the weakly sulfated one is very low (see Fig. 21).

Alcian blue technique used on CDL and PM treated with solutions to induce the different mechanical states revealed that PGs/GAGs were ubiquitously present. In CDL (see Fig. 22) it seems that there are no significant differences both on the whole amount of GAGs and on the differences related to the quantity of the different types of GAGs present in the different mechanical states. Again, PM GAGs histological quantification (see Fig. 23) showed that there are significant

differences on the content of GAGs and that there are differences related to the quantity of the different types of GAGs present in the different mechanical states. This means for both tissues that different types of GAGs are involved in the interfibrillar links of the different mechanical states.

Cuprolinic blue

Treatment of CDL and PM with Cuprolinic blue produced electron-dense precipitates associated with the surface of the collagen fibrils. No such precipitates were observed in any other location or when Cuprolinic blue was omitted from the fixative. The precipitates were roughly globular or ellipsoidal, measuring 10-20 nm in diameter. They were circumferentially arrayed around the fibrils with a longitudinal repeat period that matched the D-period of the fibril. In addition to the D-period, the collagen fibrils of the sea urchin have a repeating banded substructure, and the Cuprolinic blue precipitates were associated with a single band, which was best seen in isolated fibrils (see below).

Isolated fibrils stained with Cuprolinic blue had precipitates specifically associated with PGs/GAGs seen as small electron-dense dots at the surfaces of the fibrils (see Figs. 27 a, b).

The results obtained with Alcian blue technique on paraffin sections were further confirmed by TEM analysis of embedded tissue and extracted collagen fibrils treated with 4M Guanidine chloride and 0.1 M NaOH solutions and stained with Cuprolinic blue (see Figs. 24, 25, 26, 27 c, d). 4M Guanidine chloride removes non-covalently bound PGs from collagen fibrils, such as those of the echinoid spine ligament (Trotter and Koob, 1989). Since it had no discernible effect on the PM, it appears that covalently bound PGs dominate in this tissue. Furthermore, these results confirm that 0.1 M NaOH solution is the best to purify tissues from PGs. In addition, in thin sections the 0.1 M NaOH treated sample and above all the 4M Guanidine chloride treated sample do not preserve the integrity of collagen fibrils compared to the ASW control (see Figs. 24 b, 25 b, 26 b, c).

PGs/GAGs QUANTIFICATION: ALCIAN BLUE STAIN

The principle of the PGs/GAGs spectrophotometric quantification with Alcian blue is based on the specific interaction between sulfated polymers and the tetravalent cationic dye Alcian blue at a pH low enough to neutralize all carboxylic and phosphoric acid groups and at an ionic strength great enough to eliminate ionic interactions other than those between Alcian blue and sulfated GAGs. Hyaluronan, a nonsulfated GAG, does not react in this assay. There is no interference from proteins or nucleic acids in this method, in contrast to other dye-binding methods.

GAGs quantification was performed with a spectrophotometric method using Alcian blue dye to stain GAGs isolated from tissue with 4 M Guanidine chloride, a solution that will denature collagen and disrupt most kinds of non-covalent molecular interactions. The cross-linked collagen of CDLs and PM remains insoluble during this extraction, allowing the PGs and other soluble proteins to be separated from the bulk of the tissue by centrifugation.

This methodology is based on the protocol from Karlsson and Bjornsson (2001) modified preparing three different Alcian blue solutions at three different pH according to the principles that varying the pH the number of negative charges available to link it can vary, at pH more acid (0.2) only molecules strictly containing the sulfate group (strongly sulfated PGs) will be coloured and at pH less acid (5.6) molecules containing the sulfate group (strongly and weakly sulfated PGs) and molecules containing the carboxylic group will be coloured.

Considering the analysis in CDLs treated with different solutions (compliant corresponds to CDLs treated with PPSW, standard 45 corresponds to CDLs treated with ASW for 45 minutes and is the compliant control, standard 15 corresponds to CDLs treated with ASW for 15 minutes and is the stiff control, stiff corresponds to CDLs treated with AChSW) to obtain tissues in different mechanical states and using for each single mechanical state group the Alcian blue solution at the same pH, results that there is no statistically significant difference in PGs/GAGs amount in the different mechanical states both at the same pH conditions (see Graph 2). The only ANOVA significant test is between the compliant sample and its control, the standard 45, at pH 5.6 ($p < 0.05$).

Considering the analysis in CDLs treated with different solutions to obtain tissues in different mechanical states and using for each single mechanical state group three different pH (0.2, 1.4 and 5.6), results that there is no statistically significant difference in GAGs amount in the same mechanical state at pH 0.2, 1.4 and 5.6 (see Graph 3). The only ANOVA significant test is between the pH 1.4 and 5.6 in CDLs treated with ASW 15 ($p < 0.01$).

Considering the analysis in PMs treated with different solutions to obtain tissues in different mechanical states using for all the Alcian blue solution at the same pH or using for each single mechanical state group three different pH (0.2, 1.4 and 5.6), results that there is no statistically significant difference in PGs/GAGs amount looking at the different mechanical states in the same pH conditions (see Graph 4) and in the same mechanical state at pH 0.2, 1.4 and 5.6 (see Graph 5).

Finally, we can say that there is no statistical significance both in CDLs and PM among both GAGs content in the same mechanical state at different pH and GAGs content in the different mechanical states at the same pH. This means that there is no difference in GAGs type associated to the different mechanical states.

Furthermore, analysing the content of GAGs already associated to the isolated collagen after the extraction protocol results that in the fresh PM the GAGs amount is about 2-3 ‰, whereas in the isolated collagen fibrils the GAGs amount is very low, about 0.02 ‰ (see Graph 6). This means that the collagen extraction protocol removes most of the GAGs but those that are basic for the interaction of the fibrils with tensilin or for the biofilm production are still there.

Moreover, there is no statistically significant difference in GAGs amount among the isolated fibrils after the extraction protocol and those one isolated and treated with the purification step using 4M Guanidine chloride and 0.1 M NaOH solutions. This means that the disaggregating solution removes almost all GAGs, so the step of purification is almost useless.

PGs/GAGs CHARACTERIZATION: SDS-PAGE AND WESTERN BLOT ANALYSIS

The approach described here is to characterize the PGs and GAGs isolated from *P. lividus* CDL and PM. Once isolated with 4M Guanidine chloride, the large PGs can be separated from smaller ones by SDS-PAGE. Coomassie blue gel staining allows to characterize PGs (see Fig. 28), whereas the Alcian blue gel staining allows to characterize GAGs (see Fig. 29).

Fig. 28 shows that PGs extracted from the two different tissues are different. Large PGs between 300-200 kDa (aggrecan, versican, heparan) are present in both tissues but with a different banding pattern on the gel. Only CDLs present a PG migrating just above 120 kDa (decorin) and this is the predominant molecule in the ligaments. The core proteins of small PGs (SLRP: Small Leucine Rich Proteoglycans) migrate close together at about 40 kDa and they are present in both tissues.

Finally, the high-molecular-weight bands appear to be dominant in the PM, whereas a medium-molecular-weight band appears to be dominant in the CDLs.

Fig. 29 shows a gel electrophoresis GAGs was stained with Alcian blue solution to mark the isolated GAGs. In CDLs in the different mechanical states, GAGs pattern seem to be different but this is only one trial and this result must be confirmed. It seems that in all the samples there is a band at about 220 kDa that can be related to aggrecan PG but there is a second band present only in the stiffened sample and in its control at about 120 kDa that can be related to decorin PG.

FIBRILLIN BIOINFORMATIC ANALYSIS

Searching for all the fibrillin sequences available in GenBank database (www.ncbi.nlm.nih.gov) and applying BLASTp tool, the results are as follow: blasting *Bos taurus*,

Homo sapiens, *Sus scrofa* and *Mus musculus* fibrillin sequences with all the ORF known for *P. lividus* the result is a 42% of homology with 86 % query coverage with the fibrosurfin sequence; whereas blasting with all the ORF known for *S. purpuratus* the results are as follow: maximum similarity (99% query coverage): *B. taurus* (fibrillin2) - *S. purpuratus* (fibrillin-2-like) = 43%; *B. taurus* (fibrillin1) - *S. purpuratus* (fibrillin-2-like) = 42%; *H. sapiens* (fibrillin1) - *S. purpuratus* (fibrillin-2-like) = 44%; *H. sapiens* (fibrillin2) - *S. purpuratus* (fibrillin-2-like) = 43%; *H. sapiens* (fibrillin3) - *S. purpuratus* (fibrillin-2-like) = 41%; *S. scrofa* (fibrillin1) - *S. purpuratus* (fibrillin-2-like) = 41%; *M. musculus* (fibrillin2) - *S. purpuratus* (fibrillin-2-like) = 43%; *M. musculus* (fibrillin1) - *S. purpuratus* (fibrillin-2-like) = 42%.

FIBRILLIN CHARACTERIZATION: SDS-PAGE

The extraction of *P. lividus* CDLs with 6 M Guanidine chloride, followed by collagenase treatment, then by 6 M Guanidine chloride at least 4 times analysed by SDS-PAGE gels stained with Coomassie blue revealed the presence of a band at about 350 kDa as expected according to literature data (see Fig. 30 lane 2,3,4,5; Sakai et al., 1991; Thurmond and Trotter, 1996). This band was present in the first 4 supernatants and then it disappears. Were present also unknown species at about 240 kDa.

The same extraction performed on *P. lividus* PM did not have inexplicably any results (see Fig. 30 lane 6).

TENSILIN BIOINFORMATIC ANALYSIS AND BIOMOLECULAR CHARACTERIZATION

Searching for tensilin sequence available in GenBank database (www.ncbi.nlm.nih.gov), the results are: *C. frondosa* tensilin sequence (AY 033934.1) and a ‘predicted similar to tensilin’ sequence of *S. purpuratus* (XM 775549.2; see Seq. 1).

The *S. purpuratus* ‘predicted similar to tensilin’ sequence, whose whole genome is available on NCBI, is a ‘hypothetical protein’ record that means that it has been predicted to be an open reading frame. I successfully performed I performed the RACE (Rapid Amplification of cDNA Ends) technique and I obtained the ORF (open reading frame).

```
Query  1    MEVAFLVLLIGALSLSSADAQCA-GCSVKHPQHHFCDATFVMKVTII---------DVIL  50
            + V  ++L     S++S+  +C+  C   HPQ  FCD   V+KV I+         +V+
Sbjct  9    LLVTLVILGYFQTSMASSGIKCSHTCLSLHPQQRFCDDVVLKVKIMSRYFVNAKNEVVQ  68

Query  51   DRQGGDKLINAEINRSWKKGPSSG---DFQFYAPSSFCG-ATFDSGDTYVVTGTKEETSD  106
                      A +  S K+ P +    D  FY+PS  C  A  +  D YV+ G   +
Sbjct  69   HPYSSFVRYGARVLMSLKESPFAKEDEDIFFYSPSYDCSIAVPELKDVYVIGGKVID---  125

Query  107  GRRYWLHGSCDYM-IKWDDMSDQQKAGFKGGYKARCGECQIAESLTAASVKVEDIAANDY  165
                 +  SCD + +++D+++  Q+ GFK  Y+ +CG C I  + T   +   D+A +
Sbjct  126  --ELLVVTSCDGIAMRFDNLTSDQRRGFKDRYEEQCGFCTIQGAGTTKYIG-GDLAEDGQ  182

Query  166  PLATTYWTPTGCYYNPLMTRQFVGRKGSSVVDCEDVYGLCKPN-EADKCQWTLTPDYERC  224
               + YW+P  C+YNP  + ++ G+      DCE +Y  C+P+ +  +C W  T DY+ C
Sbjct  183  --ESGYWSPKECFYNPYPSVRYGGQ------DCETLYTFCRPHPDTGECAWEETMDYDDC  234

Query  225  LKERDD-FVKADSSAFAITRVEQCDVYTNKRKRKNCRQRFRELQAE  269
               R+  +   + S  A T   QC V   K  R  C +  ++L+ +
Sbjct  235  FDARESIWFFTEKSQPAYTCRSQCMVQPTKLLRWRCLKVIKKLEMK  280
```

Sequence 1. Alignment of *C. frondosa* tensilin sequence and *S. purpuratus* 'similar to tensilin' sequence. In yellow: high homology regions; in red: the highly conserved domain. Query = *C. frondosa* tensilin sequence; Subject = *S. purpuratus* 'similar to tensilin' sequence. Identity = 79/286 (27%), Positives = 134/286 (46%), Gaps = 31/286 (10%).

The two amino acid sequences in Seq. 1 show three regions (yellow) with a strong homology, two of which are localised in a wide highly conserved region (red). In particular the identity is 79/286 (27%), positives are 134/286 (46%) and gaps are 31/286 (10%).

This highly conserved region is not uniquely present in *C. frondosa* and *S. purpuratus* but results to possess a high conservative degree also in other echinoderms like *S. japonicus* (holothuroid) and *P. lividus* (see Seq. 2). This could mean that this is a very important region basically for the functionality of the tensilin protein.

```
ACATACGTAGTTACTGGGACAAAAAAGTTTACGGATGATGGGACTAAGTATTGGTCACACGGGT  S. japonicus
ACCTACGTAGTCACAGGGACAAAGGAGGAAACGAGCGACGGGCGGAGATACTGGCTTCATGGAT  C. frondosa
GTCTATGTCATAGGAGGAAAGGTTATAGAT--------------GAACTGCTGGTCGTCACTT  S. purpuratus
ACTTATGTGATAGGAGGTAAAATTATTGAT---------------GGACTCCTAGTTGTGTCAT  P. lividus
```

```
CATGTGACTTT--G---GTGAAGATTGGGATGACATGCCTGCCCAACAGAAGAAGGGTTTCAAG S. japonicus
CCTGCGACTATATG---ATTAAG--TGGGATGACATGTCGGACCAGCAGAAGGCGGGCTTCAAG C. frondosa
CATGTGATGGGATAGCCATGAGGTTTGATAACCTTACATCAGACCAACGAAGAGGATTCAAGG  S. purpuratus
CGTGCGATGGGATAGCAATGAAGTTTGATGTTATGACTGAAGACCAACGGATAGGATTTCTGG  P. lividus
```

Sequence 2. Alignment of the nucleotide sequences of *S. japonicus, C. frondosa, S. purpuratus* and *P. lividus* of the highly conserved domain. The *S. purpuratus* and *P. lividus* sequences are highlight respectively in blue and green as in Seq. 4.

In addition, performing the blast of the 'predicted similar to tensilin' with all the EST (Expressed Sequence Tag) in GenBank database a *P. lividus* mRNA sequence is obtained (AM565277.1), with a very high homology rate.

Proceeding with the BLASTp with *P. lividus* EST and all the proteins of the NCBI database I obtained very interesting data. As expected, at the first place I have found the 'predicted similar to tensilin' sequence of *S. purpuratus.* Other sequences with high homology are a TIMP-2 precursor (XP 001198302.1) of *S. purpuratus* and the tensilin sequence of *C. frondosa*. Moving through lower places we can find sequences belonging to animals phylogenetically more distant from echinoderms: TIMP-1 precursor of *Macaca mulatta* (NP 001028111.1), TIMP 1 precursor of *B. taurus* (NP 776896.1) and TIMP-1 precursor of *H. sapiens* (NP 003245.1).

In Seq. 3 are represented the fragments of the *P. lividus* and *S. purpuratus* sequences in comparison with none TIMP domains of other animals and in table 4 are listed the percentages of homology between the *C. frondosa* tensilin and *S. purpuratus* similar to tensilin sequences with known proteins in other animals.

```
1.  3.CSP.[1].HPQQAFCN.[1].DIVIRAKAVNKKEV.[12].RIQYEIKQIKMFKG.[2].QDIEFIYTA 66
2. 25.CSV.[1].HPQHHFCD.[1].TFVMKVTIIDVILD.[ 4].DKLINAEINRSWKK.[3].SGDFQFYAP 81
3. 30.CMP.[1].HPQTHFAQ.[1].DYVVQLRVLRKSDT.[ 4].RTTYKVHIKRTYKA.[7].LRDGRLSTP 90
4. 34.CLS.[1].HPQQRFCD.[1].DVVLKVKIMSRYFV.[13].FVRYGARVLMSLKE.[6].DEDIFFYSP 102
5. 34.CLS.[1].HPQRKFCD.[1].DAVMKVKITSRVFV.[13].FVRYGGSVITTLKD.[6].GGDIFFYSP 102
```

Sequence 3. Alignment of a portion of the *S. purpuratus* and *P. lividus* tensilin sequence compared with none TIMP domains of other animals: 1. TIMP 1 precursor [*Bos taurus*]; 2. Tensilin [*Cucumaria frondosa*]; 3. TIMP-isoform B [*Drosophila melanogaster*]; 4. Predicted similar to tensilin [*Strongylocentrotus purpuratus*]; 5. EST tensilin-like [*Paracentrotus lividus*].

Cucumaria frondosa **Tensilin**	***Strongylocentrotus purpuratus*** **Similar to tensilin**	***Paracentrotus lividus*** **EST**
tissue inhibitor of metalloproteases-like [*Nasonia vitripennis*] wasps 79%	tissue inhibitor of metalloproteinase 3-like [*Saccoglossus kowalevskii*] worms 79%	?
tissue inhibitor of metalloproteases [*Drosophila melanogaster*] flies 77%	metalloproteinase inhibitor 3-like [*Bombus terrestris*] bees 71%	
Metalloproteinase inhibitor 3 [*Harpegnathos saltator*] ants 73%	Metalloproteinase inhibitor 3 [*Camponotus floridanus*] ants 70%	
metalloproteinase inhibitor 4 precursor [*Mus musculus*] mouse 65%	tissue inhibitor of metalloproteinase-2b [*Takifugu rubripes*] fishes 54%	
metalloproteinase inhibitor 2 precursor [*Bos taurus*] ungulates 52%	tissue inhibitor of metalloproteinase 2b [*Sparus aurata*] fishes 52%	
tissue inhibitor of metalloproteinase 4 [*Homo sapiens*] 65%	tissue inhibitor of metalloproteinase 4 [*Homo sapiens*] 65%	
tissue inhibitor of metalloproteinase-3 [*Homo sapiens*] 50%	tissue inhibitor of metalloproteinase-3 [*Homo sapiens*] 50%	

Table 4. Percentages of homology between the *C. frondosa* tensilin and *S. purpuratus* similar to tensilin sequences with known proteins in other animals. Nothing is known about *P. lividus* homologies.

The presence of highly horizontally conserved sequences in animals often belonging to different phyla testify the importance of the role of the TIMP family, whose objective is probably to avoid the excessive degradation of the ECM by MMPs during the phenomena of collagen remodelling. These proteins, in fact, are involved in a lot of physiologic processes like the degradation of the ECM proteins like collagen and PGs (Wöessner, 1991). This capacity allows them to perform a leading role in the processes of MCTs remodelling (Nagase and Wöessner, 1999).

Performing an alignment with the BLASTn algorithm with the *P. lividus* EST and the 'predicted similar to tensilin' sequence of *S. purpuratus* an high identity percentage is obtained, 74% (550/742) and 9 gaps that corresponds to 1% of the nucleotide sequence (see Seq. 4).

```
Query  35   GCACCATGGCGATAAGAGTTGTAGGTCCACTACTTGTGACCCTCGTGATCCTGGGCTACT  94
            ||| |||||||||||||  | |||| | ||| ||||  ||| ||||| ||||||  ||
Sbjct  43   GCATCATGGCGATAAGACCTTTAGGACAACTCCTTGCCACCATCGTGTTCCTGGCTTATC  102

Query  95   TCCAGACATCGATGGCCTCCTCAGGTATCAAGTGCAGCCATACCTGTTT---ATCACTGC  151
            | ||| |||| ||||| || ||   |  | | ||||||  | ||| | |   ||| ||||
Sbjct  103  TTCAGGCATCAATGGCTTCTTCCCTT--CGA-TGCAGC--TCCCTCTGTGAGATC-CTGC  156

Query  152  ATCCTCAGCAACGCTTCTGTGATGACGATGTAGTTCTGAAGGTGAAAATCATGTCCCGGT  211
            | |||||   |   ||||| ||||| |||| |||| ||||||||||||||  || |||
Sbjct  157  ACCCTCAAAGAAAATTCTGCGATGATGATGCAGTTATGAAGGTGAAAATCACTTCTCGGG  216

Query  212  ATTTTGTGAACGCTAAGAACGAGGTAGTGCAGCATCCCTACAGTAGTTTTGTTCGCTACG  271
             ||||||| ||||| | ||||||| ||||   ||| |  | || |||||||||| ||||
Sbjct  217  TTTTTGTGGACGCTGACAACGAGGCAGTGGTCCATGCAAAAAGCAGTTTTGTTCGTTACG  276

Query  272  GGGCACGGGTCCTCATGTCCTTGAAGGAGTCACCATTTGCCAAGGAGGATGAAGACATCT  331
            ||| | | ||  ||| | |||||||||| ||| | ||||| ||||| | ||  |||||||
Sbjct  277  GGGGAAGTGTAATCACGACCTTGAAGGATTCAACCTTTGCTAAGGACGGTGGTGACATCT  336

Query  332  TCTTCTACTCTCCAAGCTATGATTGTTCTATAGCGGTACCAGAACTCAAGGACGTCTATG  391
            |||||||||| || |||||    || || ||  |   ||||||  || ||||    ||||
Sbjct  337  TCTTCTACTCACCTAGCTACACCTGCTCCATCCCTACACCAGATATCGAGGATACTTATG  396
```

```
Query  392  TCATAGGAGGAAAGGTTATAGATGAACTGCTGGTCGTCACTTCATGTGATGGGATAGCCA  451
            | |||||||| ||  |||| |||| ||| || || ||  | || || ||||||||||| |
Sbjct  397  TGATAGGAGGTAAAATTATTGATGGACTCCTAGTTGTGTCATCGTGCGATGGGATAGCAA  456

Query  452  TGAGGTTTGATAACCTTACATCAGACCAACGAAGAGGATTCAAGGACAGATACGAGGAGC  511
            ||| |||||||    | ||   ||||||||| | ||||||   || ||||||| |||| |
Sbjct  457  TGAAGTTTGATGTTATGACTGAAGACCAACGGATAGGATTTCTGGGCAGATACAAGGATC  516

Query  512  AATGTGGCTTCTGTACGATCCAGGGGGCTGGTACCACCAAATACATAGGGGGTGACCTGG  571
            ||||||| ||||| |||||||| || ||||| || ||||| || || || || |    ||
Sbjct  517  AATGTGGTTTCTGCACGATCCAAGGTGCTGGCACAACCAAGTATATTGGTGGCGTAGAGG  576

Query  572  CAGAAGATGGGCAGGAGTCAGGGTACTGGAGTCCAAAAGAATGTTTCTATAACCCCTACC  631
            | ||    |||||||||||||||||||||||  || ||   || |||| ||||||    |
Sbjct  577  CTGAGCTGGGGCAGGAGTCAGGGTACTGGAGCACAGAAATGTGCTTCTTTAACCCTATTC  636

Query  632  CATCCGTCAGATACGGCGGGCAGGACTGCGAGACCCTGTATACCTTCTGCAGGCCCCACC  691
            |||| |  |||||||| ||  |||||||||||||||| ||| ||||||||| ||||| |
Sbjct  637  CATCTGAGAGATACGGTGGAAAGGACTGCGAGACCCTCTATTCCTTCTGCAAGCCCCGCT  696

Query  692  CAGATACCGGTGAATGTGCGTGGGAGGAAACGATGGACTATGATGACTGCTTCGATGCCA  751
            | ||||| ||||| || || |||||||   | |||||||| |||||||||| ||   ||
Sbjct  697  CTGATACTGGTGAGTGCGCATGGGAGGCCGCCATGGACTACGATGACTGCTTTGAGAACA  756

Query  752  GAGAATCTATCTGGTTCTTCAC  773
            | |||||| | ||||||||||
Sbjct  757  GGGAATCTGTATGGTTCTTCAC  778
```

Sequence 4. Alignment of a portion of the *S. purpuratus* and *P. lividus* nucleotide tensilin sequences. In blue and green is highlighted the region that presents the highest degree of homology. Query = *S. purpuratus*; Subject = *P. lividus.*

P. lividus EST, as all the other EST, is a short sub-sequence of a cDNA sequence and represents portions of expressed genes. So, I performed the RACE (Rapid Amplification of cDNA Ends) technique to complete the ORF (open reading frame). Considering this high degree of identity, a lot of attempts were made do complete the 3' end but only the EST sequence was identified.

I also tried to complete the *P. lividus* ORF designing degenerate primers constructed in the three regions of high homology after the alignment of the *C. frondosa* tensilin sequence and the *S. purpuratus* 'predicted similar to tensilin' sequence (see Seq. 1). Finally, I found just one sequence that shows a high homology with *S. purpuratus* similar to C1qBP complement component 1, q subcomponent binding protein (XM_001177135.1; see Seq. 5).

```
Query 89    ATGCTCACAA-TGTCTTTCTAGCCAACCAGCAGTTGGGGGTAAACAGGCATTCCATCACA 147
            |||| ||||  | |||||||| |||||  |||  ||      |||| ||||||||| |||
Sbjct 1121  ATGCACACAGGTATCTTTCTATCCAACT-GCACGTG------AACATGCATTCCATAACA 1069

Query 148   TATTAACTCTGCGCATATTGTCTCTTCAAGTCAAATAGGACTCCAGTCTTCGCATATCCA 207
            | |  | | | |   ||| ||||||    ||  |  | |||| ||||||||| || |||
Sbjct 1068  TCTGTAGTATTCAGGTATAGTCTCTCAGGGTACAGCACGACTTCAGTCTTCGTATGTCCG 1009
```

```
Query 208   AAAGGGCGGCC--AGATTTAGAACAACCAAGACCAGGGACTACAATGTTCTAGGTTGGTT 265
             |  | | |||  |||||||  | ||  ||||  | | ||||||| || | || | | ||
Sbjct 1008  CACCGACAGCCGGAGATTTATTAAAAA-AAGATGACGAACTACAAAGTCCAAGATAGATT 950

Query 266   CC--CGATGCTCATTTCTTGACAAAGCCTTGGAGTTGGTTGAGGAAGCCTATGTACTGCC 323
             |   |||  |||||||||| || || |||||||||||||||| ||||| ||||| ||||
Sbjct 949   CAGTCGA--CTCATTTCTTAACGAACCCTTGGAGTTGGTTGAGAAAGCCAATGTATTGCC 892

Query 324   GATGTTCCACTGCGCTGGCTAGATCTGGAAGCTTTTCACAGAA 366
             |||||||||||| |||| ||  |||| |||||| ||||||||
Sbjct 891   GATGTTCCACTGCACTGGATAAGTCTGAAAGCTTCTCACAGAA 849
```

Sequence 5. Alignment of the nucleotide sequences of and *S. purpuratus* similar to complement component 1, q subcomponent binding protein. Query = *P. lividus* EST; Subject = *S. purpuratus* similar to complement component 1, q subcomponent binding protein. Identity is 204/283 (73%), gaps are 15/283 (5%).

Finally, a partial *P. lividus* tensilin cDNA was amplified from the PM using primers (for primer sequences see Table 1) based on the EST clone available in the GenBank database (acc. number: AM565277.1).

Regarding *S. purpuratus* tensilin protein, a full-length tensilin cDNA was isolated from the PM by means of RT-PCR using gene-specific primers designed on the sequence (acc. number: XM775549.2) available in the GenBank database (for primer sequences see Table 2). A second round of amplification was performed using an aliquot of the first reaction with two adapter primers (for primer sequences see Table 2) in order to include in the amplicon the 5' and 3' sequences necessary for the following *in vitro* translation. The cDNA was gel-purified and *in vitro* translated using the EasyXpress Insect Kit II (Qiagen) according to the manufacturer's specifications. In Fig. 31 are shown the ORF band in Agarose gel electrophoresis using the primers SF1-SR3.

COLLAGEN FIBRILS AGGREGATION ASSAY

The results obtained using the *S. purpuratus* tensilin protein on *P. lividus* and *S. purpuratus* collagens are the same so all the pictures here referred to are only the samples with *S. purpuratus* collagen.

In the 1st test 90 µl of *P. lividus* and *S. purpuratus* collagen were mixed in EGTA-ASW solution with 25 µl tensilin protein reaching the final volume of 1 ml stirring at 100 rpm 2 h RT. The final concentration of collagen was 0.09 mg/ml and the one of tensilin was 32 µg/ml. We did not see any fibril aggregation in this test (see Fig. 32). Initially was possible to observe the presence of little clots, very small, but these were unstable and once that the stirring was stopped the collagen solutions became again homogeneous.

In the 2nd test we verified the hypothesis that the amount of collagen in the first test was insufficient to generate the aggregation (see Fig. 33). So we doubled the collagen concentration (0.18 mg/ml) keeping constant the other experimental conditions. Even in this case we did not observed the formation of stable aggregates; there was no difference between the *P. lividus* and *S. purpuratus* sample and there was no difference between the samples and the controls.

In the 3rd test we decided to interrupt the stirring movement and to observe the sample to the microscope with TimeLapse tool active (see Fig. 34). We doubled again the collagen concentration (0.36 mg/ml) and the aggregation activity was observed to the light microscope. The fibril aggregation activity was not observed even in this case.

The 4th test was performed keeping the collagen concentration at 0.36 mg/ml, stirring the sample at 50rpm and tripling the concentration of the tensilin protein used. In this test we eliminated the EGTA-ASW solution to verify if this solution could interfere with the tensilin activity (see Fig. 35). As in the 1st and 2nd test here we observed the formation of little clots, but with bigger than the first two tests. In this case the clots are even more stable in time but however transitory. In this test was possible to distinguish some differences between the samples with tensilin and the controls without tensilin with the formation of bigger clots in the former.

Our results are not comparable with those one of Trotter and coworkers (1996) in which they observed by eye the formation of clots stable for days, but literature results referred to the holothurian species whereas we work on the sea urchin so is possible that in our species the tensilin protein could act in a different way.

FRACTIONS EXTRACTION AND CHARACTERIZATION: CHROMATOGRAPHY

These results arise from the collaboration and technical support of our colleagues at INEB.

Anion exchange chromatography of the PM 4M Guanidine chloride and freeze-thaw extract showed the presence of distinct proteins with widely differing charge characteristics (see Fig. 36). The flowthrough was further separated on a second anion exchange column within 0 and 1 M NaCl and different fractions were obtained with stiffening activity, which contained proteins pools in SDS-PAGE analysis (see Fig. 38). Proteins eluted from the second column at NaC1 concentrations between 0 and 1 M (fractions from pool 2-4 to pool 24-28) were quantified with DC Assay and the results obtained overlap the chromatographic quantification (see Fig. 37). These proteins were also stained with Silver staining (see Fig. 38). Fractions contain proteins as below: fraction 1 to 4 do not contain proteins; fraction 5 to 8 contain proteins at ~ 220 kDa, ~ 105 kDa, ~ 90 kDa and ~ 34 kDa; fraction 9 to 12 contain proteins at ~ 220 kDa, ~ 115 kDa, ~ 90 kDa and a huge amount of a protein

at ~ 42 kDa; fraction 13 to 20 the protein pattern is similar but different from the previous, they contain a huge amount of a protein at ~ 350 kDa and at ~ 180 kDa and ~ 160 kDa and at ~ 42 kDa; fraction 21 to 28 the protein pattern is similar to the previous but in low quantity, they contains proteins at ~ 450 kDa, ~ 350 kDa, ~ 220 kDa, at ~ 180 kDa, ~ 160 kDa and at ~ 42 kDa. The only fraction that contains a protein with the apparent molecular mass at 34 kDa, similar to the value of tensilin from *C. frondosa*, is in the fraction pool 1-4. The apparent molecular mass of tensilin, a protein of 260 AA in the predicted mature form, is 33 kDa (Tipper et al., 2003). The protein with molecular mass at ~ 350 kDa could be the stiparin protein, similar to the value of stiparin from *C. frondosa* (Koob et al., 1996). The other molecular weights belong to unknown proteins.

FRACTIONS ANALYSIS: RHEOMETER TESTS

These preliminary results arise from the collaboration and technical support of our colleagues at INEB.

Rheometer tests were used to characterize the *P. lividus* insoluble collagen and the soluble ultrapure bovine collagen as themselves and to analyse the fractions extracted with the anion exchange chromatography from *P. lividus* PM. Were made comparison between the two kinds of collagens for the different types of tests at two temperatures (25°C and 37°C) and for the same kind of collagen were made comparison in the answers for the same test at the two temperature. All the following results were analysed taking into account the control results.

Analysing the bovine and echinoderm collagen behaviours at 25°C, using the table of shear rates log test (that is a viscometry shear rate table test in a logarithmic scale), it is evident that both in *P. lividus* insoluble collagen and in bovine soluble ultrapure collagen, by increasing the shear rate from 10^{-1} to 10^{2} s^{-1}, the viscosity decreases, respectively of two and one orders of magnitude (see Graph 7). More in detail, both collagens are characterized by a viscosity of 0.12 Pa*s for a shear rate of 0.1 s^{-1}. The rheometer performs 16 viscosity measurements in the shear rate range [0.1, 100] s^{-1}, providing a final viscosity of 1.527 10^{-3} Pa*s for the *P. lividus* insoluble collagen and of 1.603 10^{-2} Pa*s for the bovine soluble ultrapure collagen at a shear rate of 100 s^{-1}. The registered slope value of the bovine curve is -1.0577 10^{-3}, whereas that of the *P. lividus* curve is -1.252 10^{-3}.

Analysing the bovine and echinoderm collagen behaviours at 37°C, using the table of shear rates log test, it is evident that the behaviours of *P. lividus* insoluble collagen and bovine soluble ultrapure collagen, by increasing the shear rate from 10^{-1} to 10^{2} s^{-1}, are completely separable (see Graph 8). The trends of both curves are linear and monotone decreasing: indeed, by increasing the

shear strain rate from 10^{-1} to about 10 s^{-1}, the viscosity decreases from 0.177 to 0.017 Pa*s for the bovine collagen and from 20.89 to 0.596 Pa*s for the echinoderm insoluble collagen.

Analysing the bovine and echinoderm collagen behaviours at 25°C, using the shear rate ramp log isothermal test (that is a viscometry shear rate ramp in logarithmic scale), it results that, by increasing in 2 minute the shear strain rate from 0.123 to 8.065 s^{-1}, the viscosity trends of the *P. lividus* insoluble collagen and of the bovine soluble ultrapure collagen are completely different from each other (see Graph 9). Parity in shear strain rate variation performed in 2 minutes, the two samples behave in two different ways: regarding the *P. lividus* insoluble collagen, if the shear stress applied to the sample increases from 8.120 10^{-3} to 0.034 Pa, the shear viscosity decreases from 0.066 to 4.201 10^{-3} Pa*s; whereas, for the bovine soluble ultrapure collagen, if the shear stress applied to the sample increases from 0.013 to 0.185 Pa, the shear viscosity decreases from 0.104 to 0.023 Pa*s. For example, considering the same shear stress data at 0.024 Pa, the *P. lividus* insoluble collagen viscosity is 6.906 10^{-3} Pa*s, whereas the bovine soluble ultrapure collagen viscosity is 0.091 Pa*s. Moreover, the slope value of the bovine curve is -0.470 and the one of the *P. lividus* insoluble collagen is -2.40.

Analysing the bovine and echinoderm collagen behaviours at 37°C, using the shear rate ramp log isothermal test, it results that, by increasing in 2 minute the shear strain rate from 0.123 to 8.065 s^{-1}, the viscosity trends of the *P. lividus* insoluble collagen and of the bovine soluble ultrapure collagen are completely different from each other (see Graph 10). Parity in shear strain rate variation performed in 2 minutes, the two samples behave in two different ways: regarding the *P. lividus* insoluble collagen, if the shear stress applied to the sample increases from 2.629 to 4.897 Pa, the shear viscosity decreases from 20.890 to 0.596 Pa*s; whereas, for the bovine soluble ultrapure collagen, if the shear stress applied to the sample increases from 0.022 to 0.139 Pa, the shear viscosity decreases from 0.177 to 0.017 Pa*s. Moreover, the slope value of the bovine curve is -1.365 and the one of the *P. lividus* insoluble collagen is -8.948.

Analysing the bovine and echinoderm collagen behaviours at 25°C, using the shear stress ramp with yield stress analysis (that is a viscometry shear stress ramp in logarithmic scale), it results that, by increasing in 1 minute the shear stress from 0.138 to 90.130 Pa, the viscosity trends of the *P. lividus* insoluble collagen and of the bovine soluble ultrapure collagen are both linear, with monotonically decreasing curves (see Graph 11). In particular, the viscosity pattern of the *P. lividus* insoluble collagen is more constant but when the shear stress reaches the 58.50 Pa, the shear viscosity reaches its maximum at 0.302 Pa*s after the first 11 points with a mean of 2 10^{-3} Pa*s, whereas the viscosity pattern of the soluble ultrapure bovine collagen can be linearized changing the shear stress in a monotonically decreasing curve varying from 0.027 to 5.130 10^{-3} Pa*s. Moreover,

the slope value of the bovine curve is -2.474 10^{-4}, and the one of the *P. lividus* insoluble collagen is for the first 11 points -0.310 10^{-3} whereas for the consequent 3 points is +7.06 10^{-3}.

Analysing the bovine and echinoderm collagen behaviours at 37°C, using the shear stress ramp with yield stress analysis, it results that, by increasing in 1 minute the shear stress from 0.138 to 90.130 Pa, the viscosity trends of the *P. lividus* insoluble collagen and of the bovine soluble ultrapure collagen are completely different from each other (see Graph 12). In particular, the viscosity pattern of the *P. lividus* insoluble collagen shows an extraordinary behaviour, whereas the viscosity pattern of the soluble ultrapure bovine collagen can be linearized changing the shear stress in a monotonically decreasing curve varying from 0.017 to 3.744 10^{-3} Pa*s. Analysing the *P. lividus* insoluble collagen behaviour, it results that by increasing the shear stress from 0.138 to 0.503 Pa the viscosity reaches its maximum moving from 0.451 to 1.471 10^{3} Pa*s, then it starts to decrease constantly till the shear stress of 10.38 Pa when reaches the minimum viscosity of 0.073 Pa*s and then the viscosity starts again to increase with a slight positive slope. Moreover, the slope value of the bovine curve is -1,46 10^{-4}, and the one of the *P. lividus* insoluble collagen is for the first 4 points +4.018 10^{3} whereas for the maximum to the minimum points is -148.828 and then for the last 6 points is +2.396 10^{3}.

I also performed the oscillation amplitude table that is an amplitude sweep stress controlled analysis with LVER (Linear Viscoelastic region) determination for low viscosity materials - within this region a sample obeys Hooke's law: the stress will be proportional to the strain.

Both at 25 and at 37°C the oscillation amplitude table shows that for both the *P. lividus* insoluble collagen and the soluble ultrapure bovine collagen the behaviours are linear and predictable but completely separable (see Graph 13). In particular, in the ultrapure bovine soluble collagen at 25°C the G' varies from 0.029 to 0.014 Pa and G" from 0.146 0.126 Pa and at 37°C the G' varies from 0.028 to 0.014 Pa and G" from 0.067 to 0.053 Pa, so the measures at the two temperatures are comparable and it can be concluded that the ultrapure bovine soluble collagen at 25 and 37°C shows a behaviour liquid alike. Instead, in the *P. lividus* insoluble collagen the properties are higher: at 25°C the G' varies from 37.080 to 0.121 Pa and G" from 8.047 to 1.523 Pa and at 37°C the G' varies from 51.760 to 42.780 Pa and G" from 10.850 to 10.820 Pa.

Comparing the bovine collagen data collected with the table of shear rates log test at 25 and 37°C (see Graph 14), the maximum viscosity at 25°C is 0.122 Pa*s whereas the one at 37°C is 0.476 Pa*s. The two curves cross the minimum viscosity 0.020 Pa*s at a shear strain rate 6.318 s^{-1}.

Comparing the bovine collagen data collected with the shear rate ramp log isothermal test at 25 and 37°C, results that the two curves are overlapped (see Graph 15).

Comparing the bovine collagen data collected with the shear stress ramp with yield stress analysis at 25 and 37°C (see Graph 16), it results that at 25°C at the lowest shear stress 0.138 Pa the viscosity is 0.024 Pa*s, whereas at the maximum shear stress 90.140 Pa the viscosity is 5.130 10^{-3} Pa*s. At 37°C at the lowest shear stress 0.138 Pa the viscosity is 0.017 Pa*s, whereas at the maximum shear stress 90.140 Pa the viscosity is 3.744 10^{-3} Pa*s.

Comparing the *P. lividus* insoluble collagen data collected with the table of shear rates log test at 25 and 37°C (see Graph 17), it results that the two curves are parallel, linear, monotonically decreasing and they do not cross. At 25°C the viscosity goes from 0.127 to 2.110 10^{-3} Pa*s, whereas at 37°C the viscosity goes from 10.760 to 0.207 Pa*s, so there are two degrees of magnitude of difference.

Comparing the *P. lividus* insoluble collagen data collected with the shear rate ramp log isothermal test at 25 and 37°C, results that increasing in 2 minute the shear strain rate from 0.123 to 8.065 s^{-1} the behaviours at 25 and 37°C are completely different (see Graph 18). For the same shear strain rate variation in 2 minutes the two sample behave in two different way: at 25°C the shear viscosity decreases from 0.066 to 4.201 10^{-3} Pa*s, whereas at 37°C the shear viscosity decreases from 20.890 to 0.596 Pa*s. Hence, when time is constant (2 minutes) the *P. lividus* insoluble collagen at 37°C reaches the same viscosity of the same sample at 25°C with a higher shear stress.

Comparing the *P. lividus* insoluble collagen data collected with the shear stress ramp with yield stress analysis at 25 and 37°C (see Graph 19), it results that the behaviours remain distinct till the shear stress reaches 58.5 Pa and the two curves cross at a viscosity of 0.30 Pa*s.

In addition, viscometry tests were performed in order to analyse the rheological properties of the insoluble and soluble collagen isolated from *P. lividus* PM and bovine ultrapure collagen after adding the chromatographic fractions isolated from PMs with the anion exchange chromatography. Only the fractions from 5 to 25 were analysed taking into account of the results obtained with the SDS-PAGE and the quantification with DC Assay. Not all the fractions gave the same replies and in particular analysing each single fraction tested on echinoderm and bovine collagen in viscometry and oscillation tests at 25 and 37°C, it is important to notice that above all the fractions 9 and 12 gave us a significant replay. Here below are reported only the results concerning the fraction 9, since the results for both fractions are comparable.

Analysing the bovine and echinoderm collagen behaviours at 25°C adding 100 µl of fraction 9, using the table of shear rates log test, it is evident that both in *P. lividus* insoluble collagen and in bovine soluble ultrapure collagen with and without 100 µl of fraction 9, by increasing the shear rate from 10^{-1} to 10^{2} s^{-1}, the viscosity decreases, respectively of two and one orders of magnitude (see Graph 20). More in detail, at 0.1 s^{-1} shear rate the samples are characterised by different viscosities

as listed below: *P. lividus* insoluble collagen 0.127 Pa*s and *P. lividus* insoluble collagen plus fraction 9 1.754 Pa*s, bovine collagen 0.122 Pa*s and bovine collagen plus fraction 9 0.245 Pa*s. The rheometer performs 16 viscosity measurements in the shear rate range [0.1, 100] s^{-1}, providing a final viscosity at a shear rate of 100 s^{-1} as listed below: *P. lividus* insoluble collagen 1.527 10^{-3} Pa*s, *P. lividus* insoluble collagen plus fraction 9 0.040 Pa*s, bovine collagen 0.016 Pa*s and bovine collagen plus fraction 9 0.010 Pa*s.

Analysing the bovine and echinoderm collagen behaviours at 25°C adding 100 µl of fraction 9, using the shear rate ramp log isothermal test, it results that, by increasing in 2 minute the shear strain rate from 0.123 to 8.065 s^{-1}, the viscosity trends of the *P. lividus* insoluble collagen and of the bovine soluble ultrapure collagen are completely different from each other (see Graph 21). Parity in shear strain rate variation performed in 2 minutes, the four samples behave in four different ways: regarding the *P. lividus* insoluble collagen, if the shear stress applied to the sample increases from 8.120 10^{-3} to 0.034 Pa, the shear viscosity decreases from 0.066 to 4.201 10^{-3} Pa*s; regarding the *P. lividus* insoluble collagen plus fraction 9, if the shear stress applied to the sample increases from 0.186 to 0.529 Pa, the shear viscosity decreases from 7.165 to 0.066 Pa*s; whereas, for the bovine soluble ultrapure collagen, if the shear stress applied to the sample increases from 0.013 to 0.185 Pa, the shear viscosity decreases from 0.104 to 0.023 Pa*s; for the bovine soluble ultrapure collagen plus fraction 9, if the shear stress applied to the sample increases from 0.024 to 0.146 Pa, the shear viscosity decreases from 0.201 to 0.018 Pa*s.

Analysing the bovine and echinoderm collagen behaviours at 25°C adding 100 µl of fraction 9, using the shear stress ramp with yield stress analysis, it results that, by increasing in 1 minute the shear stress from 0.138 to 90.130 Pa, the viscosity trends of the *P. lividus* insoluble collagen and of the bovine soluble ultrapure collagen are completely different from each other (see Graph 22). It results that, by increasing in 1 minute the shear stress from 0.138 to 90.130 Pa, the viscosity trends of the bovine soluble ultrapure collagen with or without fraction 9 are both linear, with monotonically decreasing curves. In particular, the viscosity pattern of soluble ultrapure bovine collagen can be linearized changing the shear stress in a monotonically decreasing curve varying from 0.027 to 5.130 10^{-3} Pa*s and the viscosity pattern of soluble ultrapure bovine collagen plus fraction 9 can be linearized changing the shear stress in a monotonically decreasing curve varying from 0.020 to 4.349 10^{-3} Pa*s. On the contrary, the viscosity pattern of the *P. lividus* insoluble collagen shows an extraordinary behaviour: the viscosity pattern of the *P. lividus* insoluble collagen can be linearized for the first 11 points changing the shear stress in a monotonically decreasing curve varying from 5.193 10^{-3} to 2.121 10^{-3} Pa*s, whereas analysing the *P. lividus* insoluble collagen plus fraction 9 behaviour, it results that by increasing the shear stress from 0.138 to 1.842

Pa the viscosity decreases moving from 61.780 to 0.035 Pa*s, then it starts to increase till the shear stress of 10.38 Pa when reaches the second maximum viscosity of 0.359 Pa*s and then the viscosity starts again to decrease to a final viscosity 5.634 10^{-3} Pa*s.

Discussion

The main general aim of this project was to acquire the appropriate knowledge of the model we want to get inspiration from, MCT, and to understand how it natural actually works. The research work was developed according to the specific objectives in order to define the basic biology of natural MCTs, particularly the key-components and their fundamental interactions; this was achieved through morphological, biochemical, biomolecular and biomechanical characterizations.

COLLAGEN

Collagen, the most abundant protein in animals, is mainly located in the extracellular matrix, and confers mechanical stability, promotes elastic energy storage but also regulates cell adhesion, supports chemotaxis and migration.

Many collagens are preserved from invertebrates to vertebrates, where their molecular hallmarks are the repetitions of Gly-X-Y sequences in which the amino acid residues in -X and -Y position are proline and hydroxyproline, and have a triple helical structure that is built by three polypeptide chains. The molecules are deposited side by side and parallel but staggered with respect to each other creating a periodicity known as the D-band. Multiple fibrils assemble with the aid of cross-linking macromolecules (PGs) resulting in fibres. The collagen fibrils aggregate into more complex supramolecular structures to became part of the structural connective tissues (Scott, 1995; Brinckmann et al., 2005; Exposito et al., 2010). Mutable adult connective tissues such as tube foot, spine ligament and peristome can rapidly change their mechanical properties, a process believed to involve collagen fibrils (Motokawa, 1984).

The morphological characterization presented in this thesis revealed that in typical sea urchin MCT, CDL and PM, collagen is composed by fibrils with a variable diameter and organized respectively into parallel and web-arranged fibres that determine the tensile strength of the ligament and the complex movements of the membrane, including protraction/retraction, lateral tilting, dilatation/restriction. etc. In particular, the diameters of fibrils for CDLs were 20-150 nm and for PM were 30-380 nm; the D-period of CDL was 58-63 nm and for PM was 59-63 nm. Other differences were present between the two tissues, also by analysing them with other techniques and this is consistent with the different functions that the two tissues perform (see below).

In literature different examples of D-period collagen are described, the measurements belonging to many kinds of tissues and animal species: Young (1985) working on the rabbit scleral matrix found a periodicity of 48 nm and on human scleral matrix of 53 nm; Birk et al. (1988), working on the chicken embryos corneal matrix, found a periodicity of 66±7.5 nm; Burke et al. (1989), working on the *S. purpuratus* peristome tissue, found a periodicity of 44.4 nm; Trotter and Koob (1989), working on the *E. tribuloides* catch apparatus, found a periodicity of 65.7±3.28 nm; Revenko et al. (1994), working on the rat tail ligament, found a periodicity of 69-71 nm; Trotter et al. (1994), working on the dermis of *C. frondosa*, found a periodicity of 65.7±0.5 nm

All this data differ significantly from the periodicity of 67 nm found for vertebrate type I collagen. This difference presumably results from dissimilar packing arrangements in the fibres, which in turn may reflect differences in the biochemical properties of the constituent collagen molecules. The contrasting properties shown by echinoderm collagen with respect to that of mammals and chicken may in part be responsible for the unique characteristics of MCTs and the rapidly mutable nature of these echinoderm connective tissues.

From literature it is known that fibrillar collagen is present in type I, II, III, V, XI, XXIV and XXVII and in echinoderms both embryonic and adult tissues contain collagen (Exposito et al., 2010; Burke et al., 1989; Trotter and Koob, 1989). Collagens have been isolated from a number of adult sea urchin tissues including test, tube foot, peristome and spine ligament (Pucci-Minafra and Galante, 1978; Burke et al., 1989; Tomita et al., 1994; Trotter et al., 1994).

Insoluble and soluble collagens were successfully isolated for the first time in literature from CDL and PM of the sea urchin *Paracentrotus lividus*. These collagens analysed by TEM were intact and perfectly suitable for biofilm production. The only structural difference is that in the isolated collagen the D-period range was 62-66 nm, which is different from the previous information about intact tissue, probably due to an elastic reaction of the collagen when extracted with the disaggregating solution.

Burke et al. (1989) isolated collagen from sea urchin peristome tissue and found two species of apparent molecular masses of 120 and 63 kDa. Our biochemical analysis of CDL and PM revealed two collagenous species of apparent molecular masses of 140 and 116 kDa. The additional species of 55 and 53 kDa were derived from the pepsin used in the purification protocol. The results reported here confirm the collagenous nature of the 116 and 140 kDa species and the relative staining intensities of the 116 and 140 kDa species suggest that they exist as a heterotrimer of $(116)_2$ $(140)_1$, typical of vertebrate type I collagen. Type I fibrillar collagen molecules appear to be commonly associated with adult sea urchin tissues. Trotter and Koob (1989) have isolated a collagen from the mutable spine ligament of a sea urchin. Their analyses characterized the isolated

protein as a type I fibrillar collagen consisting of an $(\alpha_1)_2(\alpha_2)_1$, arrangement. Similarly, Tomita et al. (1994) isolated and characterized a fibrillar type-collagen from the adult test of *Hemicentrotus pulcherrimus*.

Furthermore, analysing echinoderm collagen with antibody that distinctly react with collagen type I and type III we can conclude that for sure *P. lividus* collagen possessed an antigenicity common with mammalian collagen type I and not with mammalian collagen type III.

Biomolecular analyses with BLAST tools yielded to the conclusion that sea urchin collagen molecules enjoy a considerable degree of sequence homology with their vertebrate counterparts, in particular with type I. In a related report Tomita et al. (1994) have published a partial cDNA sequence encoding a fibrillar type-collagen from the adult test of the sea urchin *H. pulcherrimus*. Again, significant sequence homologies with vertebrate type I collagen were found.

Taking this into consideration we used commercial collagen type I as a positive control in our investigation the FT-IR data revealed that insoluble and soluble *P. lividus* collagen had strong similarities with mammalian collagen type I. In literature, FT-IR analysis has been used to differentiate between different collagen types on the basis of their structural parameters (Petibois et al., 2006; Belbachir et al., 2009). The amide groups (amide I, II, III and A) vibrations of protein backbones received particular attention, since they are present in all proteins and provide information on secondary conformation. The results confirmed that PM collagens have strong similarities to mammalian type I. However, differences were observed in other spectral regions, suggesting the possible presence of collagen other than type I. This is consistent with what is known for mature connective tissues of mammalians, such as cornea, skin, and cartilage, which contain heterotypic collagen fibrils consisting of more than one collagen type (Canty and Kadler, 2002).

PROTEOGLYCANS AND GLYCOSAMINOGLYCANS

The extracellular matrix of *P. lividus* CDL, PM and of the main connective tissues of vertebrates is not exclusively composed of fibrous proteins, such as collagen and fibrillin; it also contains proteoglycans (PGs). PGs fill the interstitial space of the extracellular matrix in the form of a hydrogel, performing several functions such as buffering, binding and having force-resistance properties. The interfibrillar cohesion is maintained partly by the PGs-fibril relationship (PGs may be covalently and noncovalently attached to fibrils) that must hold fibrils against fluids flow and tissue stress history, preventing uncontrollable sliding, thus contributing to the stability of collagen fibres (Erlinger et al., 1993; Scott and Thomlinson, 1998). PGs in CDL and PM were visualized at a specific position in the D-period of collagen fibrils. Interfibrillar PGs were already observed in

holothurian dermis and sea urchin spine ligament (Erlinger et al., 1993; Trotter et al., 1994; Trotter et al., 2000). PGs probably stabilize collagen fibrils acting as binding sites for specific proteins responsible for interfibrillar cohesion (Scott et al., 1998; Wilkie, 2005).

PGs are also composed of GAGs side chains that are covalently linked to a specific protein core. GAGs chains are unbranched polysaccharides composed of repeating disaccharides units that can be divided into sulphated (chondroitin, dermatan, heparin and keratin sulfate) and nonsulfated (hyaluronic acid; Junqueira, 1983; Raspanti et al., 2008).

GAGs were correctly visualized using the Cuprolinic blue stain distributed along the collagen fibrils of PM and CDL in specific positions as previously reported in literature (Trotter and Koob 1989; Trotter et al., 1994; Raspanti et al., 2008). The most important thing revealed by Cuprolinic blue analysis is the difference in PGs/GAGs presence and collagen fibrils integrity among standard and treated samples with 4M Guanidine chloride and 0.1 M NaOH solutions. Guanidine chloride removes non-covalently bound PGs from collagen fibrils, such as those of the echinoid spine ligament (Trotter and Koob, 1989). Since it had no discernible effect on the PM, it appears that covalently bound PGs dominate in this tissue. 0.1 M NaOH solution is the best to purify tissues from PGs.

In addition, in thin TEM sections, the 0.1 M NaOH treated sample and above all the 4M Guanidine chloride treated sample do not preserve the integrity of collagen fibrils compared to the ASW control and this represent a fundamental knowledge for the production of collagen biofilm and the further cell cultures or the challengefull construction of the smart biomaterial. In fact, the usage of this kind of fibrils could create problems in the fibril-fibril cohesion and fibril-cell attachment, so we consider it not suitable for cell cultures.

GAGs were also deeply analysed at LM using another stain, the Alcian blue, a polyvalent basic dye used to stain acidic polysaccharides such as GAGs in cartilages and other body structures, some types of mucopolysaccharides. For many of these targets it is one of the most widely used cationic dyes for both light and electron microscopy (Scott, 1970; Hayat 1993). The ionic bonding between cationic dyes and the negatively charged GAGs is generally thought to be proportional to the number of negative charges present on the GAG chain that is, both sulfate and carboxyl groups. GAGs quantification was performed with a spectrophotometric method using Alcian blue dye to stain GAGs isolated from tissue using different Alcian blue solutions at three different pH according to the principles that varying the pH, the number of negative charges available to link it can vary. In particular, at pH more acid (0.2) only molecules strictly containing the sulfate group (strongly sulfated PGs) will be coloured and at pH less acid (5.6) molecules

containing the sulfate group (strongly and weakly sulfated PGs) and molecules containing the carboxylic group will be coloured.

The spectrophotometric quantification with Alcian blue technique in the CDLs and PM of *P. lividus* showed that there is no statistical significance among GAGs content in the same mechanical state at different pH and GAGs content in the different mechanical states at the same pH. This means that the strongly sulfated GAGs and the weakly sulfated GAGs are present with the same amount in all the different mechanical states and that in each single mechanical state all the classes of sulfated GAGs are present. The only ANOVA significant tests are in CDL samples: (1) between the pH 1.4 and 5.6 in CDLs treated with ASW 15 ($p < 0.01$), this would say that in the standard state the less acid PGs/GAGs (molecules containing strongly and weakly sulfated groups and molecules containing the carboxylic group) are less represented than the ones medium acid; (2) between the compliant sample and its control at pH 5.6 ($p < 0.05$), this would say that in the "plastic" state the total amount of GAGs is higher than the one in the standard state and this is consistent with the hypothesis that when the tissue is in the compliant state there are more GAGs free to link the Alcian blue dye than the ones that are free in the standard state, since in the standard state more GAGs are involved in interfibrillar links.

This suggests that GAGs act exclusively as binding sites for effector molecules (e.g. tensilin) but the chemistry associated with MCTs is very complex and probably using this biochemical technique there are some gaps still to fill.

Furthermore, analysing the content of GAGs already associated to the isolated collagen after the extraction protocol results that in the fresh PM the GAGs amount is about 2-3 ‰, whereas in the isolated collagen fibrils the GAGs amount is very low, about 0.02 ‰. This means that the collagen extraction protocol removes most of the GAGs but those that are basic for the interaction of the fibrils with tensilin or for the biofilm production are still present. Moreover, there is no statistically significant difference in GAGs amount among the isolated fibrils after the extraction protocol and those one isolated and treated with the purification step using 4M Guanidine chloride and 0.1 M NaOH solutions. This means that the disaggregating solution removes almost all GAGs, so the step of purification is almost useless. Therefore, knowing that the purifications step partially degrades collagen fibrils making them not more suitable for biomaterial production we decided to eliminate the purification step.

PGs and GAGs were also analysed by SDS-PAGE and Western blot and the results yielded to the conclusion that the different amount of the different sized PGs is consistent with the different organization of the fibrils in the two tissues: in the CDL collagen fibrils are arranged in fibres which run parallel, whereas in the PM the fibres are arranged as a web. Therefore, in the CDL fibrils need

of medium-size PGs to link the parallel fibres whereas much larger PGs are necessary to link the web of fibres in the PM. Note that a PG migrating just above 120 kDa (decorin) is the predominant molecule in tensile samples. A PG that enters the running gel but migrates more slowly (biglycan) is present only in the stiff samples. The core proteins of these small PGs migrate close together at about 45 kDa. Large PG (aggrecan) is present in the stacking gel of compressed samples but does not form a discrete band.

From these trials arise the hypothesis that even if with the other techniques seems to be no difference in GAGs typology related to the different mechanical states, the SDS-PAGE shows that specific GAGs are always present in the tissue but only in the stiffening state is possible that one other GAG is produced or released or anyway detectable by Alcian blue dye.

FIBRILLIN

The mechanical integrity and strength of the ECM is provided by collagen fibres. However, they are delimited by a network of fibrillin containing-microfibrils, which is the elastic component of MCTs (similar structures were already identified in the sea cucumber dermis) providing resilience but also helping, for example, CDL to re-shorten after elongation (Wilkie, 2005).

The protein fibrillin is a major component of the beaded microfibrils of mammals and 10-14 nm microfibrils from the fibrillin family have been described for a number of animal species, both vertebrates and invertebrates (Sakai et al., 1991; Thurmond et al., 1997). With only slight differences, they have similar morphologies in electron micrographs of tissue sections from *C. frondosa* (Thurmond et al., 1997), lobster (Davison et al., 1995), and mammals (Inoue and Leblond, 1986). A partial sequence of a jellyfish fibrillin gene has also been published (Reber-Mullet et al., 1995), suggesting the evolutionary conservation of the fibrillin domain of this protein.

Extraction of *P. lividus* CDLs with 6 M Guanidine chloride analysed by SDS-PAGE gels stained with Coomassie blue revealed the presence of a band at about 350 kDa as expected according to literature data (Sakai et al., 1991; Thurmond et al., 1997).

Extensive extraction and collagenase degradation of *P. lividus* PM failed to extract a fibrillin-like molecule, and left an insoluble microfibrillar residue, probably due to strong links between fibrillin and collagen that need of a different chemical approach to be isolated.

This protein must be further analysed in echinoderm mutable tissue to discover its real function in this complex system.

TENSILIN AND AGGREGATION ASSAY

A partial *P. lividus* tensilin cDNA was amplified from the PM using primers based on the EST clone available in the GenBank database. A lot of attempts were made do complete the 3' end and the ORF but only the EST sequence was identified. It is possible to hypothese that the cause is a self-folding inner to the 3' end of the sequence that is a sequence bending on itself at the level of the 3' end for unknown causes. This makes impossible the annealing step of the primers to the 3' tail and so the amplification itself. Or it can be a mismatching of the primer, that is the lack of a perfect correspondence between the azotate bases of the primer and those one of the sequence, and this entails the interruption of the PCR reaction.

I also tried to complete the *P. lividus* ORF designing degenerate primers constructed in the three regions of high homology after the alignment of *C. frondosa* tensilin and *S. purpuratus* 'predicted similar to tensilin' sequences. Finally, I found just one sequence that shows a high homology with *S. purpuratus* similar to C1qBP (complement component 1, q subcomponent binding protein). In *H. sapiens* the C1qBP is a 282 AA protein whose specific function is unknown, but is known that it acts to the immune system level linking the head of the immunity complex C1q and inhibiting the activation of the C1 subunit. It is very interesting to note that our sequence, similar to C1qBP, has a very high sequence homology with *S. purpuratus* TIMP 1. Furthermore, C1q, the protein inactivated by C1qBP, has a sequence collagen-like recognized by MMPs which, cutting at this level, can inactive C1q (Ruiz et al., 1999). Hence, becomes plausible to hypothese that our sequence similar to C1qBP, even if is a protein that normally belongs to the immunity system, in *P. lividus* could execute a role to MCT level. However, this hypothesis must be confirmed considering the deep complexity of the entire MCT system.

Regarding *S. purpuratus* tensilin protein, a full-length tensilin cDNA was isolated from the PM by means of RT-PCR using gene-specific primers designed on the sequence available in the GenBank database. A second round of amplification was performed using an aliquot of the first reaction with two adapter primers in order to include in the amplicon the 5' and 3' sequences necessary for the following *in vitro* translation. The cDNA was gel-purified and *in vitro* translated using the EasyXpress Insect Kit II according to the manufacturer's specifications.

Repeating and modifying the protocol by Trotter et al. (1996) for he fibril aggregation assay was possible to observe only the presence of little clots, very small, but unstable and once that the stirring was stopped the collagen solutions became again homogeneous. The explanations are different: the *in vitro* produced tensilin could not have the same function or the same efficiency or could not work alone. MCTs confirmed themselves as a complex model that is almost difficult to

reproduce in a detailed way and even if each single component can be isolated, then is difficult to recombine all of them and recreate the whole system functioning.

BIOMECHANICAL ANALYSIS WITH RHEOLOGY

The Rheometer Kinexus Malvern with geometry CP 0.5/40 SR0432 SS and solvent trap 55mm C0127 SS was used to analyse the rheological properties of the insoluble and soluble collagen isolated from the *P. lividus* PM and bovine ultrapure collagen and samples made mixing all the collagens with all the chromatographic fractions. Were performed the following viscometry tests: (1) Table of shear rates log; (2) Shear rate ramp log isothermal; (3) Shear stress ramp with yield stress analysis and the following oscillation test: Amplitude sweep stress controlled with LVER determination for low viscosity materials. From this new approach arose very interesting preliminary results.

By observing the behaviour of the two collagens, it is possible to say that: increasing the shear rate, since the shear rate is a measurement of how fast the sample is flowing, the *P. lividus* insoluble collagen at 25°C is less viscous than the bovine collagen, on the contrary, parity in shear strain rate at 37°C, the insoluble *P. lividus* collagen is 10 times more viscous than the bovine one; when shear rate ramp time is constant (2 minutes) at 25°C, the *P. lividus* insoluble collagen reaches the same viscosity of the soluble ultrapure bovine collagen with a lower shear stress, on the contrary, at 37°C the *P. lividus* insoluble collagen reaches the same viscosity of the soluble ultrapure bovine collagen with a higher shear stress; at 25°C by increasing in 1 minute the shear stress, the viscosity trends of the *P. lividus* insoluble collagen and of the bovine soluble ultrapure collagen are both linear, with monotonically decreasing curves but the *P. lividus* viscosity is lower than the bovine one, on the contrary, at 37°C the viscosity pattern of the *P. lividus* insoluble collagen is much higher than the bovine one and shows an extraordinary behaviour reaching a viscosity of $1.471\ 10^3$ Pa*s. In conclusion comparing how the two collagens behave in the same mechanical conditions we can conclude that when the bovine collagen has a more constant and predictable response the *P. lividus* one reacts every time with an “extreme” response.

The two collagen were also analysed in LVER because in this region the modulus of the material will appear constant at a constant frequency (the linear region is dependent upon frequency, it attenuates at higher frequencies), but outside of this region the material’s response is non-linear. The resulting graph can give an indication of stability: while sample structure is maintained, the complex modulus (G*) is constant; when the applied stress becomes too high, breakdown occurs and the modulus decreases. G*(Pa) shows the measured sample’s stiffness. In

our experiments the measures at the two temperatures are comparable and it can be concluded that the *P. lividus* insoluble collagen at 25 and 37°C shows behaviour that is solid alike, whereas the bovine collagen shows behaviour that is liquid alike.

Analysing the response of the bovine and echinoderm collagens for the same test at the two temperatures: with the table of shear rates log test is evident that the viscosity properties of this material at 37°C are higher than the ones at 25°C; with the shear rate ramp log isothermal test results that the two curves are overlapped; whereas with the shear stress ramp with yield stress analysis for bovine collagen the viscosity properties at 25°C are higher than the ones at 37°C, on the opposite, for echinoderm collagen the viscosity properties 37°C are clearly higher than the ones at 25°C. So, it seems that working in constant shear rate the two materials have both a higher viscosity at 37°C, whereas working in constant shear stress the bovine collagen has a higher viscosity at 25°C and the *P. lividus* collagen has a higher viscosity at 37°C.

Viscometry tests were performed in order to analyse the rheological properties of the insoluble and soluble collagen isolated from the *P. lividus* PM and bovine ultrapure collagen after adding the chromatographic fractions isolated from PMs with the anion exchange chromatography. These experiments were done in the prospective to discover new effector proteins able to stiffen the collagen as stiparin and tensilin do. Analysing the bovine and echinoderm collagen behaviours at 25°C adding 100 µl of chromatographic fraction: increasing the shear rate the *P. lividus* insoluble collagen is less viscous than the bovine collagen but when an aliquot of chromatographic fraction is added to the sample *P. lividus* insoluble collagen exhibit an increased viscosity; using the shear rate ramp log isothermal test, it results that the viscosity trend of the *P. lividus* insoluble collagen plus chromatographic fraction shows the same viscosity of the other samples for an higher shear stress; using the shear stress ramp with yield stress analysis, it results that the viscosity trends of the bovine soluble ultrapure collagen with or without chromatographic fraction are both linear, with monotonically decreasing curves, on the contrary, the *P. lividus* insoluble collagen plus chromatographic fraction behaviour is higher than all the other samples with a trend completely opposite to the *P. lividus* insoluble collagen at 37°C one. Concluding, we extracted some fractions from *P. lividus* PM that contain effectors molecules which can modify the standard properties of collagen in particular increasing its normal viscosity.

Furthermore, adding the chromatographic fraction to collagen, I was expecting a sort of “aggregation” visible by eye but the collagen fibril aggregation reported in literature usually results in a low viscosity. The general aggregation usually can occur with high dimension and low density (high viscosity) clots or low dimension and high density (low viscosity) clots. In our case was

possible to observe high dimension and low density (high viscosity) clots, and this is in contrast with what Tamori et al. (2003) have found working with tensilin.

Conclusions

There has been a significant expansion in knowledge about the molecular organisation of MCT in the last few years. Most relevant in mutability is the isolation and characterisation to varying extents of a number of molecules that contribute to, or influence, interfibrillar cohesion. In addition, it is a concern that these studies have been performed on a small numbers of structures and species; so it is not known how representative these results are in terms of MCTs features and behaviours in the whole phylum. There is, in particular, a notable scarcity of information on the molecular biology of *P. lividus* and of MCTs in general.

Although there are some gaps in the bulk of information related to MCTs, the potential to undergo rapid, drastic and reversible changes in their passive mechanical properties makes the MCTs a source of inspiration and a possible supply of marine-derived resources for the ex-novo design and development of biomimetic smart materials: these latter could be potentially used for *in vitro* and *in vivo* applications whenever a controlled and reversible plasticization and/or stiffening of the biomaterial (film, 3D scaffold, etc…) is required.

Biomimicry is a promising discipline of Biotechnology addressed to novel material design inspired by animal tissues and has potential applications even in the field of tissue engineering and regenerative medicine. The MIMESIS project, of which this thesis is an integral part, has being developed within this scientific context. In this project we take inspiration from natural tissues belonging to very common marine invertebrates, echinoderms, with the final perspective to promote them and their particular connective tissues as promising models for developing innovative biomimetic biomaterials.

References

- Allen T.D., Schor S.L., Schor A.M. (1984). An ultrastructural review of collagen gels, a model system for cell–matrix, cell–basement membrane and cell-cell interactions. Scanning Electron Microscopy, 1: 375-390.
- Andrietti F., Candia Carnevali M.D., Wilkie I.C., Lanzavecchia G., Melone G., Celentano F.C. (1990). Mechanical analysis of the sea urchin lantern: the overall system in *Paracentrotus lividus*. Journal of Zoology, 220: 345-366.
- Barbaglio A., Tricarico S., Ribeiro A., Ribeiro C., Sugni M., Di Benedetto C., Wilkie I.C., Barbosa M., Bonasoro F., Candia Carnevali M.D. (2012). The mechanically adaptive connective tissue of echinoderms: its potential for bio-innovation in applied technology and ecology. Marine Environmental Research, 76: 108-113.
- Barocas V.H., Moon A.G., Tranquillo R.T. (1995). The fibroblast-populated collagen microsphere assay of cell traction force - Part 2: Measurement of the cell traction parameter. Journal of Biomechanical Engineering, 11: 161-170.
- Belbachir K., Noreen R., Gouspillou G., Petibois C. (2009). Collagen types analysis and differentiation by FTIR spectroscopy. Analytical and Bioanalytical Chemistry, 395: 829-837.
- Bergman I., Loxley R. (1963). Two improved and simplified methods for the spectrophotometric determination of hydroxyproline. Analytical Chemistry, 35(12): 1961-1965.
- Birk D.E., Fitch J.M., Babiarz J.P., Linsenmayerr T.E. (1988). Collagen Type I and Type V are present in the same fibril in the avian corneal stroma. The Journal of Cell Biology, 106: 999-1008.
- Bonasoro F., Candia Carnevali M.D., Wilkie I.C. (1995). The peristomial membrane of regular sea-urchins: functional morphology of the epidermis and coelomic lining in *Paracentrotus lividus* (Lamarck). Bollettino di Zoologia, 62: 121-135.
- Brinckmann J., Notbohm H., Müller P. (2005). Collagen: primer in structure, processing, and assembly. In: Brinckmann J., Notbohm H., Müller P.K. (eds), Topics In Current Chemistry Volume 247. Springer-Verlag, Berlin Heidelberg.
- Brockes J.R., Kumar A. (2008). Comparative aspects of animal regeneration. Annual Review of Cell and Developmental Biology, 24: 525-549.

- Brusca R.C., Brusca G.J. (1990). Invertebrates 2nd ed. Sinauer Associates, Sunderland, MA.
- Burke R.D., Bouland C., Sanderson A.I. (1989). Collagen diversity in the sea urchin, *Strongylocentrotus purpuratus*. Comparative Biochemistry and Physiology – Part B, 94(1): 41-44.
- Candia Carnevali M.D., Bonasoro F., Andrietti F., Melone G., Wilkie I.C. (1990). Functional morphology of the peristomial membrane of regular sea-urchins: structural organization and mechanical properties in *Paracentrotus lividus*. In: De Ridder C., Dubois P., LaHaye P., Jangoux M. (eds), Echinoderm research: proceedings of the 2nd European Conference on Echinoderms, pp. 207-216. Balkema, Rotterdam.
- Candia Carnevali M.D., Wilkie I.C. (1992). Gli straordinari tessuti connettivi degli echinodermi. Le scienze, 86: 59-70.
- Candia Carnevali M.D., Bonasoro F. (2001)a. Introduction to the biology of regeneration in echinoderms. Microscopy Research and Technique, 55: 365-368.
- Candia Carnevali M.D., Bonasoro F. (2001)b. Microscopic overview of crinoid regeneration. Microscopy Research and Technique, 55(6): 403-426.
- Canty E., Kadler K. (2002). Collagen fibril biosynthesis in tendon: a review and recent insights. Comparative Biochemistry and Physiology – Part A, 133: 979-985.
- Castillo J., Smith D., Vidal A., Sierra C. (1995). Catch in the primary spines of the sea urchin *Eucidaris tribuloides*: a brief review and a new interpretation. The Biological Bulletin, 188: 120-127.
- Cluzel C., Lethias C., Garrone R., Exposito J.Y. (2000). Sea urchin fibrillar collagen 2 α chain participates in heterotrimeric molecules of (1α)22α stoichiometry. Matrix Biology, 19: 545-547.
- Cluzel C., Lethias C., Garrone R., Exposito J.Y. (2003). Distinct maturations of n-propeptide domains in fibrillar procollagen molecules involved in the formation of heterotypic fibrils in adult sea urchin collagenous tissues. Journal of Biological Chemistry, 279: 9811-9817.
- Davison I.G., Wright G.M., DeMont M.E. (1995). The structure and physical properties of invertebrate and primitive vertebrate arteries. Journal of Experimental Biology, 198: 2185-2196.
- Djabourov M., Lechaire J.-P., Gaill F. (1993). Structure and rheology of gelatin and collagen gels. Biorheology, 30: 191-205.

- Emson R.H. (1984). Bone idle - A recipe for success?. In: Keegan B.F., O'Connor B.D.S. (eds), Echinodermata: Proceedings 5th International Echinoderm Conference, Galway, pp. 25-30. Balkema, Rotterdam.
- Erlinger R., Welsch U., Scott J.E. (1993). Ultrastructural and biochemical observations on proteoglycans and collagen in the mutable connective tissue of the feather star *Antedon bifida* (Echinodermata, Crinoidea). Journal of Anatomy, 183: 1-11.
- Exposito J.Y., Cluzel C., Garrone R., Lethias C. (2002). Evolution of collagens. The Anatomical Record, 268: 302-316.
- Exposito J.Y., Valcourt U., Cluzel C., Lethias C. (2010). The fibrillar collagen family. International Journal of Molecular Sciences, 11: 407-426.
- Fisher L.W., Whitson S.W, Avioh L.V., Termine J.D. (1983). Matrix sialoprotein of developing bone. The Journal of Biological Chemistry, 258: 12723-12727.
- Hayashi Y., Motokawa T. (1986). Effects of ionic environment on viscosity of catch connective tissue in holothurian body wall. Journal of Experimental Biology, 125: 71-84.
- Hayat M.A. (1993). Stains and Cytochemical Methods. In: Hayat M.A (eds), Chapter 8, pp. 80. Plenum Press, New York, NY.
- Hickman C.P. Jr., Roberts L.S., Larson A. (2001). Integrated principles of zoology. 11th ed. McGraw-Hill, Boston.
- Hidaka M., Takahashi K. (1983). Fine structure and mechanical properties of the catch apparatus of the sea-urchin spine, a collagenous connective tissue with muscle-like holding capacity. Journal of Experimental Biology, 103: 1-14.
- Hill R. (2001). Role of Ca^{2+} in excitation-contraction coupling in echinoderm muscle: comparison with role in other tissues. Journal of Experimental Biology, 204: 897-908.
- Inoue S., Leblond C.P. (1986). The microfibrils of connective tissue: I. Ultrastructure. American Journal of Anatomy, 176: 121-138.
- Jeffrey D.R., Watt I. (2003). Imaging hyaline cartilage. British Journal of Radiology, 76: 777-787.
- Junqueira L. (1983). Biology of collagen-proteoglycan interaction. Japanese Archives of Histology, 46: 589-629.
- Karlsson M., Björnsson S. (2001). Quantitation of proteoglycans in biological fluids using Alcian Blue. In: Walker J.M., Iozzo R.V. (eds), Methods in Molecular Biology, Vol. 171, Proteoglycan Protocols, pp. 159-173. Humana Press, Clifton, NJ.

- Koob T.J., Koob-Emunds M.M., Trotter J.A. (1999). Cell-derived stiffening and plasticizing factors in sea cucumber (*Cucumaria frondosa*) dermis. Journal of Experimental Biology, 202: 2291-2301.
- Laemmli U.K. (1970). Cleavage of structural proteins during the assembly of the head of bacteriophage T4. Nature (London), 227: 680-685.
- Lanzavecchia G., Candia Carnevali M.D., Melone G., Celentano F.C, Andrietti F. (1988). Aristotle's lantern in the regular sea urchin *Paracentrotus lividus*. I. Functional morphology and significance of bones, muscles and ligaments. In: Burke R.D., Mladenov P.V., Lambert P., Parsley R.L. (eds), Echinoderm biology, pp. 649-662. Balkema, Rotterdam.
- Lowry O.H., Rosebrough N.J., Farr A.L., Randall R.J. (1951). Protein measurement with the Folin phenol reagent. Journal of Biological Chemistry, 193: 265-275.
- Matsumura T. (1973). Shape, size and amino acid composition of collagen fibril of the starfish *Asterias amurensis.* Comparative Biochemistry and Physiology – Part B, 44(4): 1197-1205.
- Matsumura T. (1974). Collagen fibrils of the sea cucumber, *Stichopus japonicus*: purification and morphological study. Connective Tissue Research, 2: 117-125.
- Matsumura T., Shinmei M., Nagai Y. (1973). Disaggregation of connective tissue: preparation of fibrous components from sea cucumber body wall and calf skin. Journal of Biochemistry, 73: 155-162.
- Meisenberg G., Simmons W.H. (2006). Principles of medical biochemistry. Elsevier Health Sciences, pp. 243.
- Meyers M.A., Chawla K.K. (1999). Mechanical behaviour of materials. Cambridge University Press, London.
- Milligan (1946). Trichrome stain for formalin-fixed tissue. American Journal of Clinical Pathology, Technical Section, 10: 184-185.
- Morales M., Del Castillo J., Smith D.S. (1989). Acetylcholine sensitivity of the spine-test articular capsule of the sea-urchin *Eucidaris tribuloides*. Comparative Biochemistry and Physiology – Part C, 94: 547-554.
- Motokawa T. (1984). Connective tissue catch in echinoderms. Biology Reviews, 59: 255-270.
- Motokawa T. (1988). Catch connective tissue: a key character for Echinoderm's success. Echinoderm biology. In: Burke R.D., Mladenov P.V., Lambert P., Parsley R.L. (eds), Echinoderm biology, pp. 39-54. Balkema, Rotterdam.

- Motokawa T., Tsuchi A. (2003). Dynamic mechanical properties of body-wall dermis in various mechanical states and their implications for the behaviour of sea cucumbers. Biological Bulletin, 205: 261-275.
- Nagase H., Wöessner J.F. Jr. (1999). Matrix Metalloproteinases. The Journal of Biological Chemistry, 271: 21491-21494.
- Ottani V., Raspanti M., Ruggeri A. (2001). Collagen structure and functional implications. Micron, 32: 251-260.
- Petibois C., Gouspillou G., Wehbe K., Delage J.-P., Déléris G. (2006). Analysis of type I and IV collagens by FT-IR spectroscopy and imaging for a molecular investigation of skeletal muscle connective tissue. Analytical and Bioanalytical Chemistry, 386: 1961-1966.
- Pucci-Minafra I., Galante R. (1978). Identification of collagen in the Aristotle's lantern of *Paracentrotus lividus*. Journal of Submicroscopic Cytology, 10: 53-63.
- Rabilloud T. (1999). Silver staining of 2-D electrophoresis gels. Methods in Molecular Biology, 112: 297-305.
- Raspanti M., Viola M., Forlino A., Tenni R., Gruppi C. (2008). Glycosaminoglycans show a specific periodic interaction with type I collagen fibrils. Journal of Structural Biology, 164: 134-139.
- Reber-Mullet S., Spissinger T., Schuchert P., Spring J., Schmid V. (1995). An extracellular matrix protein of jellyfish homologous to mammalian fibrillins forms different fibrils depending on the life stage of the animal. Developmental Biology, 169: 662-672.
- Revenko I., Sommer F., Tran Minh D., Garrone R., Franc J.-M. (1994). Atomic force microscopy study of the collagen fibre structure. Biology of the Cell, 80: 67-69.
- Ribeiro A.R., Barbaglio A., Oliveira M., Santos R., Coelho A.V., Ribeiro C.C., Wilkie I.C., Candia Carnevali M.D., Barbosa M. (2012)a. Correlations between the biochemistry and mechanical states of a sea-urchin ligament: a mutable collagenous structure. Biointerphases, 7: 38.
- Ribeiro A.R., Barbaglio A., Oliveira M., Ribeiro C.C., Wilkie I.C., Candia Carnevali M.D., Barbosa M. (2012)b. Metalloproteinases in a sea urchin ligament with adaptable mechanical properties. PLOS ONE, in press.
- Robinson J.A. (1997). Comparative biochemical analysis of sea urchin peristome and rat-tail tendon collagen. Comparative Biochemistry and Physiology – Part B, 117: 307-313.
- Ruiz S., Henschen-Edman A.H., Nagase H., Tenner A.J. (1999). Digestion of C1q collagen-like domain with MMPs-1, -2, -3, and -9 further defines the sequence involved in the

stimulation of neutrophil superoxide production. Journal of Leukocyte Biology, 66: 416-422.

- Ruppert E.E., Fox R.S., Barnes R.D. (2007). Zoologia degli invertebrati. Un approccio funzionale evoluzionistico. In: Piccin (eds), pp. 1098. Piccin Nuova Libreria, Padova.
- Sakai L.Y, Keene D.R., Glanville R., Bachinger H.P. (1991). Purification and partial characterization of fibrillin, a cysteine-rich structural component of connective tissue microfibrils. The journal of biological chemistry, 266(22): 14763-14770.
- Santos R., Haesaerts D., Jangoux M., Flammang P. (2005). The tube feet of sea urchins and sea stars contain functionally different mutable collagenous tissues. Journal of Experimental Biology, 208: 2277-2288.
- Schowalter W.R. (1978). Mechanics of Non-Newtonian Fluids. Pergamon Press, Oxford.
- Scott J.E. (1970). Histochemistry of Alcian blue. Histochemie, 21: 277-285.
- Scott J.E. (1995). Extracellular matrix, supramolecular organisation and shape. Journal of Anatomy, 187: 259-269.
- Scott J.E., Orford C.R. (1981). Dermatan sulphate-rich proteoglycan associates with rat tail-tendon collagen at the d band in the gap region. Biochemical Journal, 197(1): 213-216.
- Scott J.E., Thomlinson A.M. (1998). The structure of interfibrillar proteoglycan bridges (shape modules) in extracellular matrix of fibrous connective tissues and their stability in various chemical environments. Journal of Anatomy, 192: 391-405.
- Sheehan D.C., Hrapchak B.B. (1980). Theory and practice of histotechnology 2nd ed. Battelle Press, Ohio.
- Shoulder M.D., Raines R.T. (2009). Collagen Structure and Stability. Annual Review of Biochemistry, 78: 929-958.
- Shpigel M., McBride S.C., Marciano S., Lupatsch I. (2004). The effect of photoperiod and temperature on the reproduction of European sea urchin *Paracentrotus lividus*. Aquaculture, 232(1-4): 343-355.
- Silver F.H., Landis W.J. (2008). Viscoelasticity, energy storage and transmission and dissipation by extracellular matrices in vertebrates. In: P. Fratzl (eds), Collagen: Structure and Mechanics, pp. 133-153. Springer, New York.
- Sterling K.A., Shuster S.M. (2011). Rates of fission in *Aquilonastra corallicola Marsh* (Echinodermata: asteroidea) as affected by population density. Invertebrate Reproduction and Development, 55(1): 1-5.

- Switzer R.C.3rd, Merril C.R., Shifrin S. (1979). A highly sensitive silver stain for detecting proteins and peptides in polyacrylamide gels. Analytical Biochemistry, 98(1): 231-7.
- Szulgit G. (2007) .The echinoderm collagen fibril: a hero in the connective tissue research of the 1990s. BioEssays, 29: 645-653.
- Takemae N., Nakaya F., Motokawa T. (2009). Low oxygen consumption and high body content of catch connective tissue contribute to low metabolic rate of sea cucumbers. Biological Bulletin, 216: 45-54.
- Tamori M., Yamada A., Nishida N., Motobayashi Y., Oiwa K., Motokawa M. (2006). Tensilin-like stiffening protein from *Holothuria leucospilota* does not induce the stiffest state of catch connective tissue. Journal of Experimental Biology, 209:1594-1602.
- Tamori M., Takemae C., Motokawa T. (2010). Evidence that water exudes when holothurian connective tissue stiffens. Journal of Experimental Biology, 213: 1960-1966.
- Taşkiran D., Taşkiran E., Yercan Y., Kutay F.Z. (1999). Quantification of total collagen in rabbit tendon by the Sirius red method. Analytical Biochemistry, 150: 86-90.
- Thurmond F.A., Trotter J.A. (1996). Morphology and biomechanics of the microfibrillar network of sea cucumber dermis. Journal of Experimental Biology, 199: 1817-1828.
- Thurmond F.A., Koob T.J., Bowness J.M., Trotter J.A. (1997). Partial biochemical and immunologic characterization of fibrillin microfibrils from sea cucumber dermis. Connective Tissue Research, 36:211-222.
- Timmons B., Akins M., Mahendroo M. (2010). Cervical remodeling during pregnancy and parturition. Trends in Endocrinology and Metabolism, 21: 353-361.
- Tipper J.P., Lyons-Levy G., Atkinson M.A.L., Trotter J.A. (2003). Purification, characterization and cloning of tensilin, the collagen-fibril binding and tissue stiffening factor from *Cucumaria frondosa* dermis. Matrix Biology, 21: 625-635.
- Tomita M., Kinoshita T., Izumi S., Tomino S., Yoshizato K. (1994). Characterizations of sea urchin fibrillar collagen and its cDNA clone. Biochimica et Biophysica Acta, 1217: 131-140.
- Tricarico S., Barbaglio A., Burlini N., Del Giacco L., Ghilardi A., Sugni M., Di Benedetto C., Bonasoro F., Wilkie I., Candia Carnevali M.D. (2012). New insights into the mutable collagenous tissue of *Paracentrotus lividus*: preliminary results. In: Kroh A., Reich M. (eds), Echinoderm Research 2010: Proceedings of the 7th European Conference on Echinoderms, Zoosymposia 7, pp 279-286. Göttingen, Germany.

- Trotter J.A., Koob T.J. (1989). Collagen and proteoglycan in a sea-urchin ligament with mutable mechanical properties. Cell and Tissue Research, 258: 527-539.
- Trotter J.A., Thurmond F.A., Koob T.J. (1994). Molecular structure and functional morphology of echinoderm collagen fibrils. Cell and Tissue Research, 275: 451-458.
- Trotter J.A., Lyons-Levi G., Luna D., Koob T.J., Keene D.R., Atkinson M.A. (1996). Stiparin: a glycoprotein from sea cucumber dermis that aggregates collagen fibrils. Matrix Biology, 15: 99-110.
- Trotter J.A., Chapman J.A., Kadler K.E., Holmes D.F. (1998). Growth of sea cucumber collagen fibrils occurs at the tips and centers in a coordinated manner. Journal of Molecular Biology, 284: 1417-1424.
- Trotter J.A., Lyons-Levy G., Chino K., Koob T.J., Keene D.R., Atkinson M.A.L. (1999). Collagen fibril aggregation inhibitor from sea cucumber dermis. Matrix Biology, 18: 569-578.
- Trotter J.A., Tipper J., Lyons-Levy G., Chino K., Heuer A.H., Liu Z., Mrksich M., Hodneland C., Dillmore W.S., Koob T.J., Koob-Emunds M.M., Kadler K., Holmes D. (2000). Towards a fibrous composite with dynamically controlled stiffness: lessons from echinoderms. Biochemical Society Transactions, 28: 357-362.
- Vogel K.G., Peters J.A. (2001). Isolation of proteoglycans from tendon. In: Walker J.M., Iozzo R.V. (eds), Methods in Molecular Biology, Vol. 171, Proteoglycan Protocols, pp. 9-17. Humana Press, Clifton, NJ.
- Wada H., Okuyama M., Satoh N., Zhang S. (2006). Molecular evolution of fibrillar collagen in chordates, with implications for the evolution of vertebrate skeletons and chordate phylogeny. Evolution & Development, 8: 370-377.
- Wessel G.M., Etkin M., Benson S. (1991). Primary mesenchyme cells of the sea urchin embryo require an autonomously produced nonfibrillar collagen for spiculogenesis. Developmental Biology, 148: 261-272.
- Wilkie I.C. (1979). The juxtaligamental cells of *Ophiocomina nigra* (Abildgaard) (Echinodermata: Ophiuroidea) and their possible role in mechano-effector function of collagenous tissue. Cell and Tissue Research, 197: 515-530.
- Wilkie I.C. (1988). Design for disaster: the ophiuroid intervertebral ligament as a typical mutable collagenous structure. In: Burke R.D., Mladenov P.V., Lambert P., Parsley R.L. (eds), Echinoderm Biology, pp. 25-38. Balkema, Rotterdam.
- Wilkie I.C. (2002). Is muscle involved in the mechanical in the mechanical adaptability of the echinoderm mutable collagenous tissue? Journal of Experimental Biology, 205: 159-165.

- Wilkie I.C. (2005). Mutable Collagenous Tissue: Overview and Biotechnological Perspective. Progress in Molecular and Subcellular Biology, Subseries Marine Molecular Biotechnology. In: Matranga V. (eds), Echinodermata, pp. 221-250. Springer-Verlag, Berlin Heidelberg.
- Wilkie I.C., Emson R.H. (1987). The tendons of *Ophiocomina nigra* and their role in autotomy (Echinodermata, Ophiuroida). Zoomorphology, 107: 33-44.
- Wilkie I.C., Candia Carnevali M.D., Bonasoro F. (1992). The compass depressors of *Paracentrotus lividus* (Echinodermata, Echinoida): ultrastructural and mechanical aspects of their variable tensility and contractility. Zoomorphology, 112: 143-153.
- Wilkie I.C., Candia Carnevali M.D., Andrietti F. (1993). Variable tensility of the peristomial membrane of the sea urchin *Paracentrotus lividus* (Lamarck). Comparative Biochemistry and Physiology - Part A, 105: 493-501.
- Wilkie I.C, Candia Carnevali M.D., Andrietti F. (1994). Microarchitecture and mechanics of the sea-urchin peristomial membrane. Bollettino di Zoologia, 61: 39-51.
- Wilkie I.C., Candia Carnevali M.D., Bonasoro F. (1999). Evidence for the 'cellular calcium regulation hypothesis' from 'simple' mutable collagenous structures: the brachial and cirral syzygial ligaments of *Antedon mediterranea* (Lamarck). In: Candia Carnevali M.D. and Bonasoro F. (eds), Echinoderm Research, pp. 119-125. Balkema, Rotterdam.
- Wilkie I.C., Candia Carnevali M.D., Trotter J.A. (2004). Mutable collagenous tissue: recent progress and an evolutionary perspective. In: Heinzeller and Nebelsick (eds), Echinoderms: München, pp. 371-378. Taylor and Francis Group, London.
- Wilkie I.C., Barbaglio A., Maclaren W.M., Candia Carnevali M.D. (2010). Physiological and immunocytochemical evidence that glutamatergic neurotransmission is involved in the activation of arm autotomy in the featherstar *Antedon mediterranea* (Echinodermata: Crinoidea). Journal of Experimental Biology, 213: 2104-2115.
- Wöessner J.F.Jr. (1991). Matrix metalloproteinases and their inhibitors in connective tissue remodelling. The FASEB Journal, 5: 2145-2154.
- Yamada A., Tamori M., Iketani T., Oiwa K., Motokawa T. (2010). A novel stiffening factor inducing the stiffest state of holothurian catch connective tissue. Journal of Experimental Biology, 213: 3416-3422.
- Young R.D. (1985). The ultrastructural organization of proteoglycans and collagen in human and rabbit scleral matrix. Journal of Cell Science, 74: 95-104.
- Zani S. (1994). Analisi dei dati statistici, vol. I. Giuffrè editore, Milano

Figures

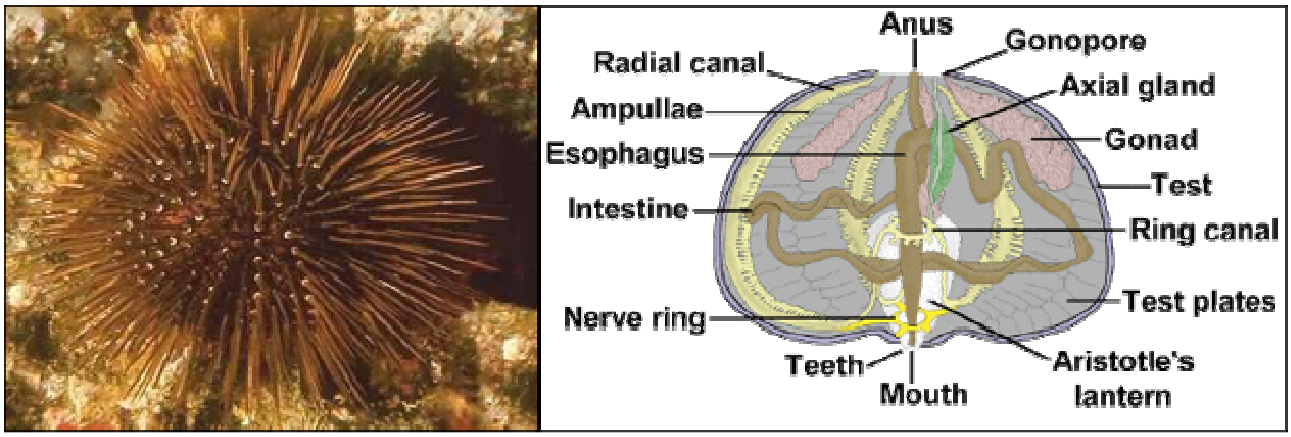

Figure 1. ***Paracentrotus lividus*****. Left: specimen of a sea urchin of the species** ***P. lividus*****. Right: aboral-oral section of a sea urchin of the species** ***P. lividus*** **with a detailed scheme of the inner organs. Brusca and Brusca, 1990.**

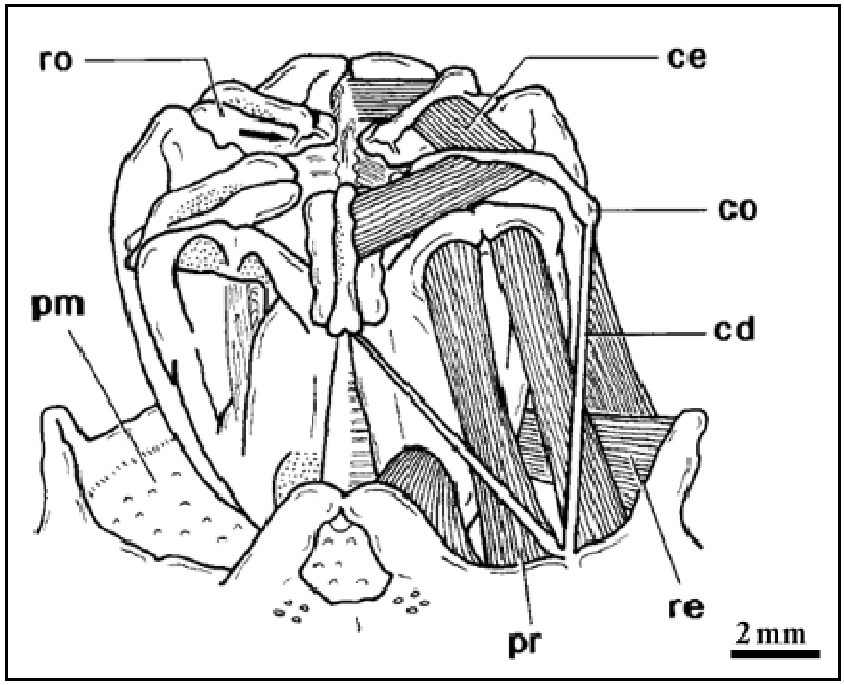

Figure 2. Diagrammatic representation of the lantern of ***P. lividus*****. The peripharyngeal coelomic membranes are omitted. Only the soft tissue components of the right side have been included; on the left side the insertion facets of the muscles are indicated by stippling, cd, compass depressor; ce, compass elevator; co, compass; pm, peristomial membrane; pr, protractor muscle; re, retractor muscle; ro, rotula. Arrow indicates one of the pair of ligaments that link the compass to the rotula. Wilkie et al., 1992.**

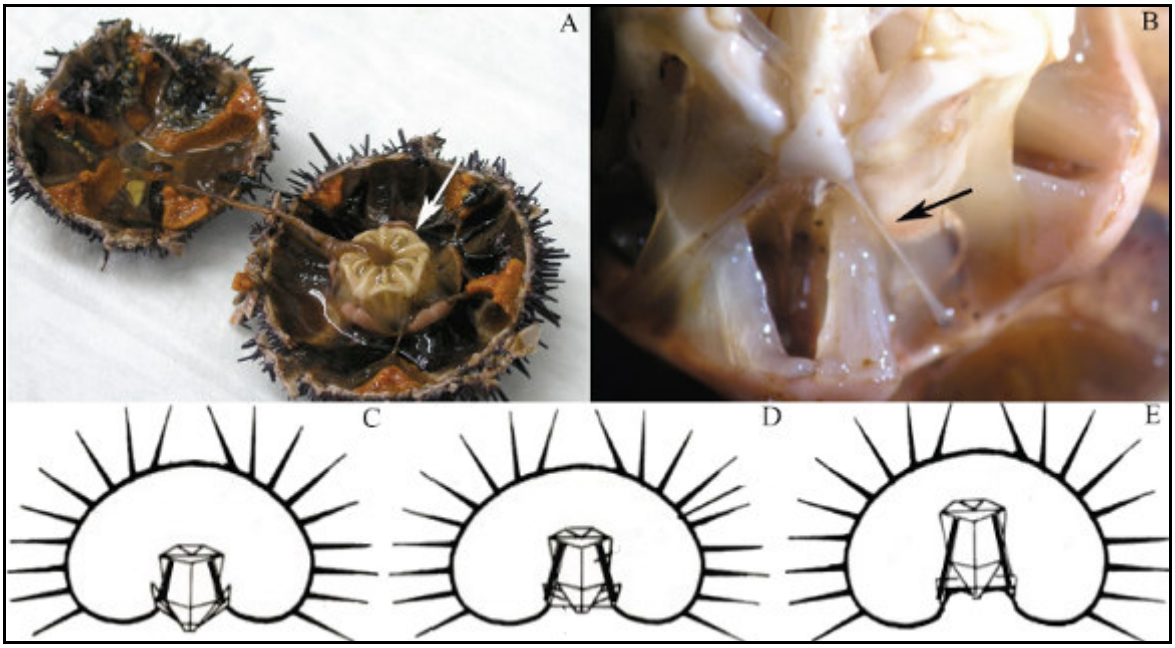

Figure 3. Anatomical relations and behaviour of CDLs. A: specimen of *P. lividus* split into two halves. The Aristotle's lantern (arrow) is observable in the oral half. B: Enlargement of the Aristotle's lantern showing the anatomical location of the CDLs (arrow). C-E: diagrams of sea urchins with lanterns in different positions; CDLs shown in black. C: Protracted position; CDLs compliant; D: Resting position; CDLs in standard state; E: Retracted position; CDLs stiff.

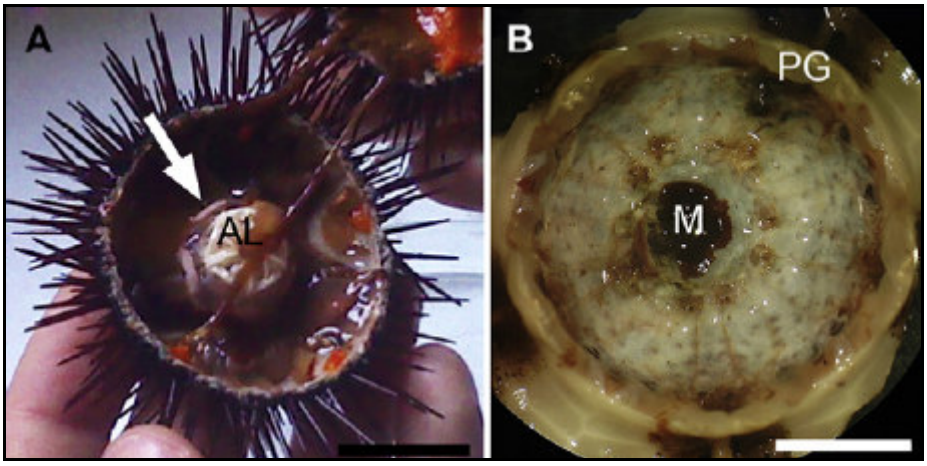

Figure 4. The PM of *P. lividus*. A: oral half of *P. lividus*. Note the buccal apparatus ("Aristotle's Lantern": AL) positioned at the centre of the PM delimited by the perignathic girdle (arrow). Bar ¼ 2 cm. B: PM of *P. lividus* after removal of the buccal apparatus. Perignathic girdle (PG), mouth (M). Bar ¼ 1 cm. Barbaglio et al., 2012.

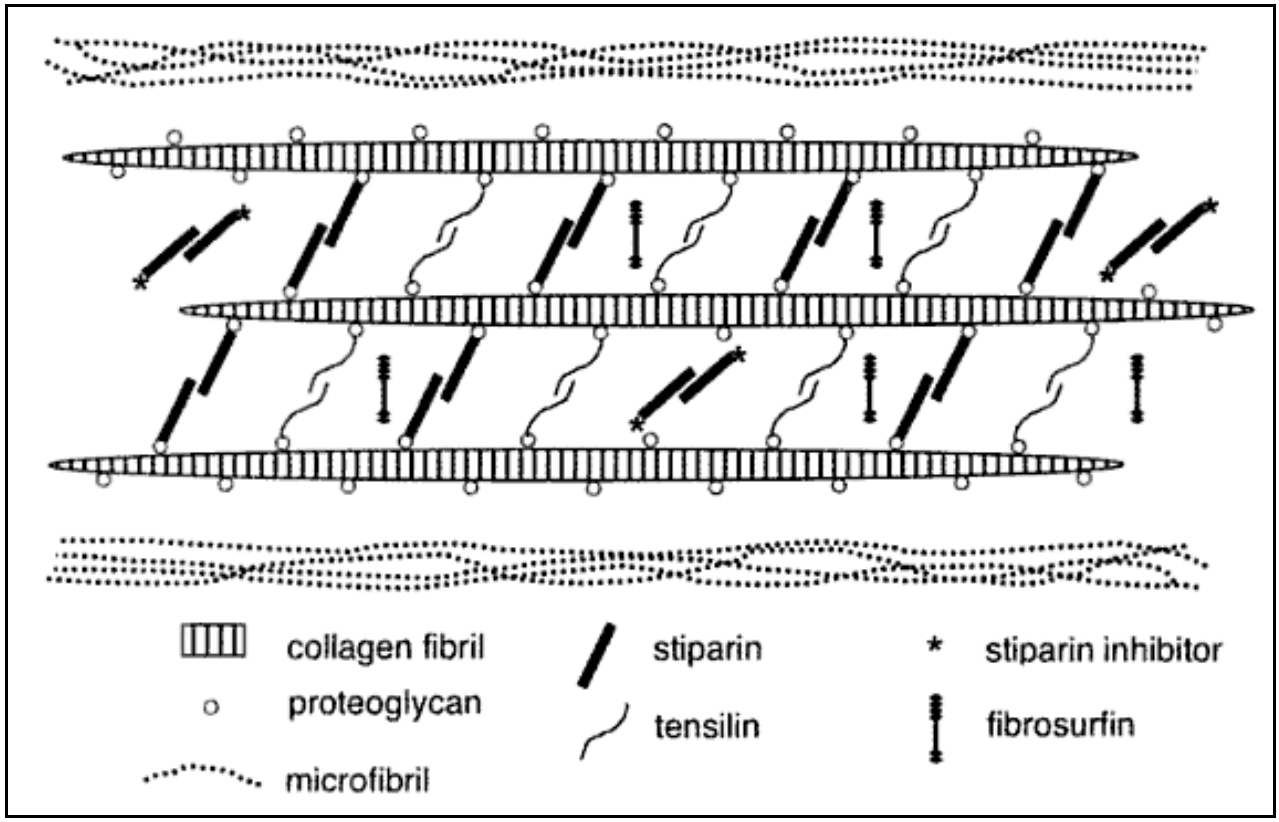

Figure 5. Model of MCT molecular organization, which is based on current evidence and assumes that the few mutable structures from which that evidence has been derived are representative. Most MCT consists of parallel aggregates of discontinuous, spindle-shaped collagen fibrils on which are attached PGs and other GAG-containing molecules whose functions include serving as binding sites for molecules responsible for interfibrillar cohesion. Amongst the latter are the proteins stiparin and tensilin, the fibril-aggregation activities of which are modified by a variety of specific inhibitors. The mechanisms by which stiparin and tensilin cause fibril aggregation are incompletely understood. For simplicity, the model assumes that they form dimers that act as interfibrillar crossbridges. Fibril bundles are delimited by loose networks of elastic fibrillin-containing microfibrils that return the tissue to its resting dimensions after it has undergone deformation when in a compliant condition. The specific functions of fibrosurfin are as yet unknown. Wilkie, 2005.

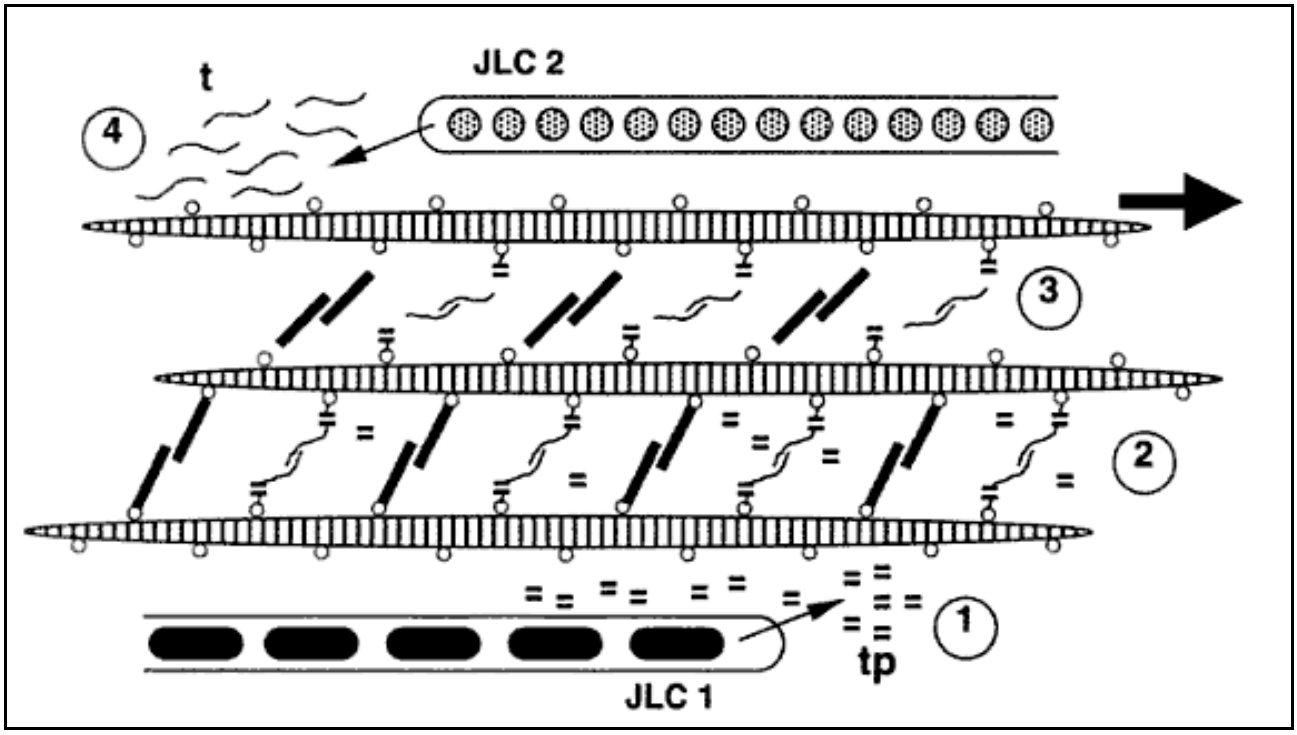

Figure 6. Model of the tensilin-tensilin protease hypothesis. MCT plasticization or destiffening results from (1) the release from, or activation by, a specific type of juxtaligamental cell (JLC 1) of tensilin protease (tp), which (2) cleaves tensilin near its GAG-binding site. This (3) allows fibrils to slide past each other, since they are held together only weakly by stiparin. Restiffening results from (4) the release of fresh tensilin (t) from a second type of juxtaligamental cell (JLC 2). MCT constituents represented as in Fig. 5. Wilkie, 2005.

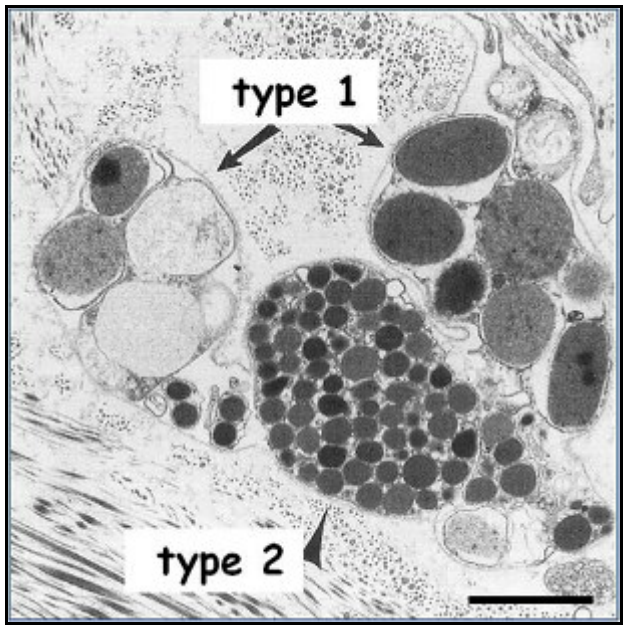

Figure 7. Electron micrograph of typical granular cells in the outer dermis. The most common granular cells contain medium-sized (arrowhead) and large (arrows) granules belonging respectively to JLC 1 and JLC 2. The collagen density is low, and the cell density is relatively high. Both panels are at the same magnification. Scale bar, 2 mm. Koob et al., 1999.

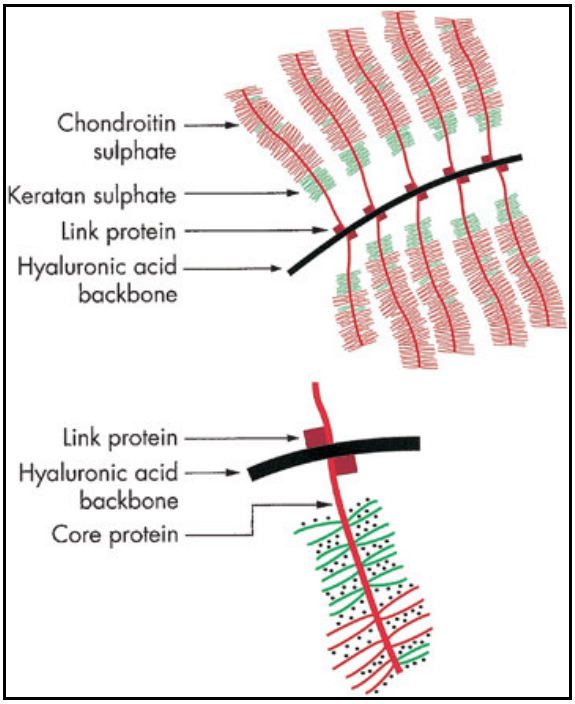

Figure 8. Schematic representation of the molecular organization of an aggregated PG molecule. Jeffrey and Watt, 2003.

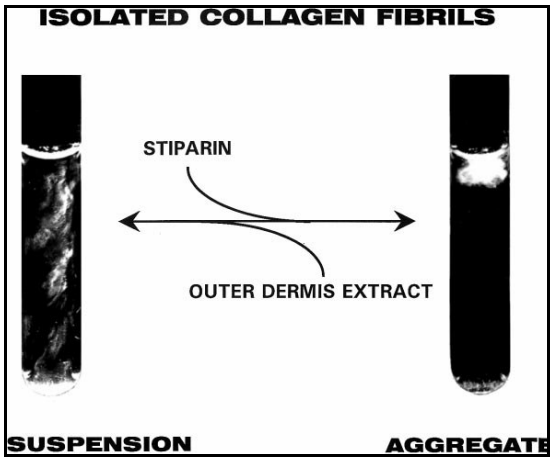

Figure 9. Collagen fibril aggregation assay. Collagen fibrils are suspended in buffered salt solutions at a concentration of 60 mg/ml of collagen. Oblique illumination shows diffuse light scattering of the suspended fibrils left. Addition of 0.25 mg of stiparin causes the fibrils to aggregate into a single clot right. Addition of outer dermis extract both inhibits and reverses the action of stiparin. Trotter et al., 1999.

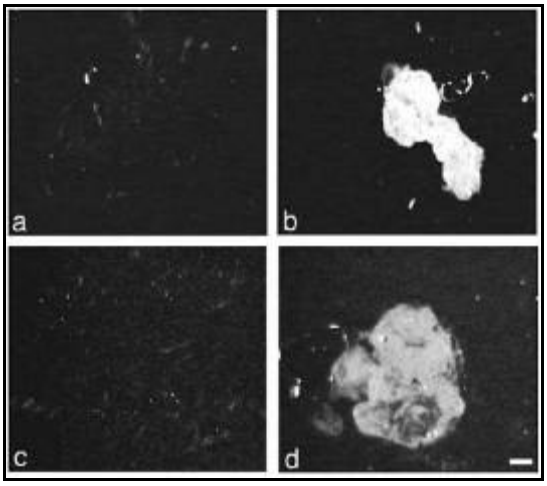

Figure 10. Collagen fibril aggregation assay in (a,b) Ca^{2+}-containing medium and (c, d) Ca^{2+}-free medium. Addition of the medium containing H-tensilin to the suspension caused the aggregation of collagen fibrils into a clot (b, d) whereas addition of the medium alone did not cause the aggregation (a, c). These dark-field light micrographs were taken at low magnification. Concentrations of collagen fibrils were the same from a to d. Scale bar, 500 µm. Tamori et al., 2006.

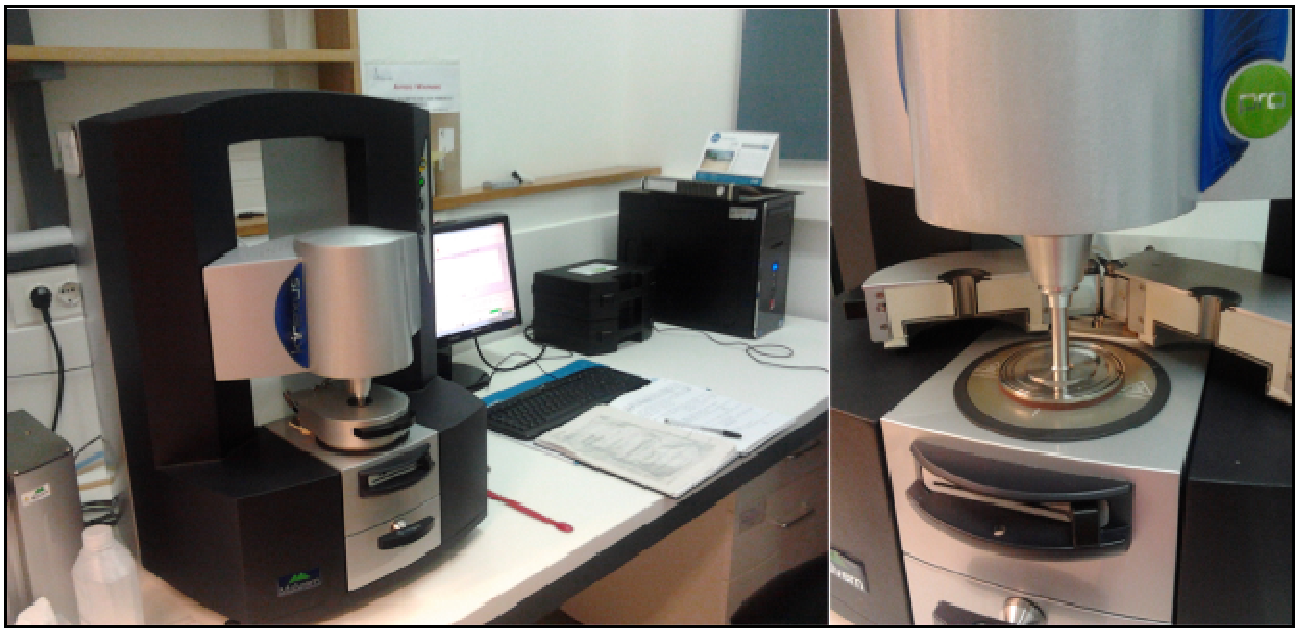

Figure 11. Marlvern Kinexus Rheometer. Left, rheometer workspace at INEB; right, detail of the rheometer with the thermic chamber opened and the come-plate geometry working on a sample.

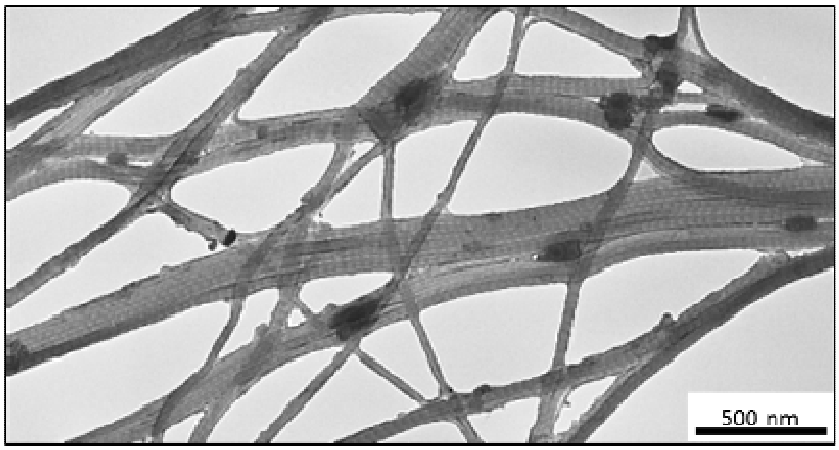

Figure 12. Transmission electron micrographs of extracted collagen fibrils from the CDL of the sea-urchin *P. lividus*. Samples were negatively stained with PTA.

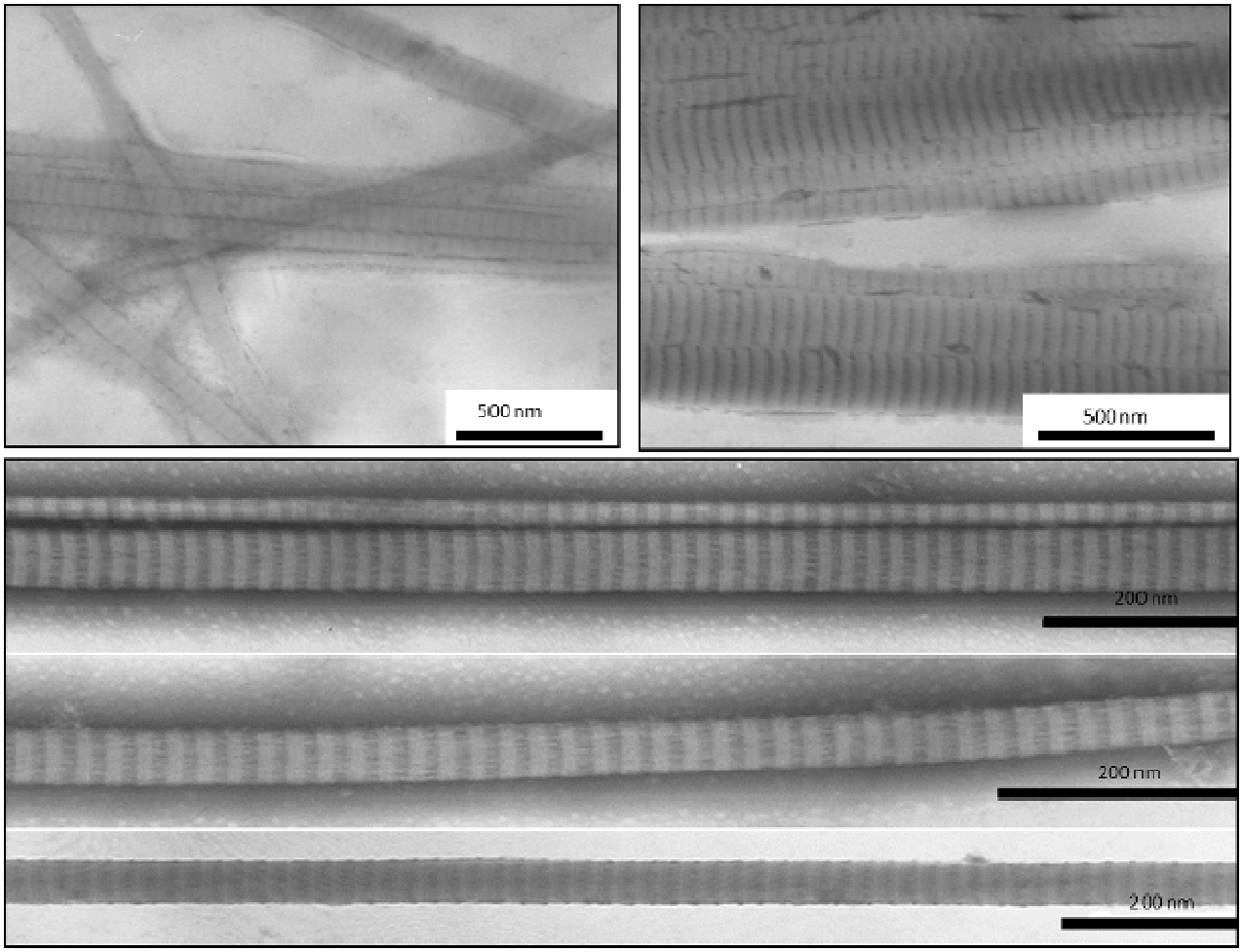

Figure 13. Transmission electron micrographs of extracted collagen fibrils from the PM of the sea urchin *P. lividus*. Samples were negatively stained with PTA.

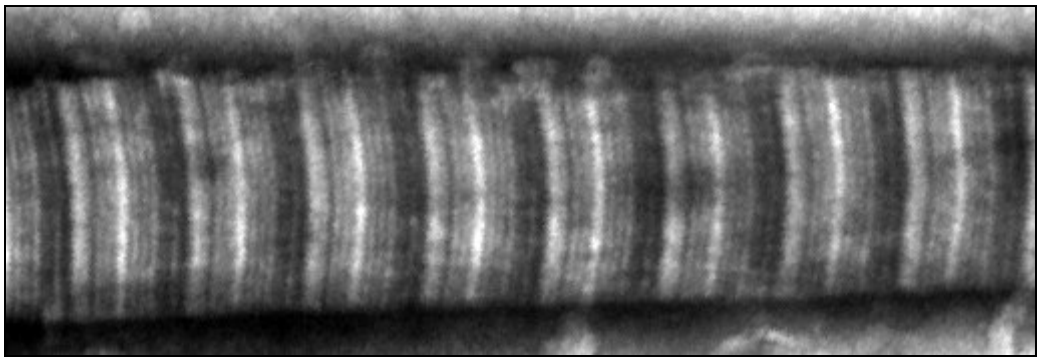

Figure 14. Transmission electron micrographs of extracted collagen fibril from the PM of the sea urchin *P. lividus.* Example of fibril used to measure the D-period.

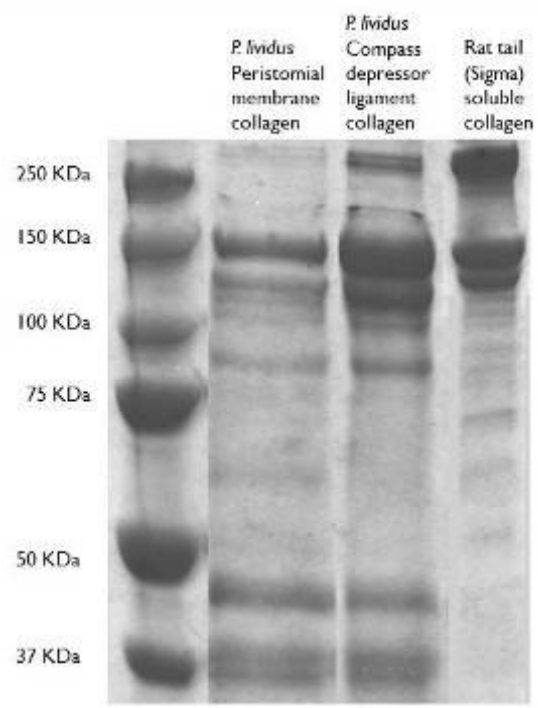

Figure 15. SDS-PAGE analysis of the *P. lividus* PM and CDL collagen. Both samples are characterized by the presence of species of apparent molecular masses 140 and 116 kDa (lane 2, 3) while the rat tail tendon preparation contained the expected species at 126 and 123 kDa (lane 4). Both preparations were also characterized by the variable presence of additional species of 55 and 53 kDa and 250 kDa.

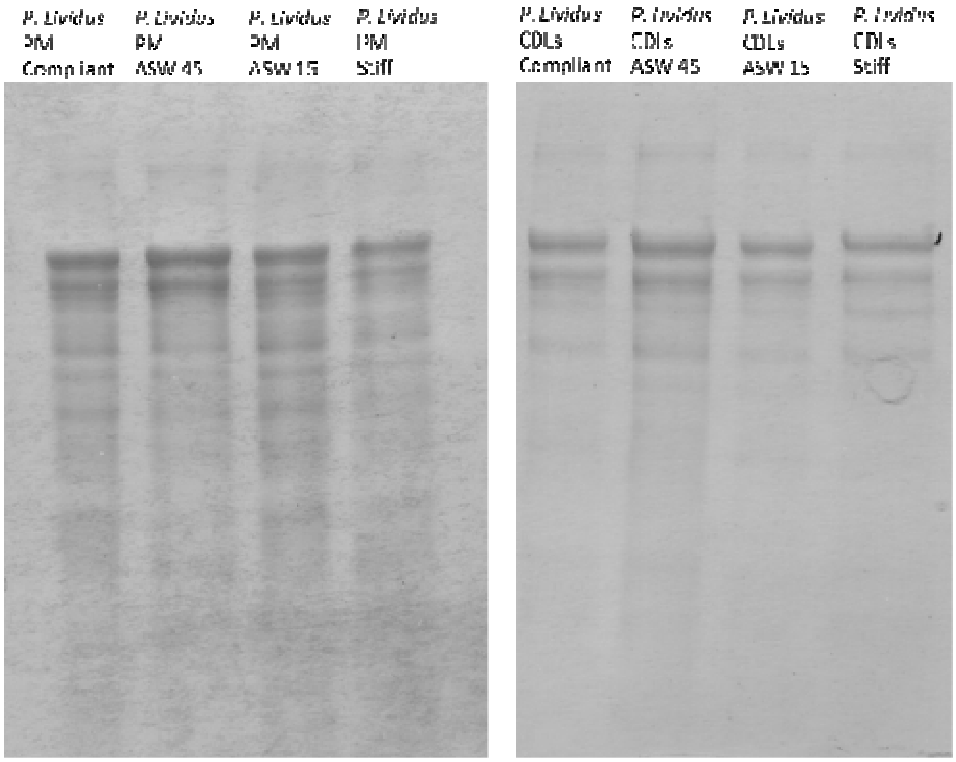

Figure 16. SDS-PAGE analysis of the *P. lividus* PM and CDL collagen isolated from tissues previously treated to induce the different mechanical states. All the samples are characterized by the presence of species of apparent molecular masses 140 and 116 kDa (lane 2, 3) independently from the mechanical state.

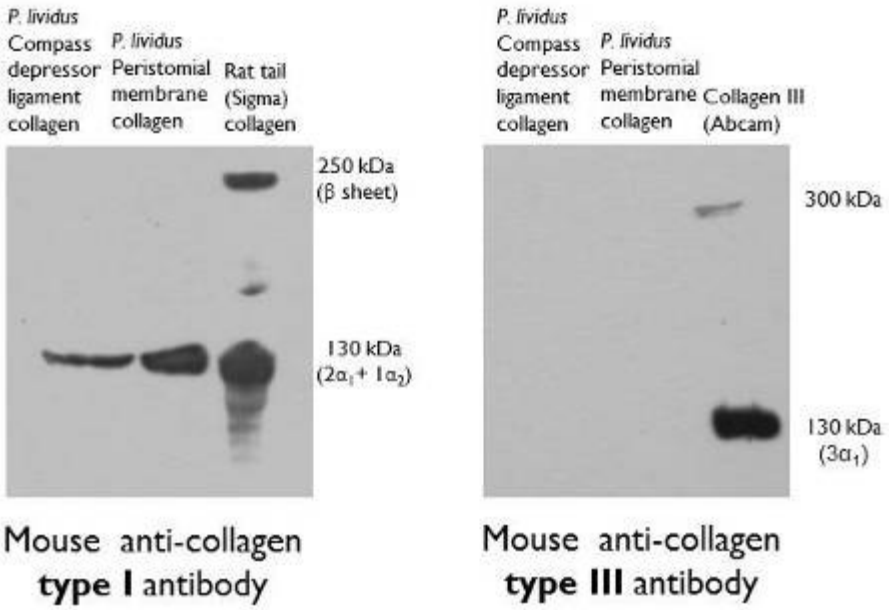

Figure 17. Western blot analysis of the *P. lividus* PM and CDL collagen. On the left *P. lividus* PM and CDL collagens were blotted with the Monoclonal Anti-Collagen Type I antibody; on the right *P. lividus* PM and CDL collagens were blotted with the Monoclonal Anti-Collagen Type III antibody. Type I collagen purified from rat tail tendon (Sigma C3867) and collagen III protein (Abcam ab 7535) were used as standards. Only the collagen III of control was recognised by the antibody. The Anti-Collagen Type III antibody did not recognise neither PM collagen nor the CDL one.

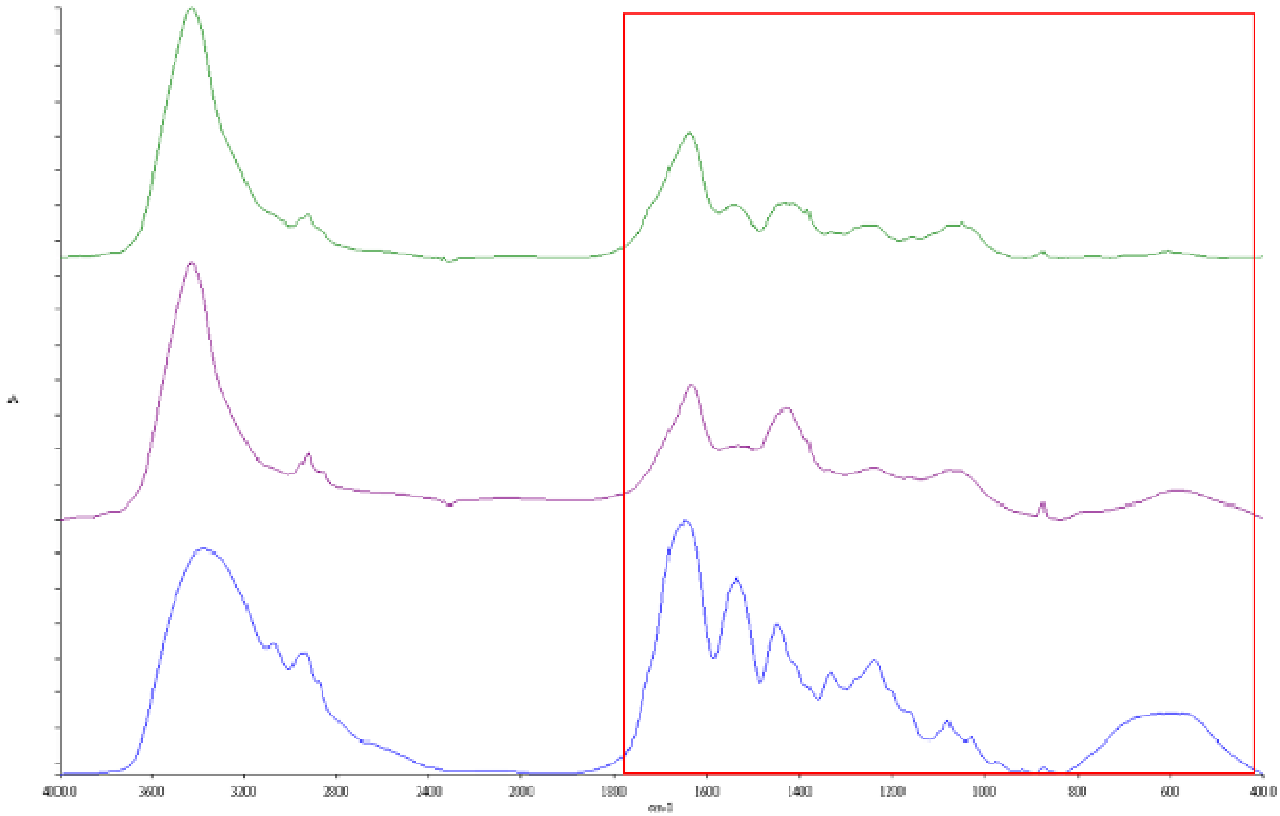

Figure 18. FT-IR analysis of *P. lividus* insoluble and soluble collagens isolated from the PM and bovine ultrapure collagen using a Perkin Elmer 2000 spectrometer. Green curve: *P. lividus* soluble sample, violet curve *P. lividus* insoluble collagen, blue curve soluble bovine collagen. The main bands of collagens arose from the peptide bond vibrations: the heights of the peaks of amide I (1640 cm^{-1}, C=O stretch), amide II (1550cm^{-1}, C-N stretch and N-H in-plane bend) 1450 cm^{-1} (CH bending) and the one between 3100 cm^{-1}-3600 cm^{-1} (OH and NH) of CDLs and collagen spectra.

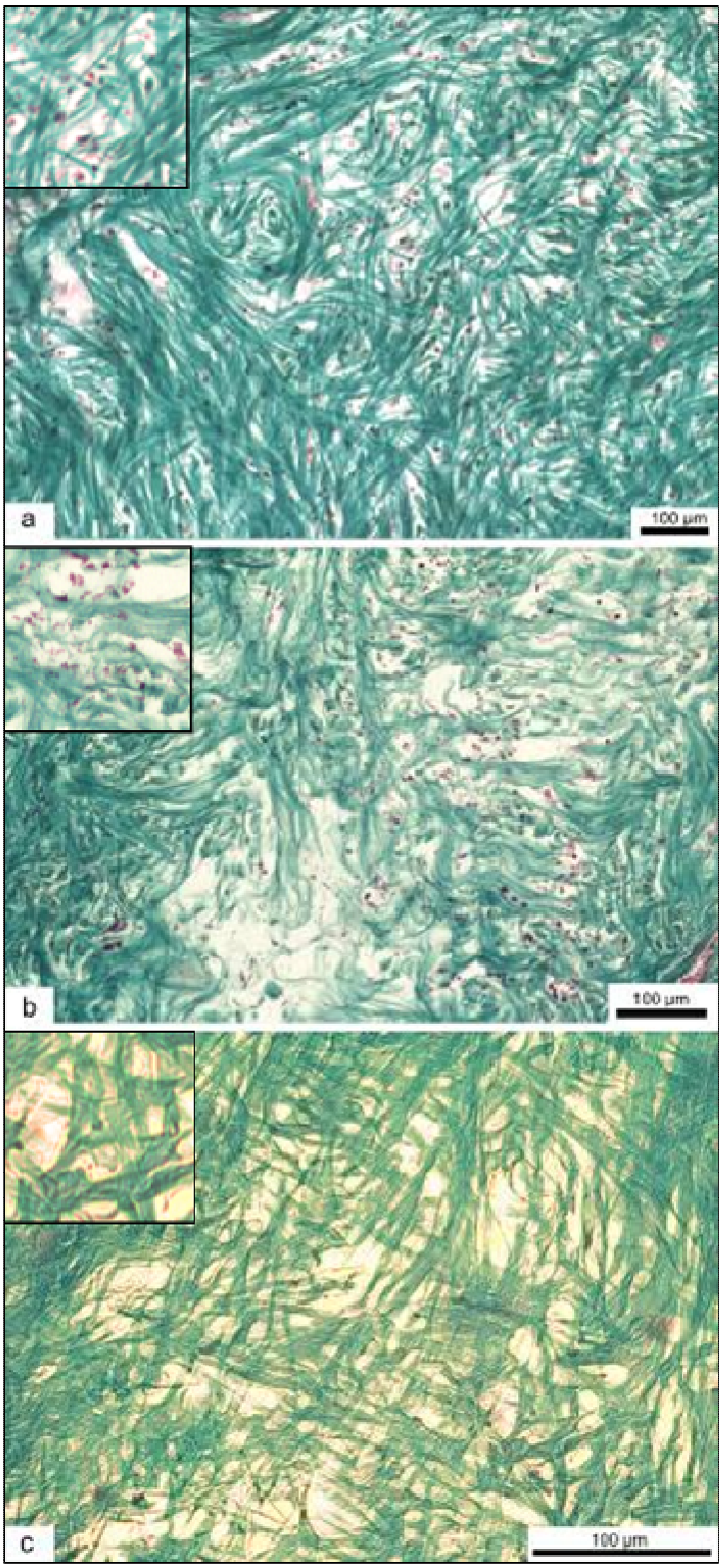

Figure 19. Milligan's Trichrome-stained sections of *P. lividus* PM. a: control tissue in ASW; b: 4M Guanidine chloride solution treated tissue; c: 0.1 M NaOH solution treated tissue. Cells (pink dots) were not affected by 4M Guanidine chloride but they were entirely removed by 0.1 M NaOH. Collagen in green. Tricarico et al., 2012.

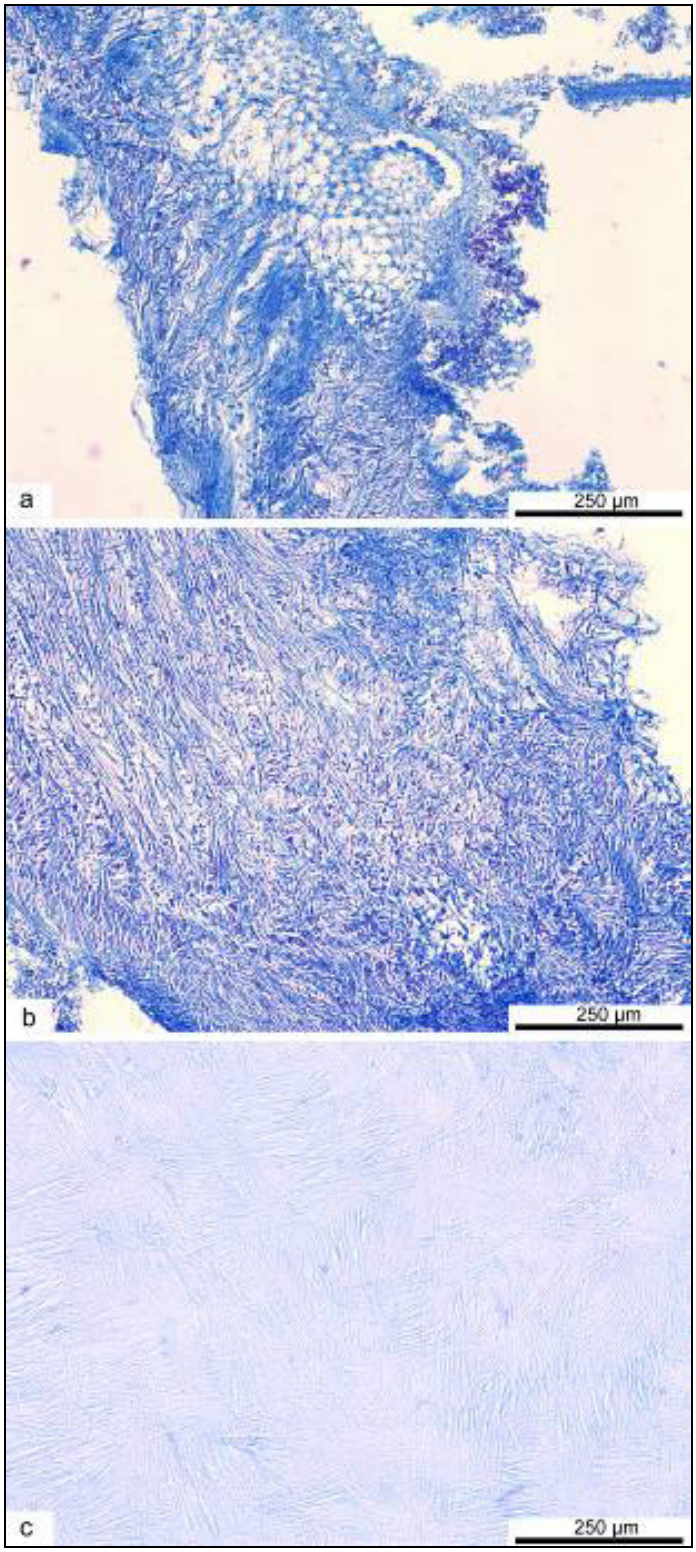

Figure 20. Alcian blue-stained sections of *P. lividus* PM using and Alcian blue solution prepared at pH 3.1. a: control tissue in ASW; b: 4M Guanidine chloride solution treated tissue; c: 0.1 M NaOH solution treated tissue. Whilst 4M Guanidine chloride did not affect the intensity of staining of the collagen fibres, this was significantly reduced by 0.1 M NaOH. Since 4M Guanidine chloride removes non-covalently bound PGs from collagen fibrils and it had no discernible effect on the PM, it can be concluded that covalently bound PGs dominate in this tissue.Tricarico et al., 2012.

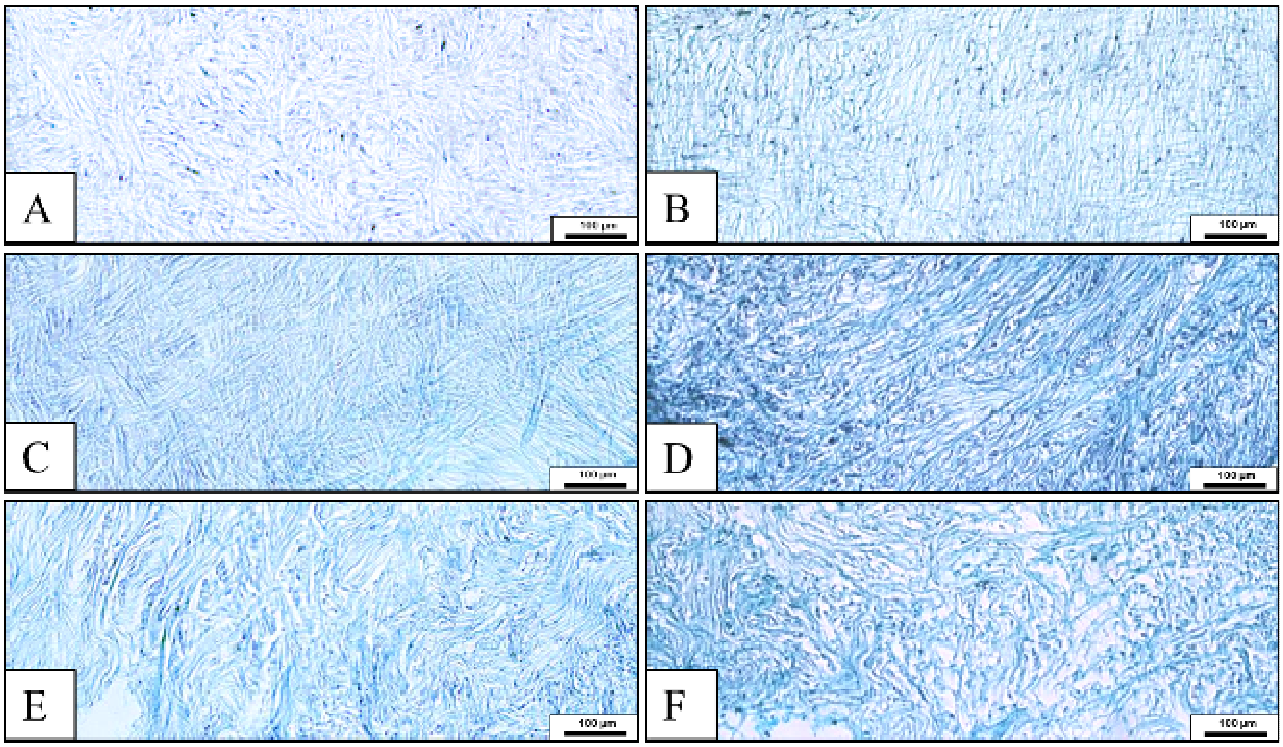

Figure 21. Alcian blue-stained sections of *P. lividus* PM. A, B: 0.1 M NaOH solution treated tissue; C, D: control tissue in ASW; E, F: 4M Guanidine chloride solution treated tissue. A, C, E: pH 5.6 to stain weakly sulfated mucins and Hyaluronic acid; B, D, F: pH 0.2 to stain strongly sulfated mucins above all chondroitin / keratan sulfate

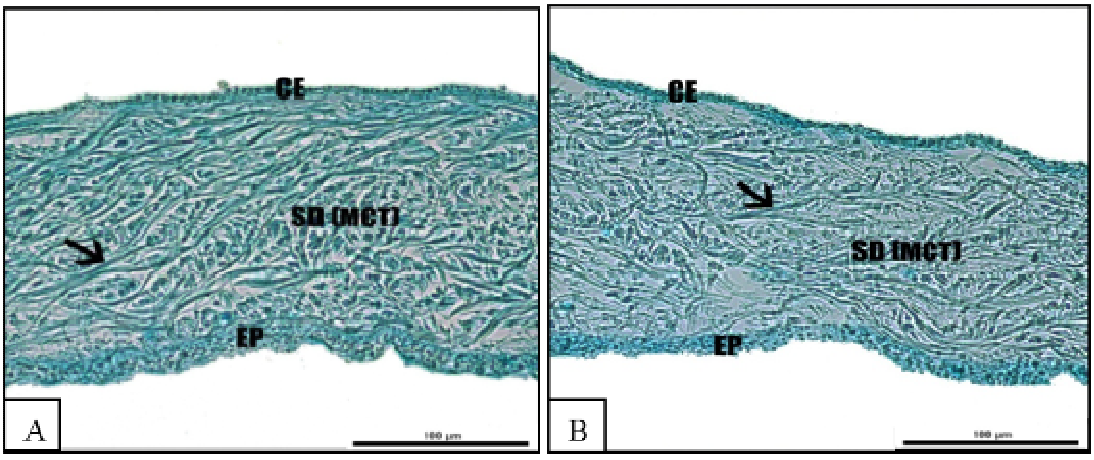

Figure 22. Transversal paraffin section of CDLs stained with Alcian blue. A: CDL sample treated with ACh and stained with an Alcian blue solution at pH 5.6; B: CDL sample treated with PPSW and stained with an Alcian blue solution at pH 5.6. EP, epidermis; SD, dermis (MCT); CE, coelomic epithelium. Arrow underline where GAGs link collagen fibrils. There are no differences related to the quantity of the different types of GAGs present in the different mechanical states.

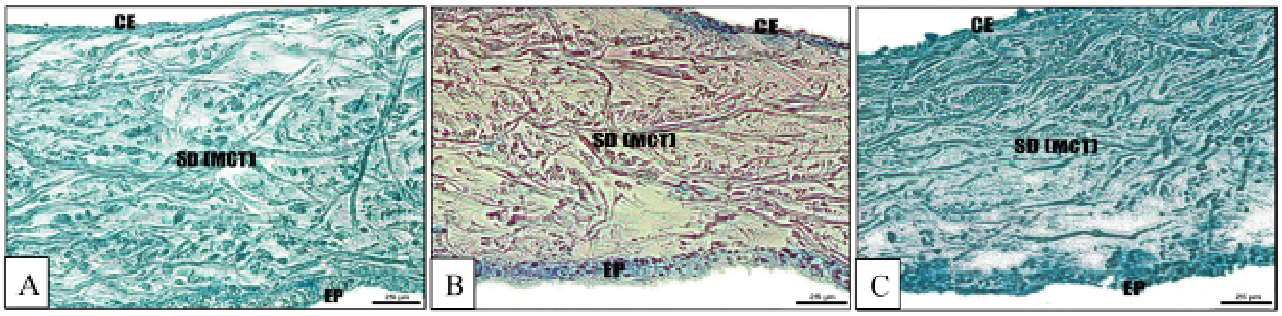

Figure 23. Transversal paraffin section of PMs treated with ASW stained with three different Alcian blue solutions. A: PM sample treated with an Alcian blue solution at pH 0.2; B: PM sample treated with an Alcian blue solution at pH 3.1; C: PM sample treated with an Alcian blue solution at pH 5.6. EP, epidermis; SD, dermis (MCT); CE, coelomic epithelium. There are differences related to the quantity of the different types of GAGs present in the different mechanical states.

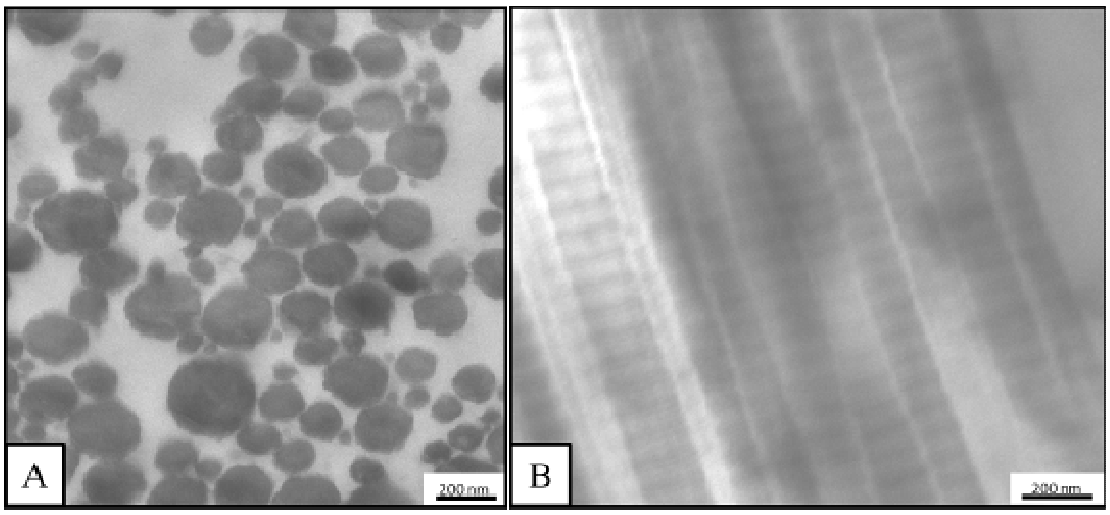

Figure 24. Transmission electron micrographs of a thin section stained with Cuprolinic blue of an intact PM treated with ASW. A: transversal section, collagen fibrils are intact, roundish and linked by PGs; B: longitudinal section, collagen fibrils are perfectly intact.

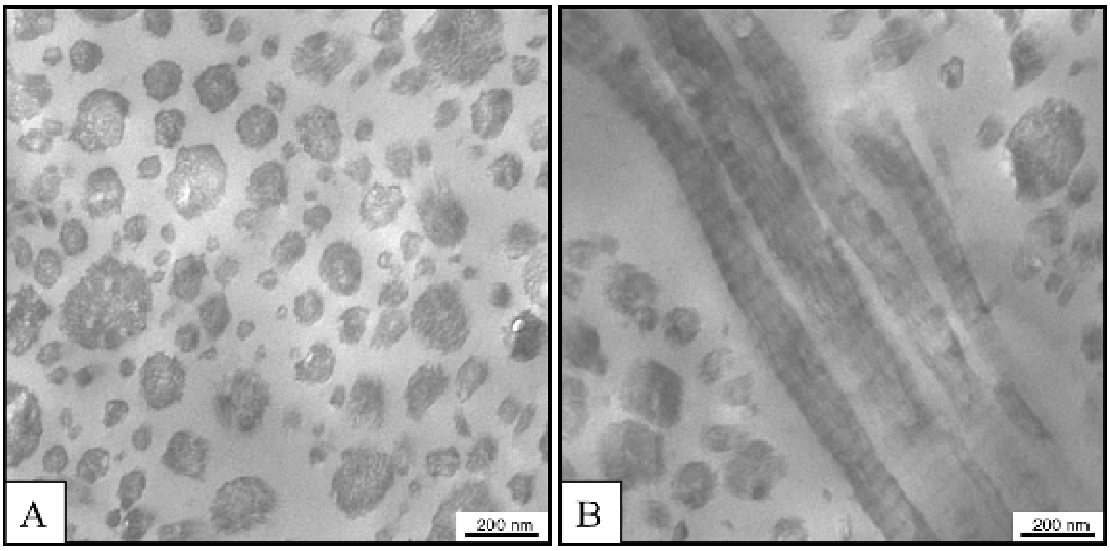

Figure 25. Transmission electron micrographs of a thin section stained with Cuprolinic blue of an intact PM treated with 0.1 M NaOH solution. A: transversal section; B: transversal and longitudinal cut fibrils. 0.1 M NaOH does not preserve the integrity of collagen fibrils.

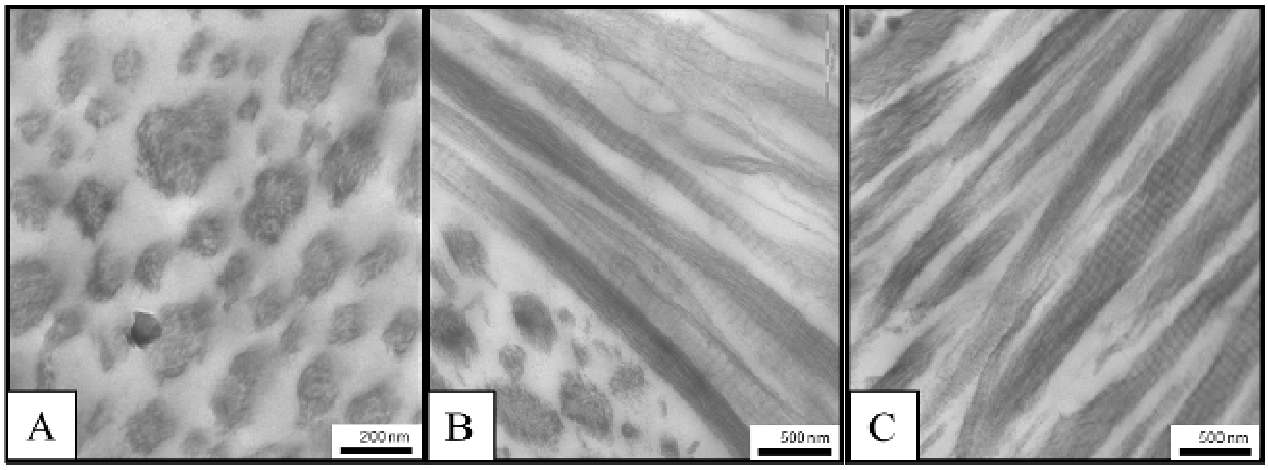

Figure 26. Transmission electron micrographs of a thin section stained with Cuprolinic blue of an intact PM treated with 4 M Guanidine chloride solution. A: transversal section; B: transversal and longitudinal cut fibrils; C: longitudinal fibrils. 4 M Guanidine chloride does not preserve the integrity of collagen fibrils.

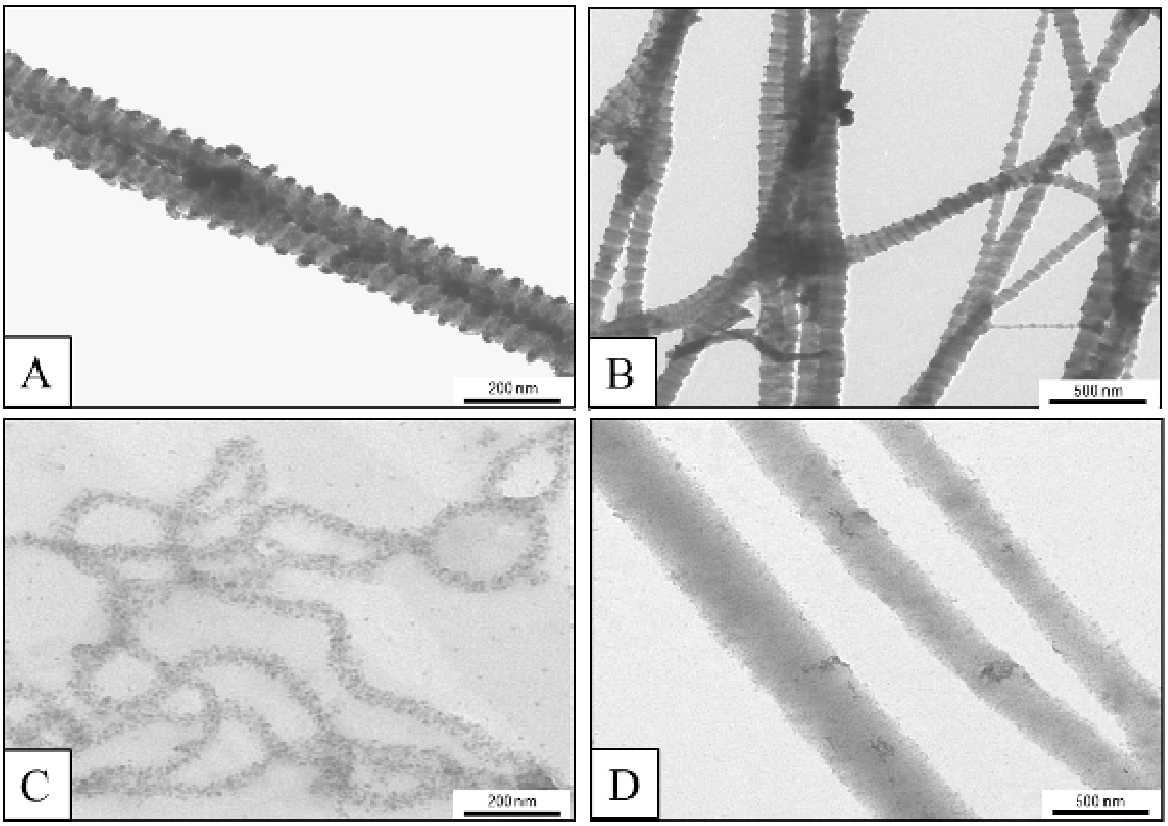

Figure 27. Transmission electron micrographs of isolated collagen stained with Cuprolinic blue. A,B: isolated fibrils according to the protocol of Matsumura (1974); C: isolated fibrils treated with 4 M Guanidine chloride solution; D: isolated fibrils treated with 0.1 M NaOH solution. 4 M Guanidine chloride and 0.1 M NaOH do not preserve the integrity of collagen fibrils and eliminate all the PGs. A, B: the small black dots that periodically recover the fibrils represent the PGs associated to the collagen fibrils stained by Cuprolinic blue.

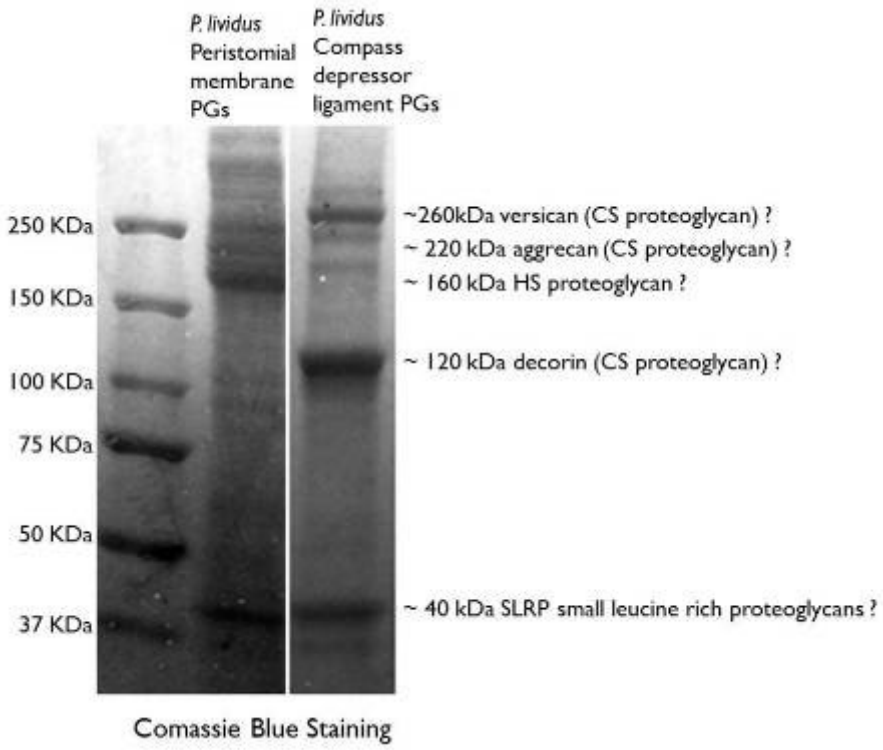

Figure 28. SDS-PAGE of PGs isolated from the CDLs and PM. After electrophoresis the gel was stained with Coomassie blue. Large PGs between 300-200 kDa (aggrecan, versican) are present in both tissues. Only CDLs present a PG migrating just above 120 kDa (decorin). The core proteins of small PGs (SLRP: Small Leucine Rich Proteoglycans) migrate close together at about 40 kDa and they are present in both tissues.

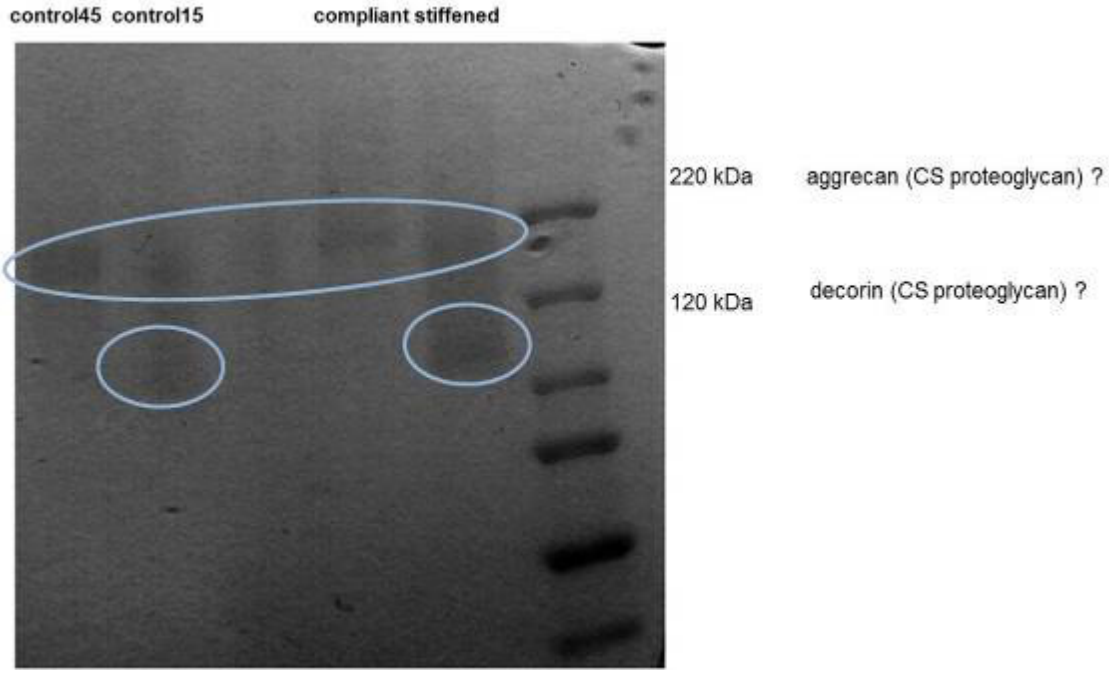

Figure 29. SDS-PAGE of GAGs isolated from the CDLs in the different mechanical states. After electrophoresis the gel was stained with Alcian blue. Control 45: GAGs isolated from CDLs treated with ASW for 45 minutes, this is the control for the compliant state; Control 15: GAGs isolated from CDLs treated with ASW for 15 minutes, this is the control for the stiffened state; Compliant: GAGs isolated from CDLs treated with PPSW; Stiffened: GAGs isolated from CDLs treated with ACh. In all the samples there is a band at about 220 kDa that can be related to aggrecan PG. Only in the stiffened sample and in its control at about 120 kDa that can be related to decorin PG.

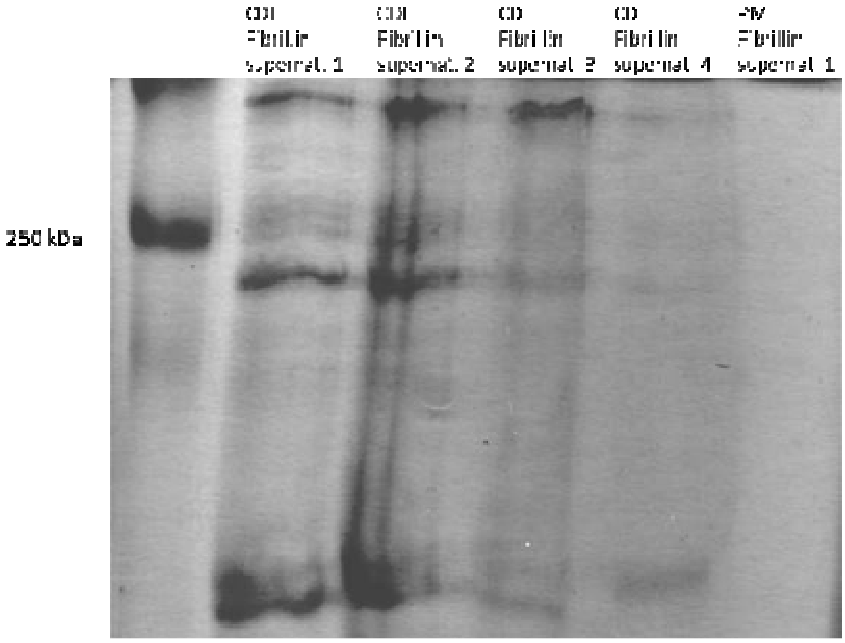

Figure 30. Characterization of fibrillin with SDS-PAGE. Extraction of *P. lividus* CDLs with 6 M Guanidine chloride, followed by collagenase treatment, then by 6 M Guanidine chloride at least 4 times analysed by SDS-PAGE gels stained with Coomassie blue revealed the presence of a band at about 350 kDa as expected according to literature data (lane 2,3,4,5). This band was present in the first 4 supernatants and then it disappears. Were present also unknown species at about 240 kDa. The same extraction performed on *P. lividus* PM did not have inexplicably any results (lane 6).

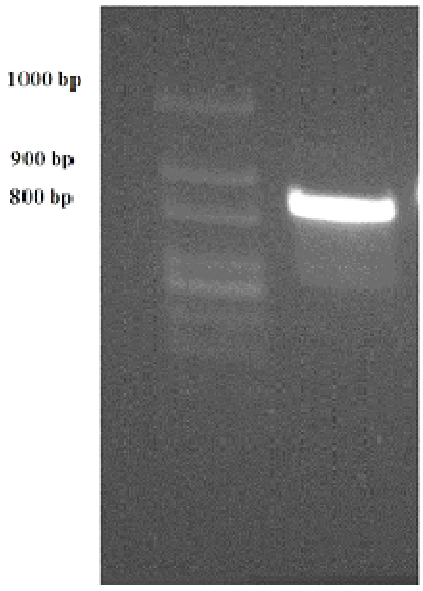

Figure 31. Agarose gel electrophoresis. The sample is the *S. purpuratus* tensilin protein obtained using the primers SF1 - SR3.

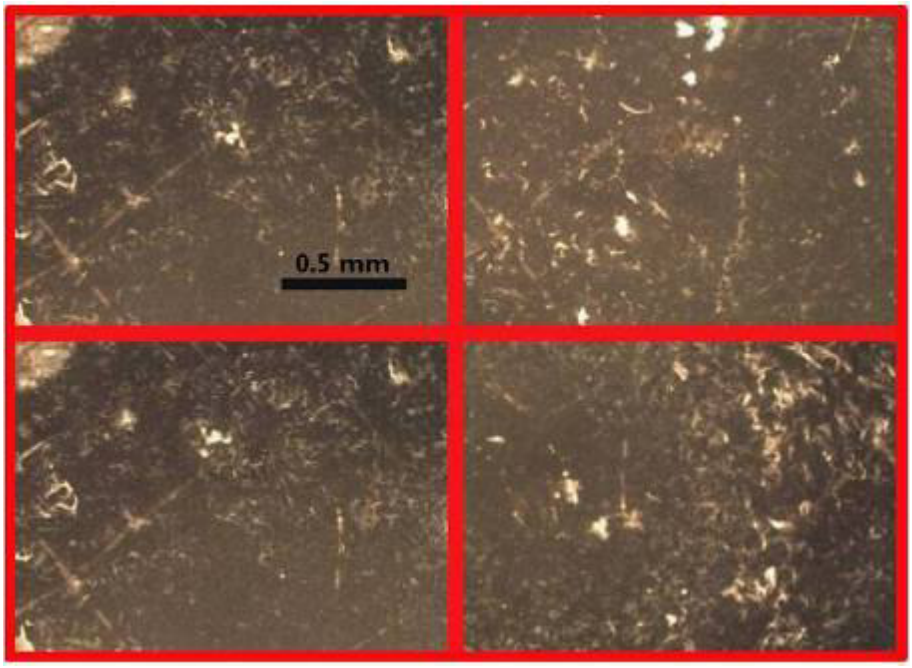

Figure 32. Aggregation assay 1st test. Up-left: collagen t0; down –left: collagen t2h; up-right: collagen + tensilin t0; down-right: collagen + tensilin t2h. 25 µl purified *purpuratus* tensilin protein, 90 µl/ml *S. purpuratus* collagen solution, 1 ml final volume with 2 mM EGTA, 0.5 M NaCl, 20 mM Tris solution, stirring speed 150/100 rpm RT. The aggregation was observed but unstable and transitory.

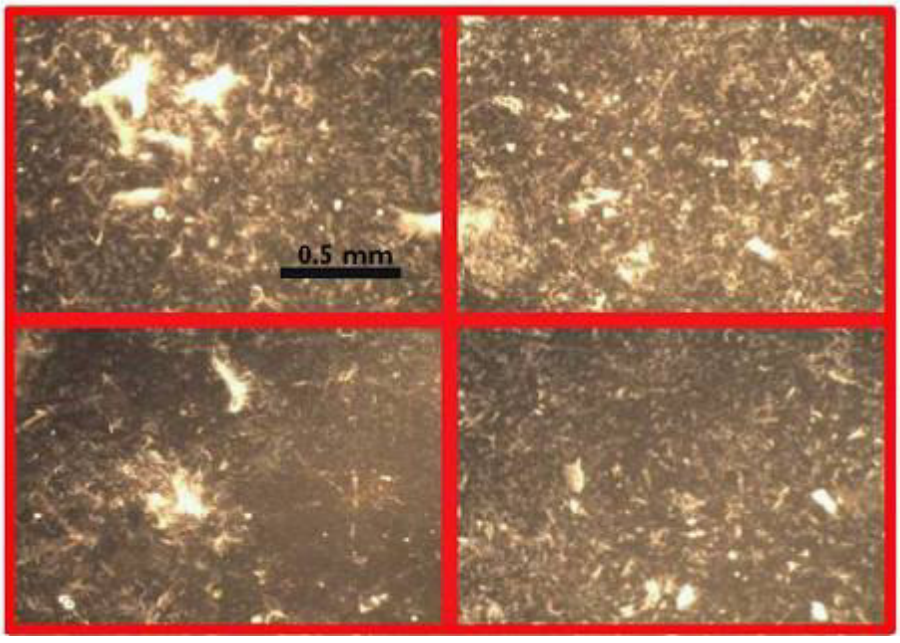

Figure 33. Aggregation assay 2nd test. Up-left: collagen t0; down –left: collagen t2h; up-right: collagen + tensilin t0; down-right: collagen + tensilin t2h. 25 µl purified *S. purpuratus* tensilin protein, 180 µl/ml *S. purpuratus* collagen solution, 0.5 ml final volume with 2 mM EGTA, 0.5 M NaCl, 20 mM Tris solution, stirring speed 100 rpm RT. The aggregation was observed but unstable and transitory.

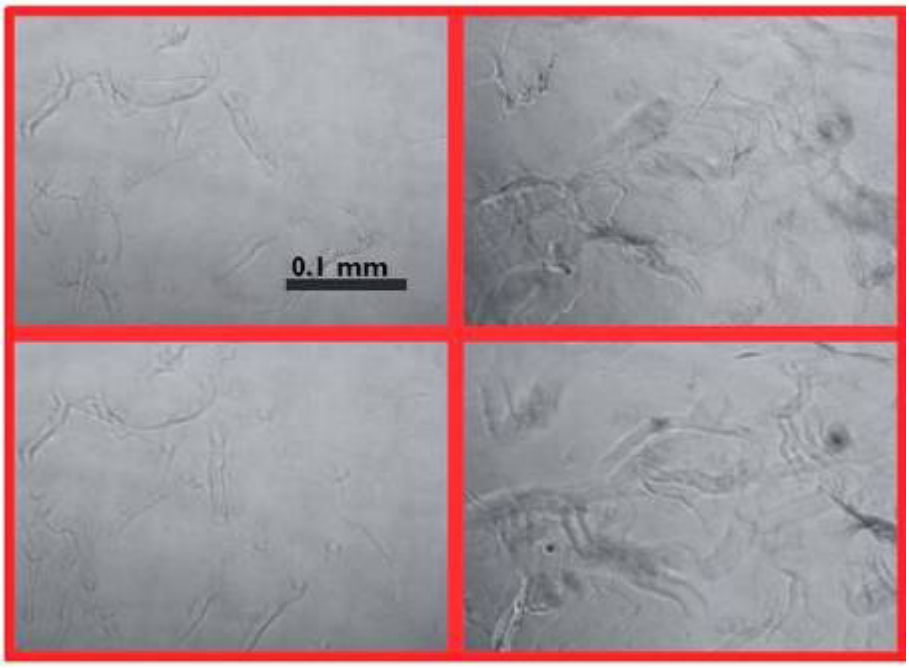

Figure 34. Aggregation assay 3rd test. Up-left: collagen t0; down –left: collagen t2h; up-right: collagen + tensilin t0; down-right: collagen + tensilin t2h. 25 µl purified *S. purpuratus* tensilin protein, 180 µl/ml *S. purpuratus* collagen solution, 0.36 ml final volume with 2 mM EGTA, 0.5 M NaCl, 20 mM Tris solution, stirring speed 0 rpm RT – Time Lapse. The aggregation was observed but unstable and transitory.

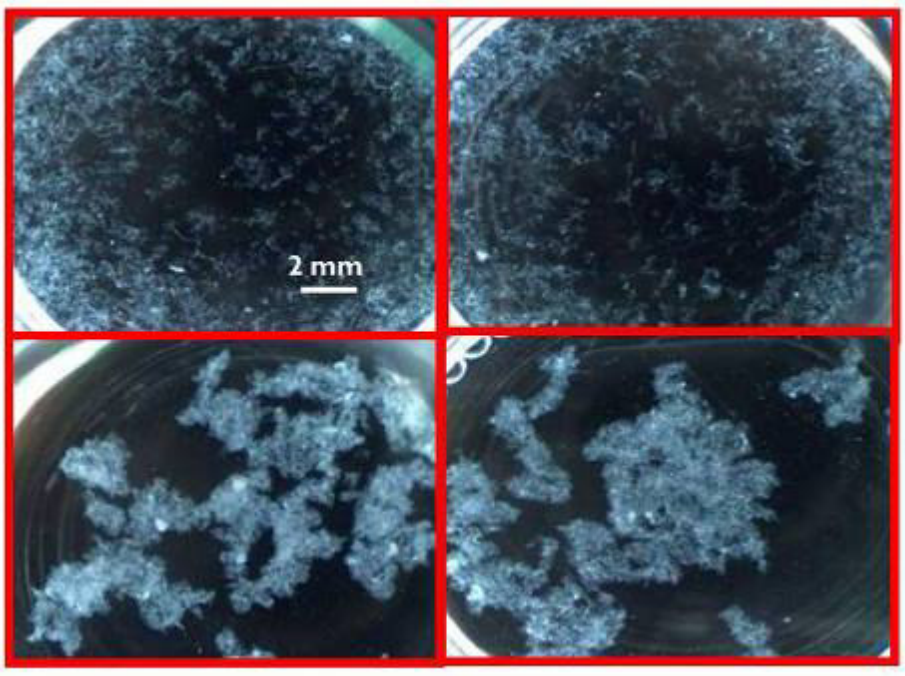

Figure 35. Aggregation assay 4th test. Up-left: collagen t0; down –left: collagen t2h; up-right: collagen + tensilin t0; down-right: collagen + tensilin t2h. 25x3 µl purified *S. purpuratus* tensilin protein, 360 µl/ml *S. purpuratus* collagen solution, 0.275 ml final volume with dH_2O, Stirring speed 50 rpm RT. The aggregation was observed but unstable and transitory.

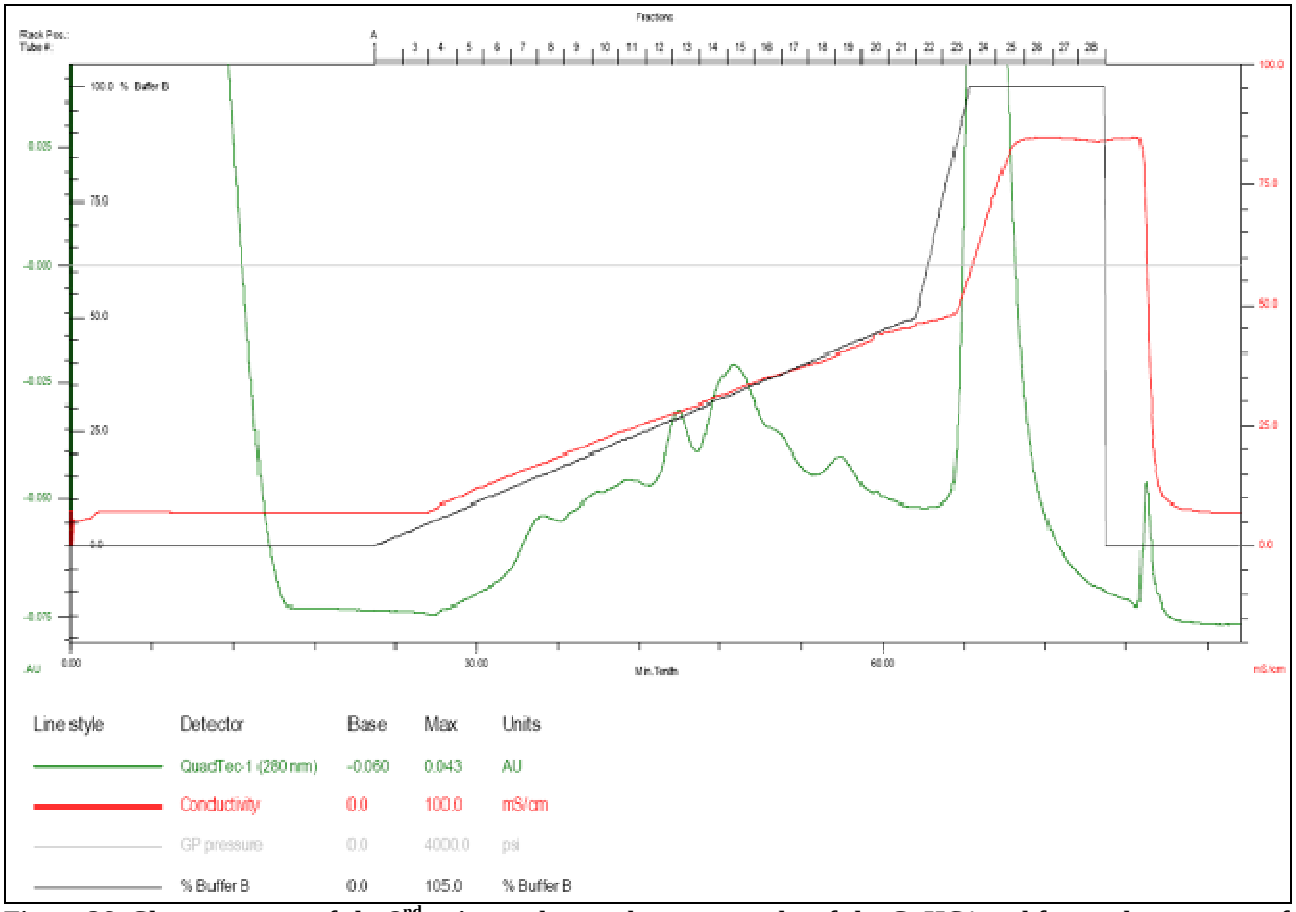

Figure 36. Chromatogram of the 2nd anion exchange chromatography of the GuHC1 and freeze-thaw extract of PM. It showed the presence of distinct proteins with widely differing charge characteristics.

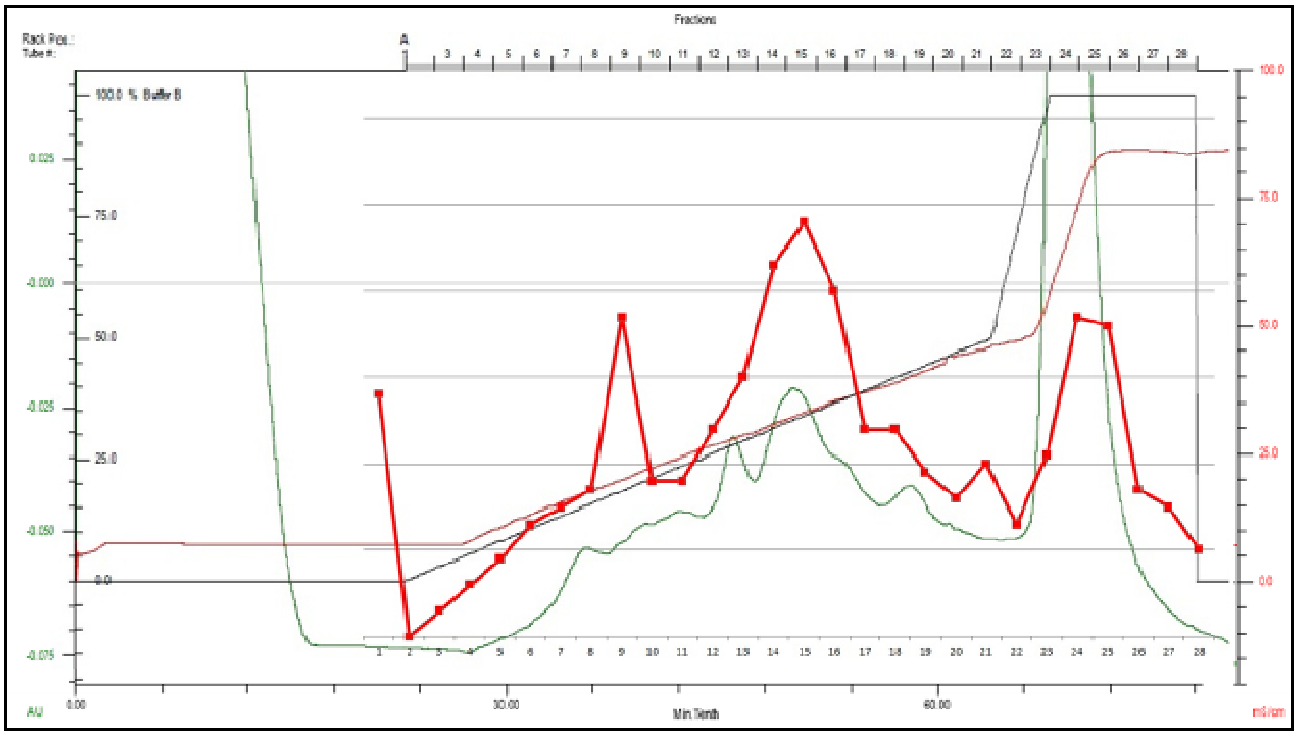

Figure 37. Chromatogram of the 2nd anion exchange chromatography of the GuHC1 and freeze-thaw extract of PM overlapped with the DC Assay protein quantification. The two results can be overlapped.

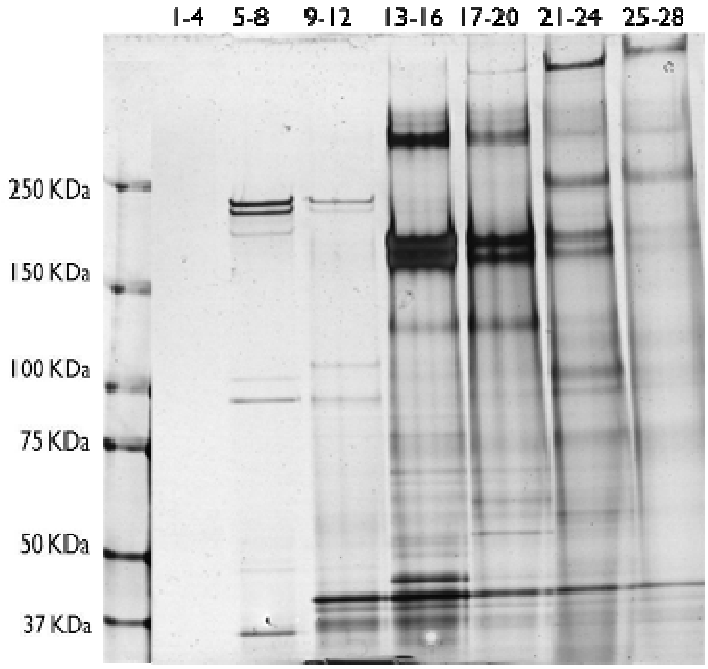

Figure 38. SDS-PAGE (3-8%) of the purified protein pools from the 2nd anion exchange chromatography. 1st lane, molecular mass marker; 2nd lane, pool fractions 1-4; 3rd lane, pool fractions 5-8; 4th lane, pool fractions 9-12; 5th lane, pool fractions 13-16; 6th lane, pool fractions 17-20; 7th lane, pool fractions 21-24; 8th lane, pool fractions 25-28.

Graphs

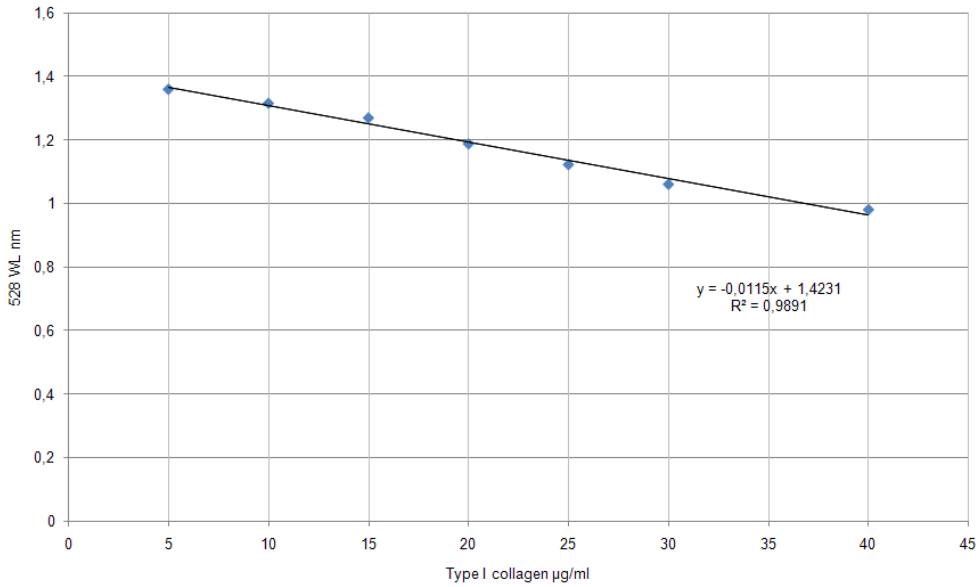

Graph 1. Standard curve showing the absorbance of Sirius red at 528 nm versus concentration of type I collagen. Each point is the mean of triplicate samples and the regression coefficient for the line is 0.989.

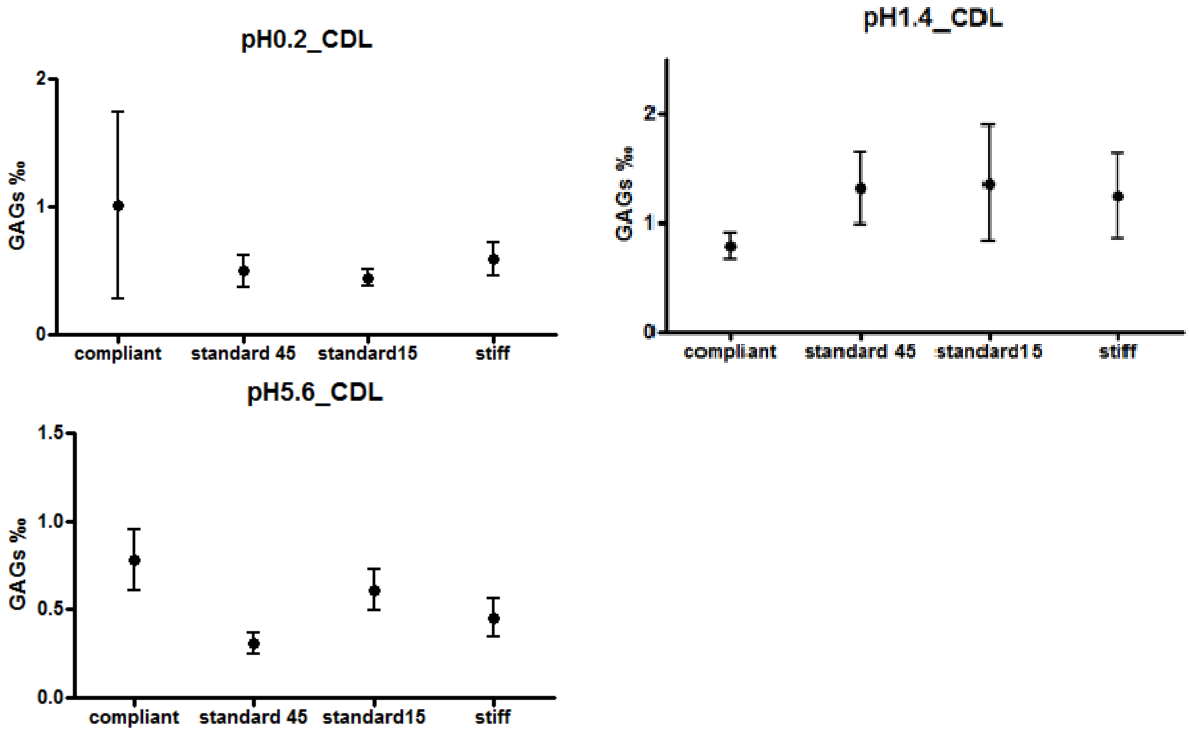

Graph 2. Alcian blue spectrophotometric quantification of PGs/GAGs in *P. lividus* CDLs in different mechanical states at the same pH. On y axis there is GAGs amount expressed ‰. On x axis there are the different mechanical states: compliant corresponds to CDLs treated with PPSW, standard 45 corresponds to CDLs treated with ASW for 45 minutes and is the compliant control, standard 15 corresponds to CDLs treated with ASW for 15 minutes and is the stiff control, stiff corresponds to CDLs treated with ACh. There is no statistically significant difference in GAGs amount in the different mechanical states at pH 0.2, 1.4 and 5.6. The only ANOVA significant test is between the compliant and standard 45 samples at pH 5.6 $p < 0.05$.

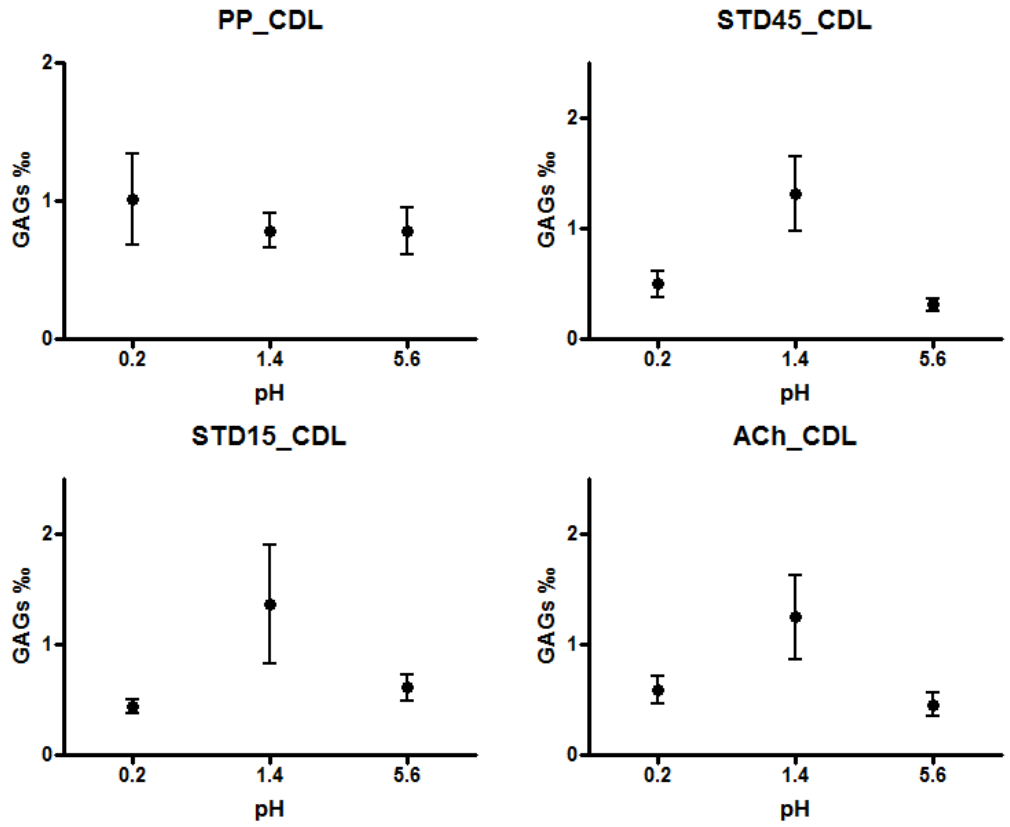

Graph 3. Alcian blue spectrophotometric quantification of PGs/GAGs in *P. lividus* CDLs in the same mechanical states considering the different pH. On y axis there is GAGs amount expressed ‰. On x axis there are the different pH: 0.2, 1.4 and 5.6. There is no statistically significant difference in GAGs amount in the same mechanical states at pH 0.2, 1.4 and 5.6. The only ANOVA significant test is between the pH 1.4 and 5.6 in CDLs treated with ASW 15 $p < 0.01$.

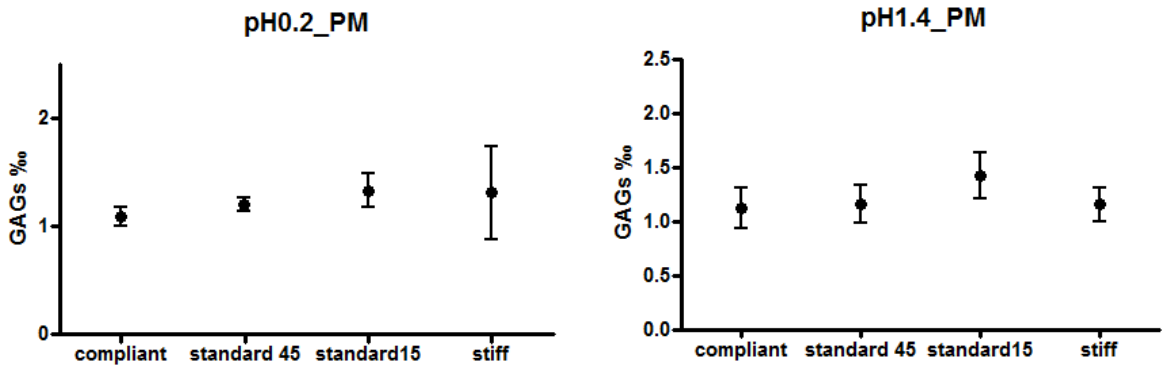

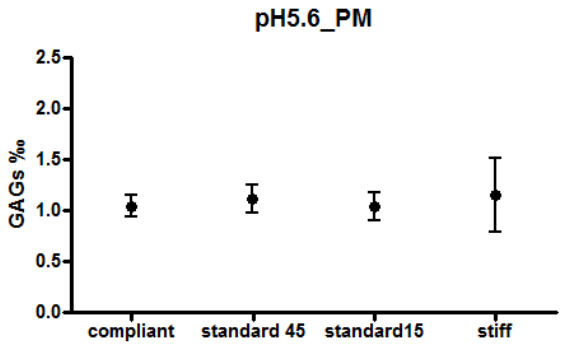

Graph 4. Alcian blue spectrophotometric quantification of PGs/GAGs in *P. lividus* PMs in different mechanical states at the same pH. On y axis there is GAGs amount expressed ‰. On x axis there are the different mechanical states: compliant corresponds to PM treated with PPSW, standard 45 corresponds to PM treated with ASW for 45 minutes and is the compliant control, standard 15 corresponds to PM treated with ASW for 15 minutes and is the stiff control, stiff corresponds to PM treated with ACh. There is no statistically significant difference in GAGs amount in the different mechanical states at pH 0.2, 1.4 and 5.6.

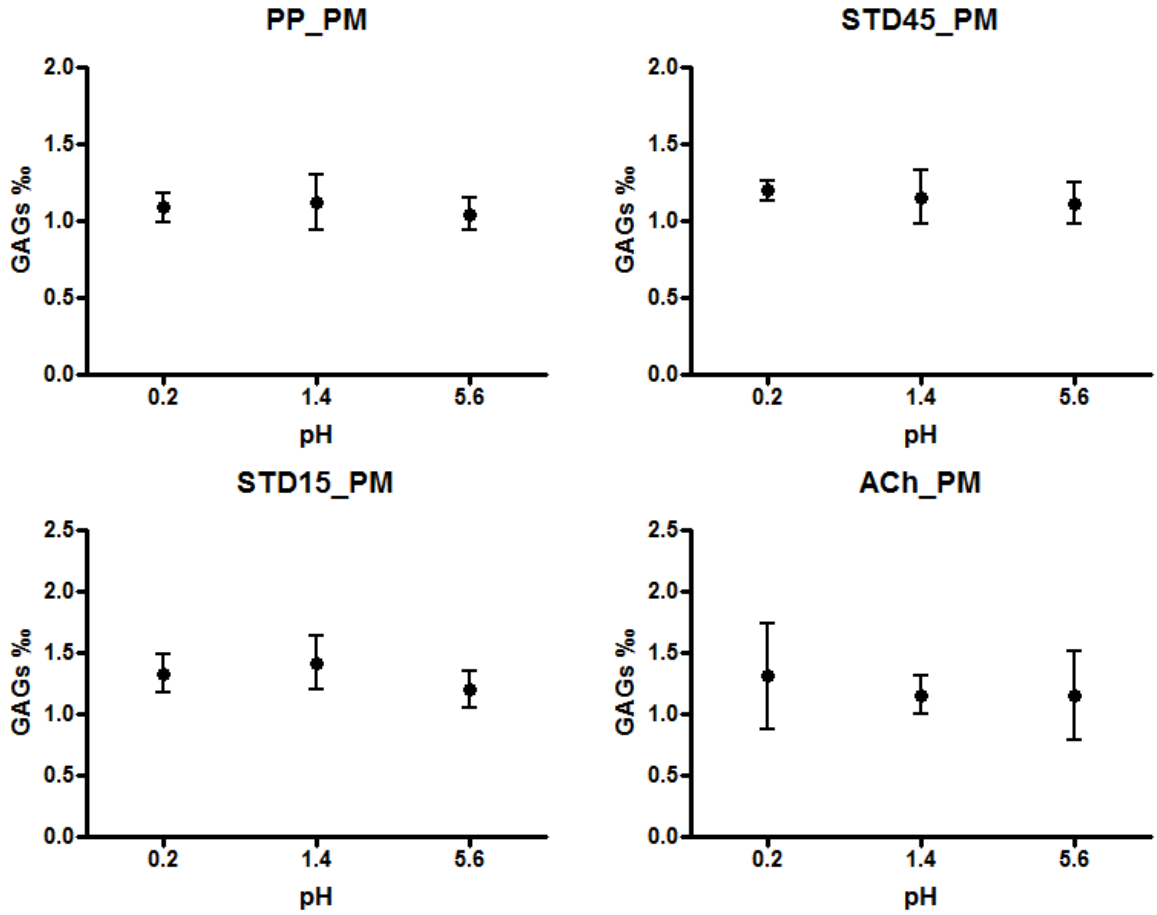

Graph 5. Alcian blue spectrophotometric quantification of PGs/GAGs in *P. lividus* PMs in the same mechanical states considering the different pH. On y axis there is GAGs amount expressed ‰. On x axis there are the different pH: 0.2, 1.4 and 5.6. There is no statistically significant difference in GAGs amount in the same mechanical states at pH 0.2, 1.4 and 5.6.

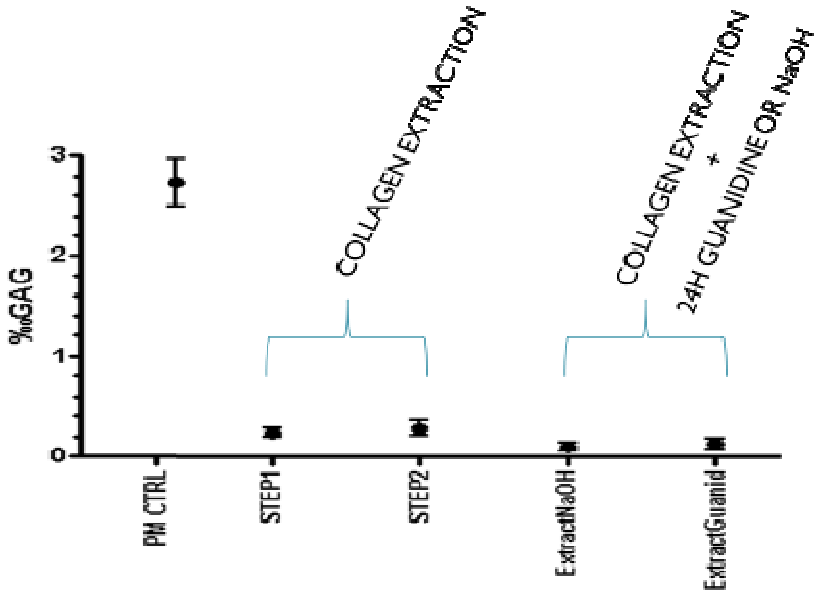

Graph 6. Spectrophotometric quantification of GAGs in fresh PM (PM CTRL), two different steps of the collagen extraction protocol (STEP1, STEP2), isolated collagen purified with 0.1 M NaOH solution (ExtractNaOH), isolated collagen purified with 4M Guanidine chloride solution (ExtractGuanid). There is no statistically significant difference among GAGs amount associated to isolated collagen and the two treatments of purification but all these samples are statistically different from the control PM. ANOVA test, $p < 0.0001$.

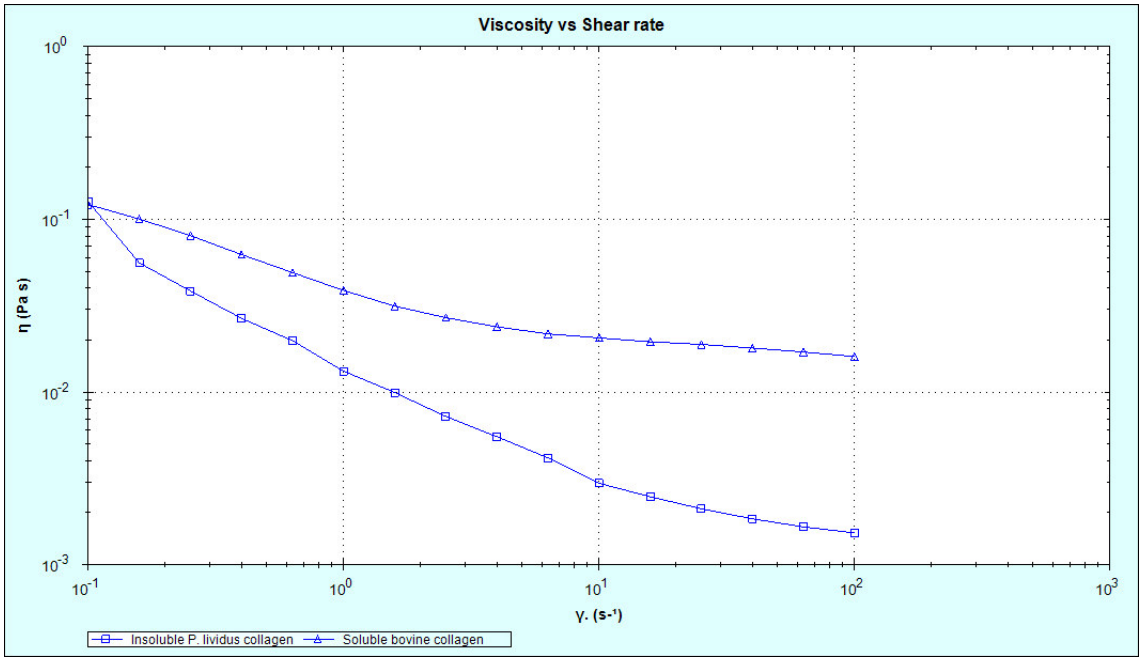

Graph 7. Table of shear rates log. Viscometry shear rate table in logarithmic scale at 25°C. The square line is the insoluble *P. lividus* collagen sample and the triangle line is the bovine soluble collagen sample. Both in *P. lividus* insoluble collagen and soluble ultrapure bovine collagen increasing the shear rate from 10^{-1} to 10^{2} s^{-1} the viscosity decreases.

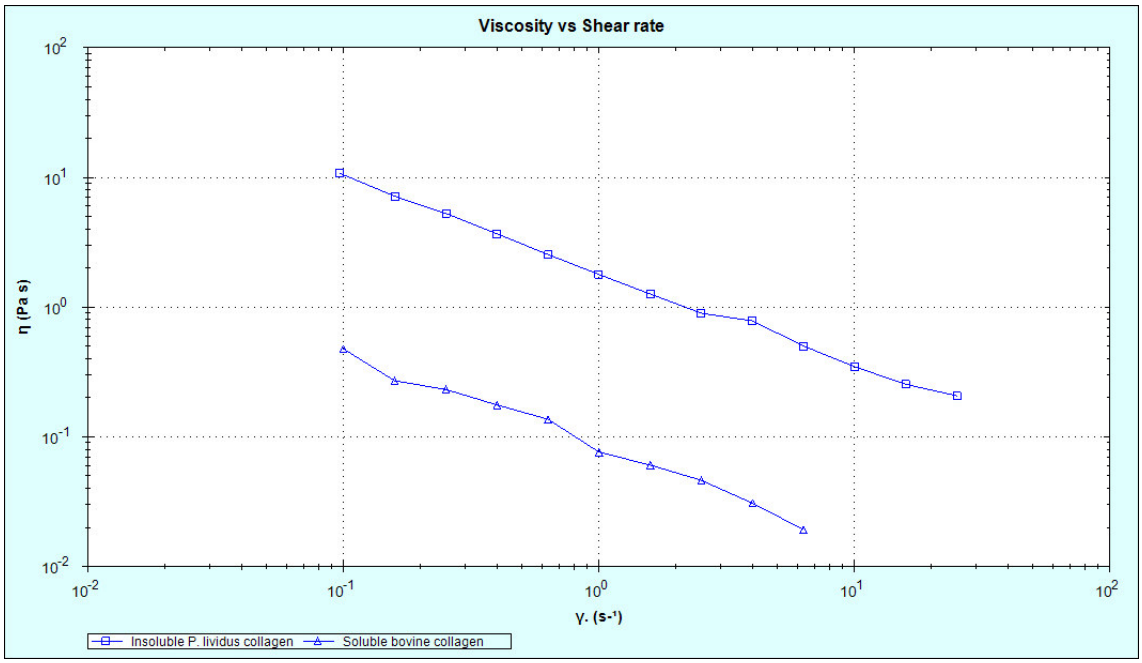

Graph 8. Table of shear rates log. Viscometry shear rate table in logarithmic scale at 37°C. The square line is the insoluble *P. lividus* collagen sample and the triangle line is the bovine soluble collagen sample. The behaviours are both linear, monotonically decreasing curves: increasing the shear strain rate from 10^{-1} to about 10 s^{-1} the viscosity decreases.

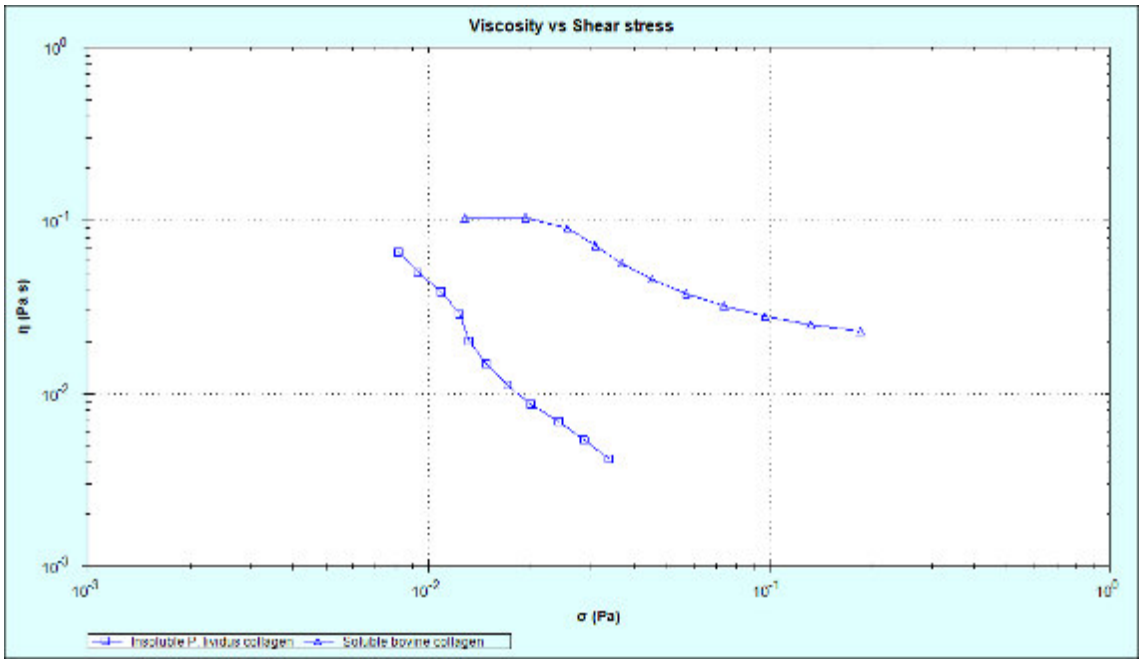

Graph 9. Shear rate ramp log isothermal. Viscometry shear rate ramp in logarithmic scale at 25°C. The square line is the insoluble *P. lividus* collagen sample and the triangle line is the bovine soluble collagen sample. Increasing in 2 minute the shear strain rate from 0.123 to 8.065 s^{-1} the behaviours of the *P. lividus* insoluble collagen and soluble ultrapure bovine collagen are completely different.

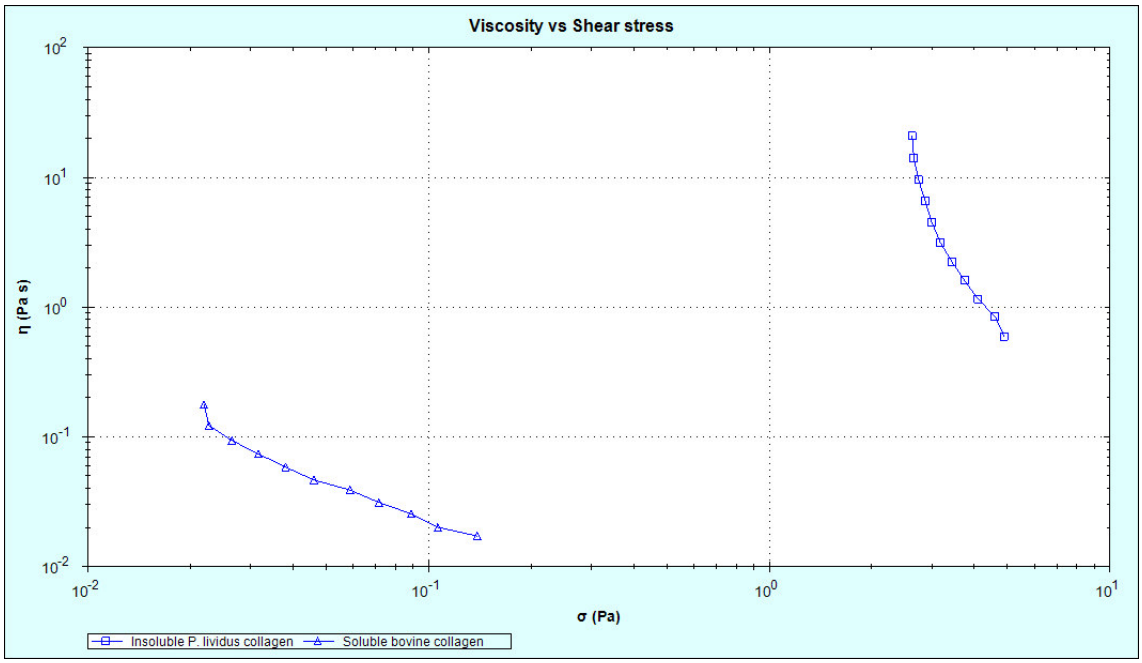

Graph 10. Shear rate ramp log isothermal. Viscometry shear rate ramp in logarithmic scale at 37°C. The square line is the insoluble *P. lividus* collagen sample and the triangle line is the bovine soluble collagen sample. Increasing in 2 minute the shear strain rate from 0.123 to 8.065 s^{-1} the behaviours of the *P. lividus* insoluble collagen and soluble ultrapure bovine collagen are completely different.

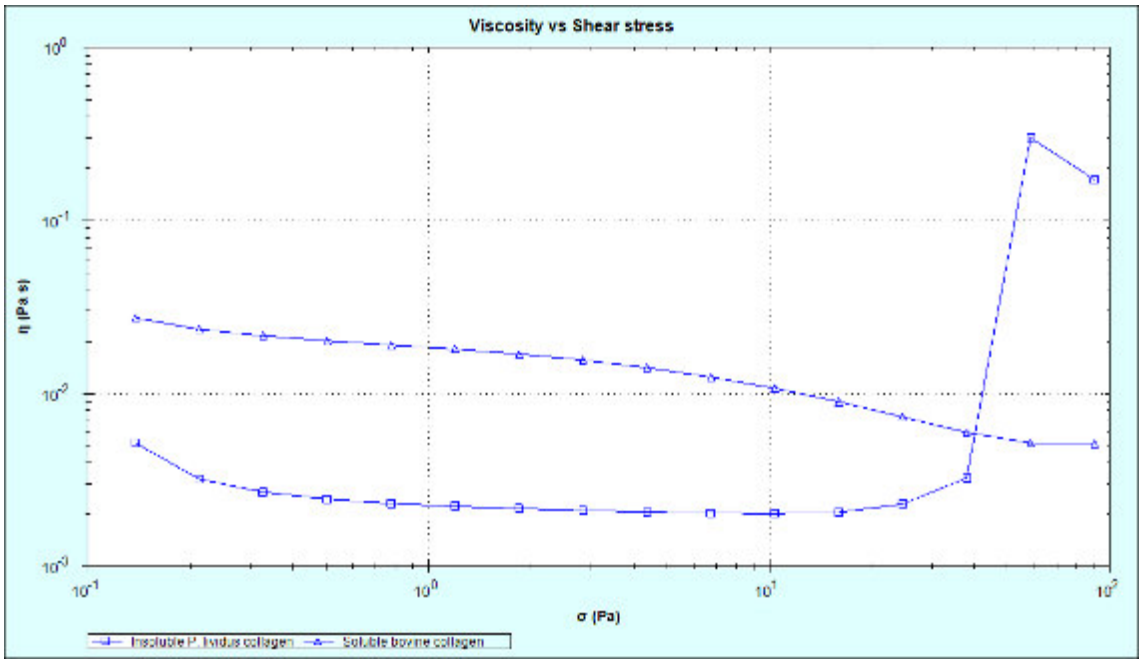

Graph 11. Shear stress ramp with yield stress analysis. Viscometry shear stress ramp in logarithmic scale at 25°C. The square line is the insoluble *P. lividus* collagen sample and the triangle line is the bovine soluble collagen sample. The behaviours are both linear, with monotonically decreasing curves.

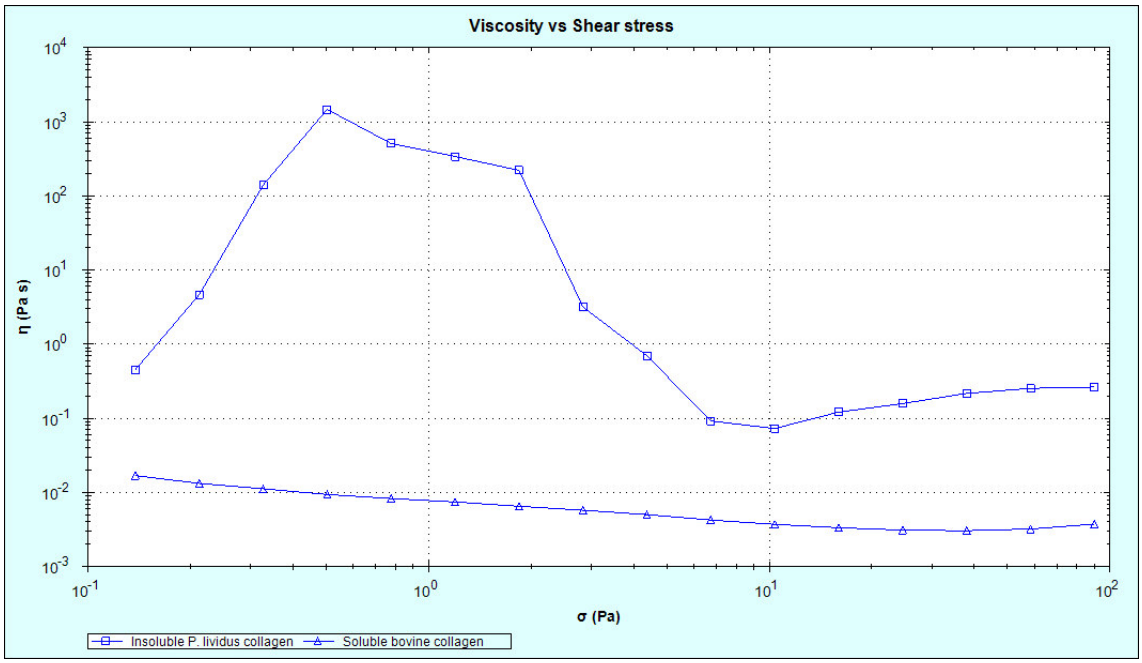

Graph 12. Shear stress ramp with yield stress analysis. Viscometry shear stress ramp in logarithmic scale at 37°C. The square line is the insoluble *P. lividus* collagen sample and the triangle line is the bovine soluble collagen sample. The viscosity pattern of the soluble ultrapure bovine collagen can be linearized changing the shear stress in a monotonically decreasing curve varying from 0.017 to 3.744 10^{-3} Pa*s, whereas the viscosity pattern of the *P. lividus* insoluble collagen shows an extraordinary behaviour.

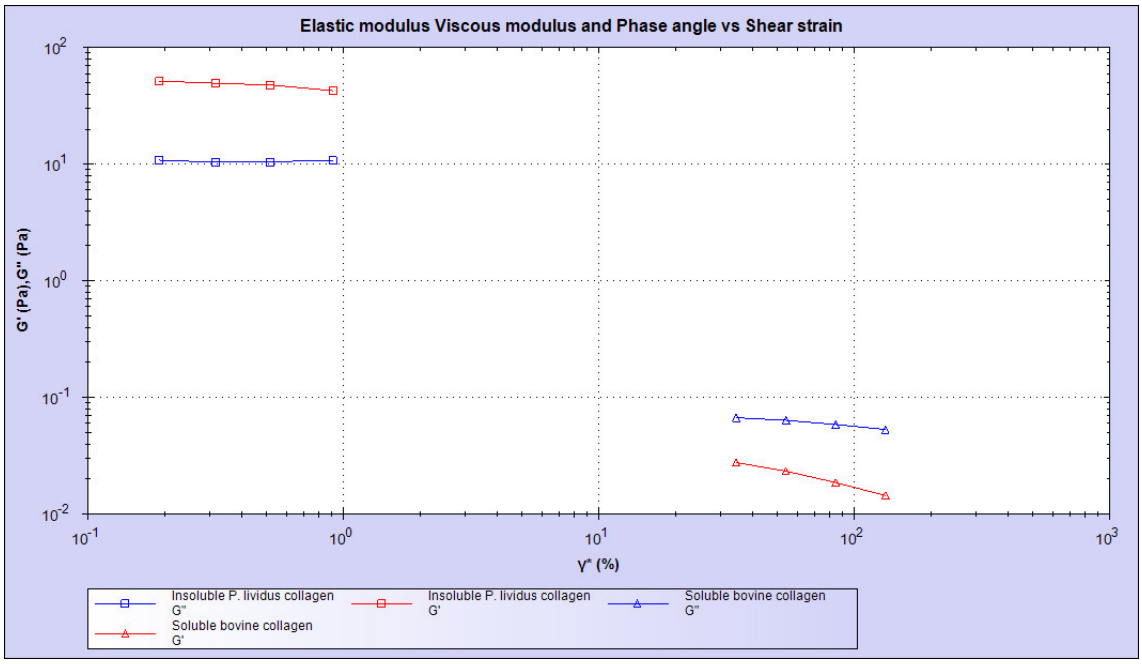

Graph 13. Oscillation amplitude table in amplitude sweep stress controlled with LVER determination for low viscosity materials at 25 and 37°C. The square line is the insoluble *P. lividus* collagen sample and the triangle line is the bovine soluble collagen sample. Both for the *P. lividus* insoluble collagen and for the soluble ultrapure bovine collagen the behaviours are linear and predictable.

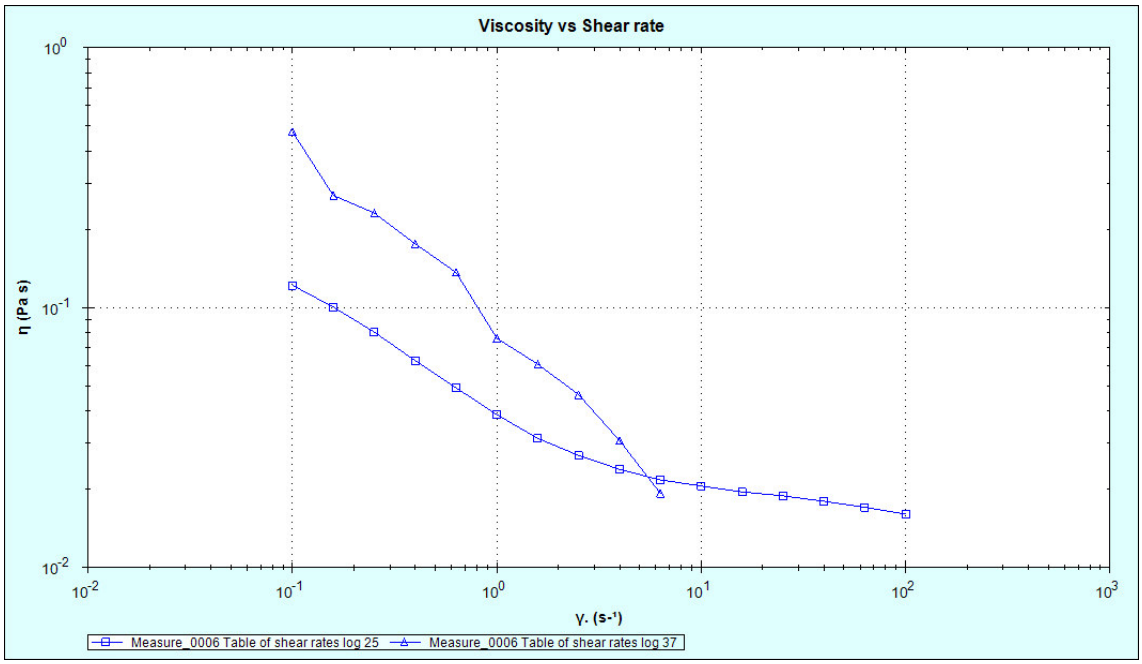

Graph 14. Table of shear rates log. Viscometry shear rate table in logarithmic scale. The square line is the ultrapure bovine collagen sample at 25°C and the triangle line is the ultrapure bovine collagen sample at 37°C. The viscosity properties of this material at 37°C are higher than the ones at 25°C.

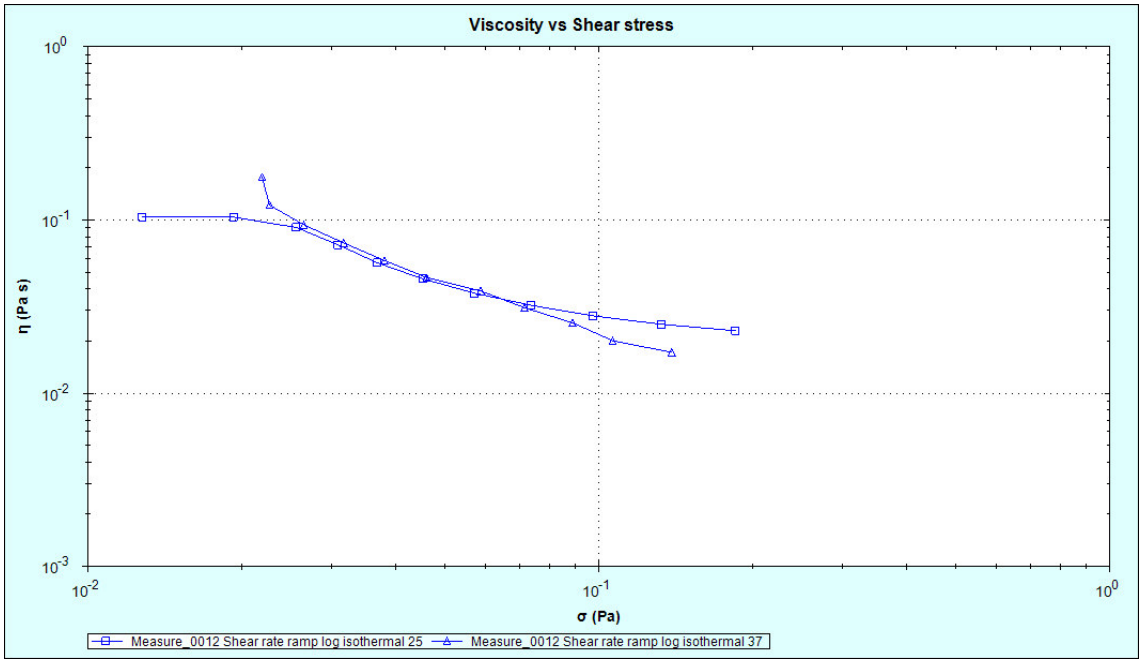

Graph 15. Shear rate ramp log isothermal. Viscometry shear rate ramp in logarithmic scale. The square line is the ultrapure bovine collagen sample at 25°C and the triangle line is the ultrapure bovine collagen sample at 37°C. The two curves are overlapped.

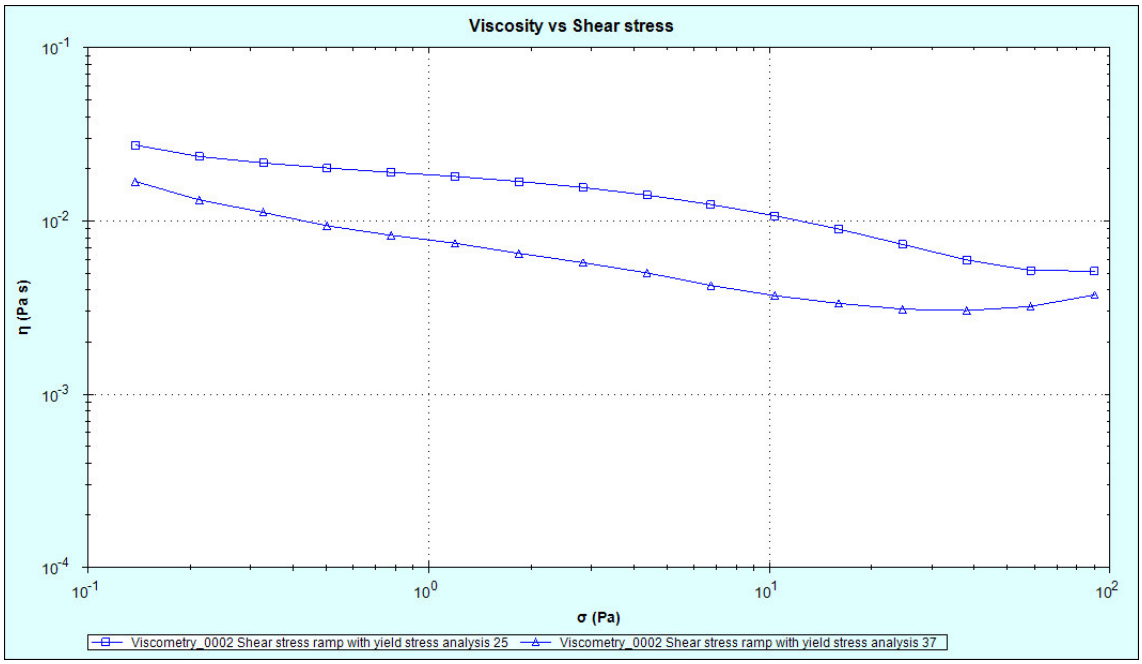

Graph 16. Shear stress ramp with yield stress analysis. Viscometry shear stress ramp in logarithmic scale. The square line is the ultrapure bovine collagen sample at 25°C and the triangle line is the ultrapure bovine collagen sample at 37°C. The viscosity properties of this material at 25°C are higher than the ones at 37°C.

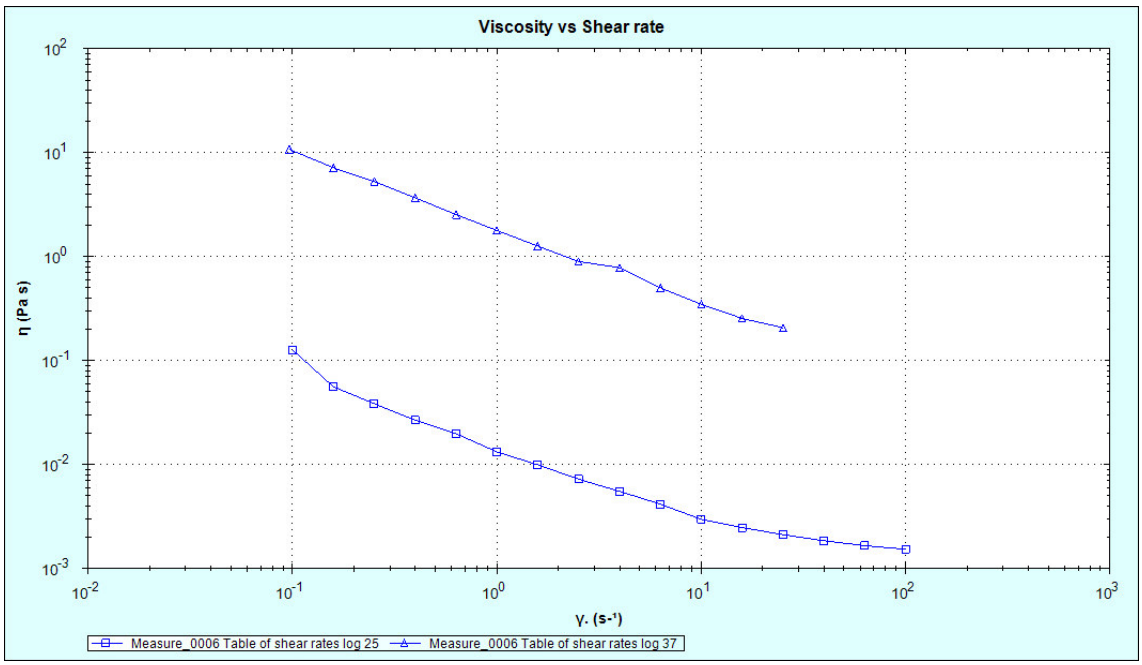

Graph 17. Table of shear rates log. Viscometry shear rate table in logarithmic scale. The square line is the *P. lividus* insoluble collagen sample at 25°C and the triangle line is the *P. lividus* insoluble collagen sample at 37°C. The viscosity properties of this material at 37°C are higher than the ones at 25°C. The two curves are parallel, linear, monotonically decreasing and they do not cross.

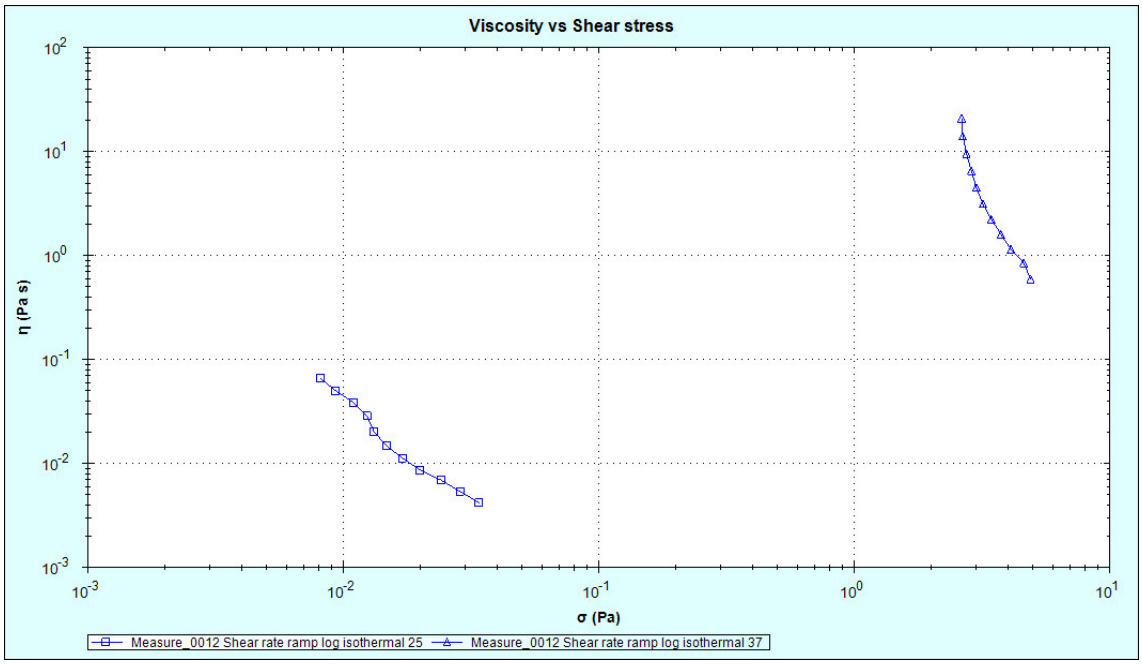

Graph 18. Shear rate ramp log isothermal. Viscometry shear rate ramp in logarithmic scale. The square line is the *P. lividus* insoluble collagen sample at 25°C and the triangle line is the *P. lividus* insoluble collagen sample at 37°C. The viscosity properties of this material at 37°C are higher than the ones at 25°C. When time is constant (2 minutes) the *P. lividus* insoluble collagen at 37°C reaches the same viscosity of the same sample at 25°C with a higher shear stress.

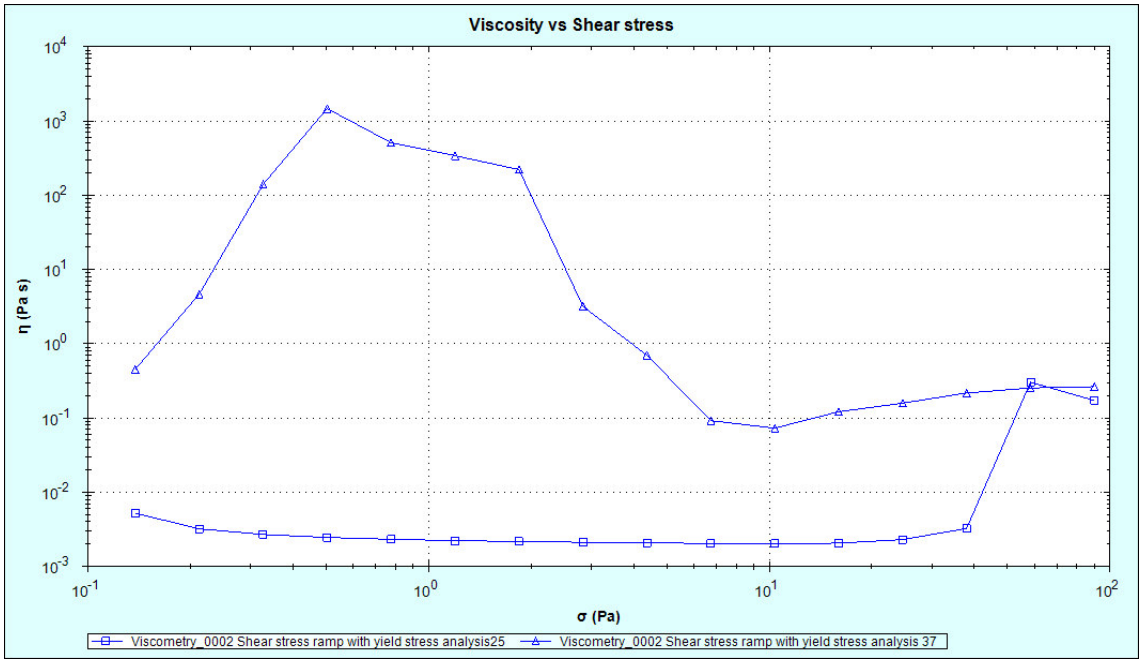

Graph 19. Shear stress ramp with yield stress analysis. Viscometry shear stress ramp in logarithmic scale. The square line is the *P. lividus* insoluble collagen sample at 25°C and the triangle line is the *P. lividus* insoluble collagen sample at 37°C. Behaviours are completely different and the viscosity properties of this material at 37°C are clearly higher than the ones at 25°C. The behaviours remain distinct till the shear stress reaches 58.5 Pa and the two curves cross at a viscosity of 0.30 Pa*s.

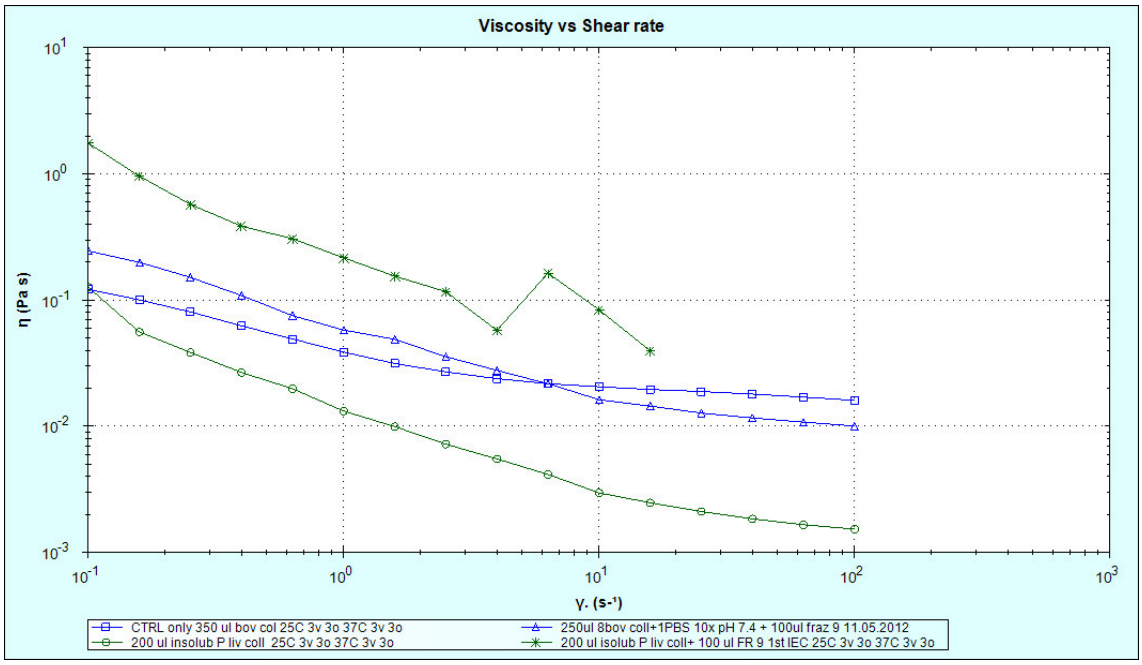

Graph 20. Table of shear rates log. Viscometry shear rate table in logarithmic scale at 25°C. The square-blue line is the bovine collagen sample, the triangle-blue line is the bovine collagen sample + fraction 9, the circle-green line is the *P. lividus* insoluble collagen sample and the star-green line is the *P. lividus* insoluble collagen + fraction 9 sample.

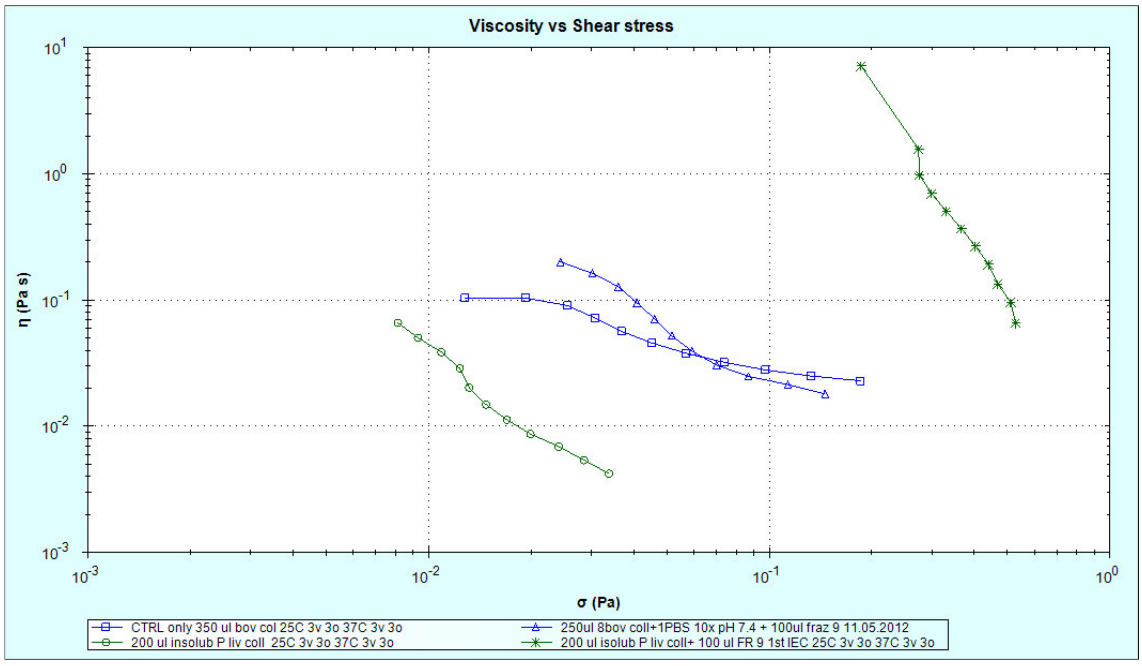

Graph 21. Shear rate ramp log isothermal. Viscometry shear rate ramp in logarithmic scale at 25°C. The square-blue line is the bovine collagen sample, the triangle-blue line is the bovine collagen sample + fraction 9, the circle-green line is the *P. lividus* insoluble collagen sample and the star-green line is the *P. lividus* insoluble collagen + fraction 9 sample.

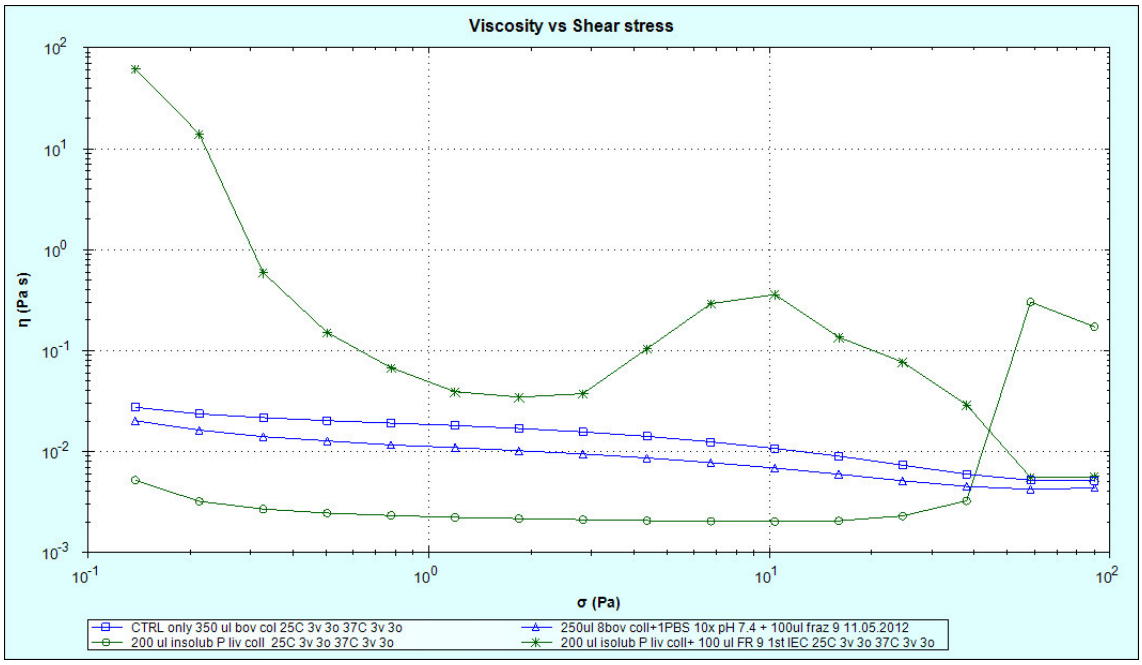

Graph 22. Shear stress ramp with yield stress analysis. Viscometry shear stress ramp in logarithmic scale at 25°C. The square-blue line is the bovine collagen sample, the triangle-blue line is the bovine collagen sample + fraction 9, the circle-green line is the *P. lividus* insoluble collagen sample and the star-green line is the *P. lividus* insoluble collagen + fraction 9 sample.